

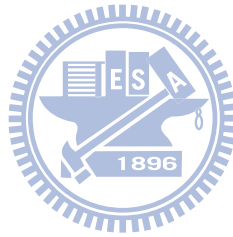
國立交通大學

材料科學與工程學系

博士論文

高分子奈米結構在生物分子上之應用

Polymer Base Nanostructures for Biological Applications



研究生：徐昭業

指導教授：黃華宗 博士

陳培菱 博士

中華民國九十八年九月

高分子奈米結構在生物分子上之應用

Polymer Base Nanostructures for Biological Applications

研究生：徐昭業

Student : Jau-Ye Shiu

指導教授：黃華宗

Advisor : Wha-Tzong Wang

陳培菱

Peilin Chen



A Thesis

Submitted to Department of Materials Science and Engineering

College of Engineer

National Chiao Tung University

in Partial Fulfillment of the Requirements

for the Degree of

Doctor of Philosophy

in

Materials Science and Engineering

September 2009

Hsinchu, Taiwan, Republic of China

中華民國九十八年九月

高分子奈米結構在生物分子上之應用

摘要

具有奈米形貌的材料表面已被廣泛的應用於生物材料上，特別是因表面形貌所造成的超疏水表面(Super Hydrophobic Surface)，由於大部分生物材料需要附著於物體上才能夠表現其應有的行為，例如：osteoclast cell 吸附於骨骼上之行為，因此了解材料表面與細胞之間的交互關係為重要的議題。本論文分為兩部分，其一主要是利用高分子材料加上奈米結構製程技術，來製備具有不同形貌之奈米基材，並用來了解生物分子在此表面上的吸附行為；更進一步利用材料表面的特性來達到操控細胞的貼附行為，如蛋白質陣(Protein arrays)列及細胞陣列(Cell arrays)；其二是利用奈米球微影術(Nanosphere Lithography)及微流體系統(Microfluidic system)製備三維多孔性結構於微流道中，並用來偵測單一 DNA 分子在其中的行為。

本論文研究第一部分主要探討如何在高分子材料表面製造出奈米尺度的形貌，其主要可分為兩種方法，一為將含氟的高分子旋轉塗佈在基材表面再利用氧電漿漿做表面處理，藉由改變氧電漿的處理時間可得到不同粗糙度的表面，其對應的水滴接觸角(Water Contact Angle)可從 120° 改變成 169° 。第二個製程是利用奈米壓印技術將高分子材料轉為具有週期性的奈米陣列形貌，其主要是先利用奈米球微影術將奈米球緊密排列於矽基板上，再利用氧電漿將奈米球縮小到適當的大小，最後再經由濺鍍金屬薄膜、舉離及蝕刻的步驟可得到具有奈米結構的矽基板；稱之為母模。將母模放置於高分子薄膜表面並加熱、加壓，等待溫度回到室溫將其分離便可得與母模相反的高分子奈米結構，其對應的水滴接觸角可達 167° 。

本論文研究第二部分是將細胞培養在這些不同粗糙度的含氟高分子表面，並進一步了解其吸附行為，本研究選擇三種不同的細胞，其中包含 NIH 3T3 小鼠纖維母細胞、CHO (Chinese Hamster Ovary) 中國倉鼠卵巢細胞及 HeLa (Human cervical

epithelioid carcinoma)子宮頸癌細胞。其結果顯示 NIH 3T3 及 CHO 細胞較容易吸附在越粗糙的表面上。因此當把材料表面製備成具有圖案化的(Square 200*200 μm)週期陣列，只有圖案內為粗糙的表面，其餘表面皆保持平整。細胞吸附之行為也會隨之改變而形成細胞陣列，最後結果也發現可利此材料表面來增加細胞基因轉染效率(Transfection Efficiency)。

本論文研究第三部分是利用電濕潤效應(Electrowetting Effect)結合超疏水表面作為蛋白質陣列的表面材料，其原理是將含氟的高分子塗佈在 ITO 電極表面，再將含有鹽離子的溶液放置於材料表面並施加電壓於電極與溶液上使其產生電場，此電場會使溶液更濕潤於表面，換句話說，當施加電壓後會使材料從疏水狀態轉為親水狀態。實驗結果發現當材料經過氧電漿處理後而成超疏水表面再施加相同的電壓下，會從超疏水(接觸角為 163 度)變成超親水(接觸角為 10 度)。當把材料表面設計成與前一部分細胞培養表面的相同圖案後，將蛋白質分子放置於其表面並施加 150V 之電壓後，發現大部份蛋白質分子僅吸附於處理過的表面，也就是說蛋白質分子可被吸附在原本是超疏水表面藉由電濕潤效應而轉為超親水的表面上。經由不同電極設計可將特殊的細胞吸附分子(Fibronectin)吸附在特定的位置，再將細胞培養於其表面上，藉此亦可得到可操控的細胞陣列，此應用可與細胞吸附於粗糙表面特性結合，最後可將兩種不同的細胞共培養(Co-culture)在同一個表面上。

本論文研究最後一部分是利用具有三維奈米多孔性結構之微流道來分析單一 DNA 分子之行為，利用奈米膠體球(Colloidal Particle)自組裝的特性將其堆疊於微流道中，等溶液揮發後並形成六角最密堆積(Hexagonal close-pack)的光子晶體於微流道內，再將其填入凝膠(So-gel)或光阻(Photoresist)充滿其餘空間，最後將膠體球溶解便可得一三維多孔性的反向結構(Inver Opal structure)，此結構由兩種不同大小所組成，一個來自於膠體球本身所佔據之空間(330nm&570nm)，另一來自於球與球連接處(40~62nm)。DNA 分子可被放入此結構中並施加電場，藉由電場的誘導帶負電的 DNA 分子會向正極靠近，當 DNA 分子經過這些微小的奈米孔洞時會被拉伸而產成形變，最後利用螢光顯微鏡可觀測到單一 DNA 分子在此結構中的行為。

Polymer Base Nanostructure for Biological Application

Abstract

Nanotechnology has been widely used for biological applications. One of the most interesting examples is the so-called superhydrophobic surface. This type of structure is influenced by material property (hydrophobicity) and surface morphology (nanostructures). Since most cells can't express cellular behavior without adhere on surfaces, it is very important to investigate the cellular adhesion on surface. For example osteoclast cells have to attach on the bone to behave normally. To understand the cell-substrate interactions, it is very important to investigate how cells adhere to the substrates and how the substrates respond to forces exerted by cells. There are two parts in this thesis; one is using low toxicity polymeric nanostructure with different morphology to study the cellular adhesion behavior by it. Further more, the cell can be controlled to pattern on selected area, as cell arrays. In the second part, the three dimensional periodic nano-porous structure in the integrated microfluidic channel was used to study single DNA behavior.

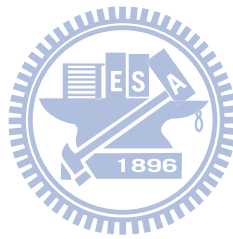
In the first part of the dissertation, there were two simple techniques to impart superhydrophobic properties to the surfaces of microdevices. In the first approach, thin films of a fluoropolymer were spin-coated on the device surfaces followed by an oxygen plasma treatment. By varying the oxygen plasma treatment time, the water contact angles on device surface could be tuned from 120° to 169°. In the second approach, a nanoimprint process was used to create nanostructures on the devices. To fabricate the nanoimprint stamps with various feature sizes, nanosphere lithography was employed to produce a monolayer of well-ordered close-packed nanoparticle array on the silicon surfaces. After oxygen plasma trimming, metal deposition and dry etching process, silicon stamps with different nanostructures were obtained. These stamps were used to imprint nanostructures on hydrophobic coatings, such as Teflon, over the device surfaces. The water contact angle as high as 167° was obtained by the second approach.

In the second part of this dissertation, the patterned nanostructure fluoropolymer surfaces were used for the study of the cell adhesion. By a combination of photolithography and oxygen plasma treatment, patterned fluoropolymer surfaces with various roughnesses have been obtained. The water contact angles measured on the surface were range from 120° to 163° , and surface roughness was measured from 2 nm to 65 nm. When these pattern surfaces were used as the substrates for the cell cultures of HeLa, NIH3T3, and CHO cells, it was found that those cell lines did not adhere to the flat fluoropolymer surfaces. However, the number of NIH3T3 and CHO cells adhered on the surfaces increase with the surface roughness. Such nanostructure materials could be used as scaffold for selected cell growth.

In the third part of this dissertation, I will describe an approach to fabricate addressable cell microarrays, which are based on the patterned switchable superhydrophobic surfaces. The switchable superhydrophobic surfaces were prepared by roughening the surface of fluoropolymers on the electrodes. Upon the application of 150 V, the water contact angle on the roughened fluoropolymer surface could be changed from 163° to less than 10° allowing the deposition of fibronectin, which could guide the growth of the cell. To pattern the cells on such device, the HeLa cell was first seeded on pre-patterned fibronectin area for incubating. After 3 hours incubation and removing suspension cell, the NIH 3T3 cell was incubated on same chip. Two different cell lines can be patterned on the same chip using the technique.

In the last part of this dissertation, I will describe a simple approach to fabricate robust three-dimensional periodic porous nanostructures inside the microchannels. In this approach, the colloidal crystals were first grown inside the microchannel using an evaporation-assisted self-assembly process. Then the void spaces among the colloidal crystals were filled with epoxy-based negative tone photoresist. After subsequent development and nanoparticle removal, the well-ordered nanoporous structures inside the microchannel could be fabricated. Depending on the size of the colloidal nanoparticles, periodic porous nanostructures inside the microchannels with cavity size of 330 and 570 nm have been obtained. The dimensions of interconnecting pores for these cavities were around 40 and 64 nm, respectively. The behavior of single λ -phage DNA molecules in these nanoporous structures was studied using fluorescence microscopy. It was found that

the length of DNA molecules oscillated in the nanoporous structures. The measured length for λ -phage DNA was larger in the 330 nm cavity than those measured in the 570 nm cavity.



誌謝

指導教授 黃華宗 教授

感謝老師在學術上的指導，並給予學生在研究上有很大的空間，也很感謝每次耐心傾聽學生的報告。

陳培菱 教授

感謝老師一路以來的教導與啟發，老師的鼓勵讓我對研究工作產生莫大的興趣。也非常感謝老師支持學生能夠參加國際會議，不僅讓學生更有國際觀，也讓學生在研究之路上得到很大的助益。

口試委員 韋光華 教授、陳三元 教授、薛景中 教授

感謝各位老師在學生論文口試的指導與建議。

交大同學 國倫、育生、國容、彥文

感謝你們在研究上的幫忙。

中研院同事 瓊雯、俊勳、柏宏、文彥、育維、潤蓉、鈞尹、世閔、帝硯、汎清、羽筑、士炘、Shobhit、Narendra

特別感謝瓊雯學姊的提攜與指導並感謝大家一路相挺，非常開心與大伙們一起工作。

Shobhit is my English teacher and buddy.

最後感謝我的家人與妻子立心一路的支持，讓我能夠順利完成學位。

TABLE OF CONTENTS

ABSTRATE.....	I
致謝.....	VI
LIST OF TABLES.....	VIII
LIST OF FIGURES.....	IX
Chapter 1 Introduction.....	1
1.1 Background.....	1
1.2 Superhydrophobic surafce.....	2
1.3 Aims and Objectives.....	6
1.4 Brief Structures of this Thesis.....	6
Chapter 2 Materials and Experimental Techniques.....	8
2.1 Materials.....	8
2.2 Cell Line.....	9
2.3.1 Preparation of Fluoropolymer Films.....	9
2.3.2 Photolithography and Oxygen Plasma Treatment for Superhydrophobic Micro Device.....	10
2.3.3 Nanosphere Lithography.....	10
2.3.4 Fabrication of Nanostamp in Silicon Base.....	11
2.3.5 Nanoimprint.....	13
2.3.6 Switchable Superhydrophobic Surfaces.....	13
2.3.7 Nanostructure in Microfluidic Channel.....	15
2.3.8 Cell Culture on Superhydrophobic Micro Arrays.....	16
Chapter 3 Superhydrophobic Coatings for Microdevices.....	17
3.1 Introduction.....	18
3.2 Experimental Section.....	21
3.2.1 Oxygen Plasma Treatment.....	21
3.2.2 Nanoimprint Process.....	21
3.3 Result and Discussion.....	22
3.3.1 Oxygen Plasma Treatment.....	22
3.3.2 Nanoimprint Process.....	26
3.4 Conclusion.....	28
Chapter 4 Observation of Enhanced Cell Adhesion and Transfection Efficiency on the Superhydrophobic Surfaces.....	30

4.1 Introduction.....	31
4.2 Experimental Section.....	33
4.2.1 Fabrication of superhydrophobic arrays.....	33
4.2.2 Protein absorption with different different surface.....	35
4.2.3 Cell Culture on superhrophobic pattern.....	35
4.2.4 Transfection of Cell.....	36
4.3 Result and Discussion.....	36
4.3.1 Water Contact Angle and Surface Roughness Measurement.....	36
4.3.2 Counting Cell Number on Pattern Surface.....	37
4.3.3 Protein Absorption Analysis.....	39
4.4 Conclusions.....	47
Chapter 5 Addressable Cell Microarrays by Switchable Superhydrophobic Surfaces	
.....	49
5.1 Introduction.....	50
5.2 Experiment Section.....	52
5.3 Result and Discussion.....	54
5.5 Conclusion.....	59
Chapter 6 Behavior of single DNA molecules in the well-ordered nanopores	60
6.1 Introduction.....	61
6.2 Materials and methods.....	63
6.2.1 Chip fabrication.....	63
6.2.2 DNA separation.....	65
6.3 Result and Discussion.....	65
6.3.1 Monolithic Integration of SU-8 Microchannels.....	65
6.3.2 Behavior of Individual DNA Molecules.....	66
6.3.3 Mobility Measurement.....	67
6.5 Conclusion.....	68
Chapter 7 Conclusions and Prospects	71
References	74
List of Publications	83
Curriculum Vitae	85

LIST OF TABLES

Table 6.1 The relationship between the silica beads, cavity size and pore size Silica particles size.....	64
---	----

LIST OF FIGURES

Chapter 1 Introduction

- Figure 1.1 Measurement of the apparent water contact angle on various size-reduced polystyrene surfaces. The solid line is calculated using the modified Cassie's formulation. The dashed line is calculated by Wenzel's model. The star is the water contact angle of double-layer polystyrene arrays that underwent 120 s of oxygen plasma treatment.....4
- Figure 1.2 SEM images (60°) of the size-reduced polystyrene beads and the water contact angle measurement on the corresponding modified surfaces (insets). The diameters of polystyrene beads and water contact angles on these surfaces were measured to be (a) 400 nm, 135°, (b) 360 nm, 144°, (c) 330 nm, 152°, and (d) 190 nm, 168°. Bar: 1 μm.....5

Chapter 2 Materials and Experimental Techniques

- Figure 2.1 The superhydrophobic micro arrays was formed on substrate after oxygen plasma etching and remove photoresist. (Square size: 200μm×200μm).....10
- Figure 2.2 Single layer polystyrene beads close-packed in pattern area on silica substrate.(Size: 400nm).....11
- Figure 2.3 The periodic chromium network on silicon substrate after oxygen plasma reducing the size of nanosphere and metal depositing. (Hole size: 200nm).....12
- Figure 2.4 The silicon stamp was made after the dry etching process and removing chromium layer by CR-7 etchant.....13
- Figure 2.5 Polymeric nanostructure obtained by nanoimprint process.....14
- Figure 2.6 Optical images of water droplet on the roughened fluoropolymer surface before (a) and after (b) applying 300 VAC to the ITO glass.....14
- Figure 2.7 Cross-sectional SEM images of nanoporous structures inside the microchannels. Bar: 4 μm.....16
- Figure 2.8 Cell seed on superhydrophobic micro arrays with volume 1000ml.....16

Chapter 3 Materials and Experimental Techniques

- Figure 3.1 Schematic for producing a superhydrophobic coating on device surfaces using

	oxygenplasma treatment. (a) The surface of the device is coated with a layer of fluoropolymer (Teflon).(b) Oxygen plasma treatment is used to roughen the surface of fluoropolymer. (c) A superhydrophobicsurface is obtained after the oxygen plasma treatment.....	20
Figure 3.2	Schematic for creating a superhydrophobic coating on device surfaces using nanoimprint process. (a) The silicon substrate is coated with a single layer of well-ordered polystyrene beads. (b) Oxygen plasma is used to reduce the size of polystyrene beads. (c) A layer of chromium is coated on top of the polystyrene beads. (d) Polystyrene beads are then removed by CH ₂ Cl ₂ solution. (e) The silicon wafer is etched by RIE. (f) The nanoimprint stamp is obtained by removing the chromium layer using CR-7 etchant. (g) The stamp is pressed against the device coated with fluoropolymer. (h) After removing the stamp from the device surface, nanostructure on the surface is obtained.....	23
Figure 3.3	SEM images of (a) flat (b) roughened fluoropolymer surfaces. Inset: water droplets on both surfaces.	24
Figure 3.4	Water contact angle measured on the roughened fluoropolymer surface as a function of oxygen plasma treatment time.	25
Figure 3.5	The XPS data of the fluoropolymer coating without oxygen plasma treatment.	26
Figure 3.6	The XPS spectra of a) F (1s), b) C (1s), c) O (1s) peaks for both the flat Teflon AF (solid line) and the roughened Teflon AF after 10 min of oxygen plasma treatment (dottedline).	27
Figure 3.7	FTIR spectra of the flat (black) and roughened (red) Teflon AF.....	27
Figure 3.8	SEM images of the nanoimprint stamp created by nanosphere lithography. (a) Bar: 2 μm; inset bar: 500 nm; (b) bar: 1 μm, the angle of SEM view: 60°..	28
Figure 3.9	SEM image of the imprinted nanostructure on the ITO glass surface. Bar: 1.5 μm, the angle of SEM view: 60°..	29

Chapter 4 Observation of Enhanced Cell Adhesion and Transfection Efficiency on the Superhydrophobic Surfaces

Figure 4.1 Patterning process for switchable superhydrophobic surfaces: A) the fluoropolymer was coated on glass substrate. B) A layer of patterned photoresist was used as the mask for the oxygen plasma treatment. C) After oxygen plasma treatment, the unprotected area was roughened. D) The

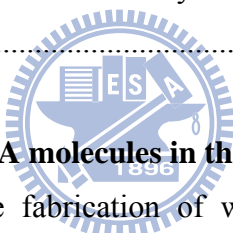
	superhydrophobic microarray was obtained by removing the photoresist. E) The cell was cultured on superhydrophobic microarray.....	34
Figure 4.2	The AFM images of (a) flat and (b) roughened Teflon AF. Bar: 1 μ m. (Measured by VEECO Innova SPM).....	37
Figure 4.3	The contact angles on the roughened Teflon AF surfaces as a function of etching time.....	38
Figure 4.4	The surface roughness on the roughened Teflon AF surfaces as a function of etching time. (Measured by VEECO Innova SPM).....	39
Figure 4.5	The fluorescence intensity of the dye conjugated fibronectins on various surfaces as a function of solution contact time. Open triangles: glass surfaces. Close triangles: PEG presenting surfaces. Open circles: roughened fluoropolymers with a contact angle of 163° . Close circles: flat fluoropolymers.....	41
Figure 4.6	The DIC images of (a) NIH 3T3 (b) CHO and (c) HeLa cells on the patterned superhydrophobic surfaces after 6 hours of incubation. Bar: 200 μ m.....	43
Figure 4.7	The time-lapse DIC images of NIH 3T3 cells on the patterned superhydrophobic surfaces after a) 0 minute, b) 50 minutes c) 100 minutes d) 3 hours of incubation. e) After washing the sample with PBS solution. Bar: 200 μ m.....	44
Figure 4.8	The averaged cell number attached on the roughened fluoropolymer surfaces as a function of water contact angle. The patterned area is $200\mu\text{m} \times 200 \mu\text{m}$. The collagen coated glass and flat fluoropolymer were used as controls.....	45
Figure 4.9	a) Transfection efficiency measured for the CHO cells on the poly D-lysine (red) and superhydrophobic surface(black). b) The CHO cells on the patterned superhydrophobic surfaces transfected with fluorescence proteins, Kaede. Bar 50 μ m. (c) The NIH 3T3 cells on the patterned superhydrophobic surfaces transfected with fluorescence proteins, GFP-actin. Bar 50 μ m.....	46

Chapter 5 Addressable Cell Microarrays by Switchable Superhydrophobic Surfaces

Figure 5.1	(a) The switchable superhydrophobic surface is fabricated by roughening a layer of fluoropolymer on the pre-patterned ITO electrodes. (b) A drop of
------------	--

fibronectin solution is added to the surface and a 150V is applied to the desired electrodes. (c) Fibronectin molecules are deposited to the array with underneath electrode activated. (d) The microarray is then used for cell culture. The cells will only attach to the area coated with fibronectin. (e) The procedure is repeated to culture the second type of cells.....53

Figure 5.2	Optical image of an addressable chip containing 4 x 4 switchable superhydrophobic microarrays.....	54
Figure 5.3	Fluorescence image of the patterned FITC conjugated anti-chicken IgG (green) and cy3 conjugated anti-rabbit IgG (red). Bar: 400 μm	55
Figure 5.4	HeLa cells patterned on the switchable superhydrophobic microarrays. Bar: 200 μm	56
Figure 5.5	Fibroblast cells patterned on the switchable superhydrophobic microarrays. Bar: 200 μm	57
Figure 5.6	Fibroblast cells (red) were first patterned on switchable superhydrophobic microarray then followed by the HeLa cells (green). Bar: 200 μm	58



Chapter 6 Behavior of single DNA molecules in the well-ordered nanopores

Figure 6.1	Schematic for the fabrication of well-order nanoporous structure in the microchannel using SU-8 photoresist. (a) Silica colloidal crystals are first grown inside the SU-8 microchannel. (b) The void spaces of the colloidal crystals are filled with SU-8 photoresist and cured in the desired area using UV radiation. (c) Inverse opal structures can be obtained after removing the silica nanoparticles with BOE solution and sealing with another layer of SU-8 photoresist. (d) The nanoporous structures are consisted of cavity d_c and interconnecting pore d_p	64
Figure 6.2	SEM images of nanoporous structures. Silica nanoparticle size (a) 300 nm, bar: 300 nm; (b) 570 nm, bar: 500 nm.....	65
Figure 6.3	Sequential images of λ -DNA migrating inside the nanoporous structure toward the anode at an applied field of 5 V/cm. Elapsed time between frames is 0.1 s. Cavity size: (a) 300 nm, bar: 20 μm and (b) 570 nm; bar: 20 μm	68
Figure 6.4	(a) Averaged DNA length in two different nanoporous structures. Applied field: 5 V/cm. 300nm (black square), 570 nm (open circles). (b) DNA length distribution in the nanoporous materials with two different cavity sizes	

(average of 500 DNA molecules).....69

Figure 6.5 The electrophoretic mobility of (a) λ -DNA and (b) M13mp18 vector as a function of the applied electric field with two different cavity size of nanoporous structures: 300 nm (black square), 570 nm (open circles) (average of 50 DNA molecules).69



Chapter 1

Introduction

1.1 Background

Surface engineering plays an important role in various biological applications, including biosensor technology [1-3] and tissue engineering. [4] In biosensor technology, the ability to create patterns of proteins and cells on the surface is very important, since it is required to monitor living cell behavior when it attach on the surface for studying cell-substrate interaction. Tissue engineering can control the shape of cell adhesion on the surface and the chemistry and topography of the surface where the cell adhered are also important for understanding the relationship between cellular attachment and material surface. Cell adhesion is an important key to biomedical and biotechnological applications. The understanding of the relationship between cell adhesion and substrate are particularly important issue. It has been known that cell attachment contain many proteins including fibronectin, serum albumin and extra cellular matrix (ECM) protein. Therefore, by controlling cell adhesion proteins onto implant surface, the cell attachment behavior is also influenced. For example, if the micro contact printing is used to print fibronectin onto patterned area, the cell can be selected to attach on that area. [5, 6] However, the properties of substrate surface also affect to cell adhesion such as hydrophobicity, surface charge, surface chemistry and roughness. Some reports have shown that cells prefer to grow on surface with specific morphology such as porous and roughness surface. [7] However, there are very limited research activities in exploring the possibility of using the surface morphology as tool for biological applications. We believe that there are many properties

should be discussed between cell-substrate interactions. Especially, by using the materials which can be changed surface morphologic to study cell adhesion.

In this thesis, I describe that use simple approach to prepare polymeric nanostructure arrays with the so-call “superhydrophobic surface”, which can be used to pattern proteins and cells. We also in investigate how the nanostructure affects the surface hydrophobicity and how is it to influence the cell adhesion. Furthermore, the behavior of cell adhesion can be controlled to attach on the selected position of the surface and two different types of cell can be cultured on the same surface.

1.2 Superhydrophobic surfaces

Superhydrophobic surfaces, inspired by the water-repellent behavior of the micro and nanostructured plant surfaces [8, 9], with a water contact angle larger than 150° , have attracted a lot of research attention recently. Because of their unusual large water contact angle, superhydrophobic surfaces can be used as self-cleaning, anti-adhesion, and oxidation-resistant coatings, [10] and it was demonstrated recently that blood cells did not adhere to such type of surfaces [11]. The water-repellent behavior of superhydrophobic surfaces has been explained by two models, [12] the Wenzel and Cassie formulations, which both predict that a nanostructured surface may amplify the surface hydrophobicity as long as a layer of low-surface-energy materials is present on the surface.

In Wenzel’s formulation, it is assumed that the liquid fills up the rough surface, therefore forming a wetted contact, and the apparent water contact angle (θ^*) can be written as

$$\cos \theta^* = \lambda \cos \theta,$$

where λ is the roughness factor which is the ratio of total surface area to the projected area on the horizontal plane and θ is the intrinsic contact angle measured on the flat surface. In Cassie’s approach, it is assumed that the liquid forms a line of contact on the

rough surface with air trapped below the contact line and the apparent contact angle can be formulated as

$$\cos \theta^* = \Phi_s (\cos \theta + 1) - 1,$$

where Φ_s is the area fraction of the liquid-solid contact to the projected surface area. In previous work, [12] we have fabricated well-ordered, tunable superhydrophobic surface whose water contact angle can be tuned from 132° to 170° (on a double-layer sample) using a combination of nanosphere lithography and oxygen plasma treatment. The water contact angle on these surfaces can be modeled by the modified Cassie's formulation without any adjustable parameter (Figure 1.1). The dynamic water contact angle measurement indicates that well-ordered two-dimensional nanostructured systems have relatively large water contact angle hysteresis (Figure 1.2).

It has been suggested that contamination, oxidation, and current conduction can be inhibited on such superhydrophobic surfaces, and the flow resistance in the microfluidic channels can also be reduced using super water-repellent materials. [13] However, to fully utilize the water-repellent properties of the nanostructured surfaces, it is necessary to investigate the relationship between the nanostructure and the water repellent behavior on surfaces and to fabricate the nanostructured surfaces with desired surface hydrophobicity. To fabricate superhydrophobic surfaces, a typical procedure is to create a rough surface covered with low surface energy molecules, such as fluoroalkylsilanes, [14] or to roughen the surface of hydrophobic materials. Several superhydrophobic surfaces have been prepared by these approaches including fluoroalkylsilane-modified inverse opal surfaces, [15] plasma polymerization, [16] anodic oxidation of aluminum, [17] gel-like roughened polypropylene, [18] plasma fluorination of polybutadiene, [19] oxygen plasma-treated poly(tetrafluoroethylene), [20, 21] densely packed aligned carbon nanotubes, [22] aligned

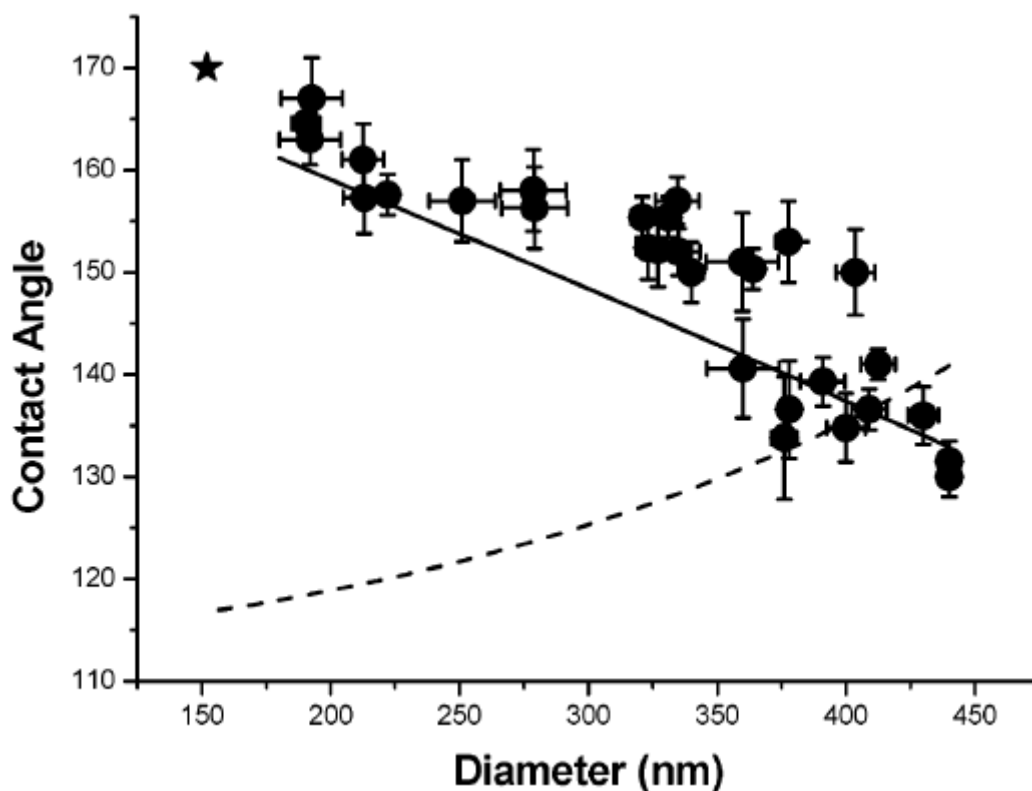


Figure 1.1 Measurement of the apparent water contact angle on various size-reduced polystyrene surfaces. The solid line is calculated using the modified Cassie's formulation. The dashed line is calculated by Wenzel's model. The star is the water contact angle of double-layer polystyrene arrays that underwent 120 s of oxygen plasma treatment. [12]

polyacrylonitrile nanofibers, [23] and solidification of alkylketene dimmer. [24] A common observation in these experiments is that the water contact angle increases as the surface roughness increases. However, in other experiments [25, 26] it has been demonstrated that smooth well-ordered microstructured surfaces could also produce superhydrophobic surfaces as long as the ratio of the liquid-solid contact area to the overall projected area remains small. It has also been pointed out [27, 28] that the three phase contact line plays a very important role in the contact angle hysteresis, which determines the sliding behavior of water droplets on surfaces.

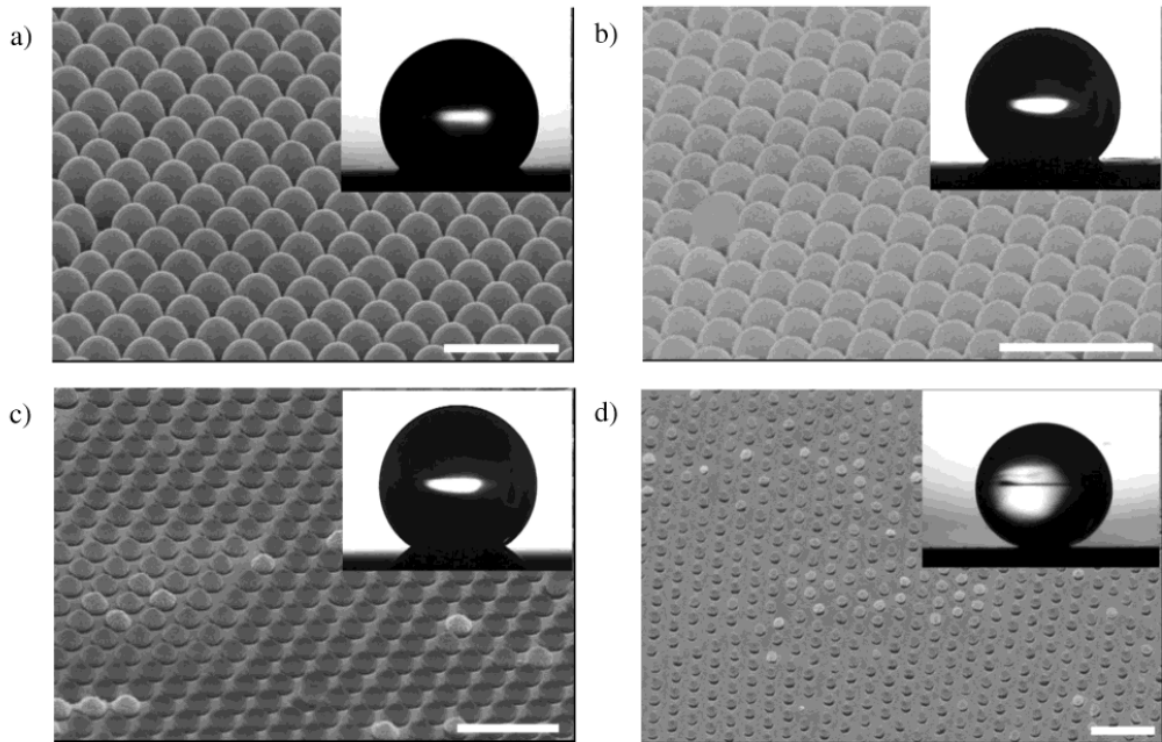


Figure 1.2 SEM images (60°) of the size-reduced polystyrene beads and the water contact angle measurement on the corresponding modified surfaces (insets). The diameters of polystyrene beads and water contact angles on these surfaces were measured to be (a) 400 nm, 135° , (b) 360 nm, 144° , (c) 330 nm, 152° , and (d) 190 nm, 168° . Bar: 1 μm . [12]

From the above discussion of fabrication procedures, it can be used to prepare superhydrophobic surfaces. However, if the superhydrophobic surfaces are to be used in a microdevice, the modification process should be compatible with the micro-fabrication techniques. For example, if one would like to engineer the surface of a microfluidic device with superhydrophobic properties to reduce the flow resistance, the superhydrophobic material should be integrated into the microfluidic system [17, 29]. Since the surfaces of the microdevices are always flat and smooth, superhydrophobic surfaces can be produced only by roughening a hydrophobic coating. However, almost none of the above-mentioned

techniques can be used directly in such type of applications. Therefore, an alternative approach for producing superhydrophobic coatings on the device surface is needed.

1.3 Aims and Objectives

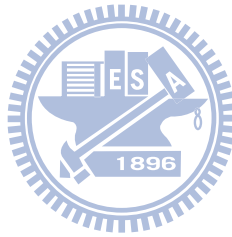
In this thesis, it has been demonstrated that there are two approaches to impart superhydrophobic properties to the surfaces of micro-devices. First, thin films of a fluoropolymer were spin-coated on the device surfaces followed by an oxygen plasma treatment. However, this approach can not be applied to every hydrophobic materials. In some condition, the surface property will be changed after gas plasma etching. Therefore, the process without changing the chemical properties of polymer should be developed. In the second approach, a nanoimprint process was used to create nanostructures on the polymeric devices. During this process, the polymer only change shape with heating and pressuring when it is filled into imprinting mold. Those two fabrication techniques can be used create superhydrophobic surface on the device which were used to study the adhesion of biological molecule, such as protein and cell. Switchable surface technique is also applied to the superhydrophobic surface to control proteins and cells adhesion by eletrowetting effect.

Another developing of robust three dimensional nanoporous inside microfluidic channel will be used to study single DNA molecule behavior. The fabrication is combined colloidal crystals and micofludic system.

The objectives of this thesis are as follows:

- To develop a simple approach to fabricate superhydrophobic micro-devices.
- To develop a fabrication nanostructure on polymer without changing its chemical property.
- To investigate cell-substrate interaction using different surface morphology.

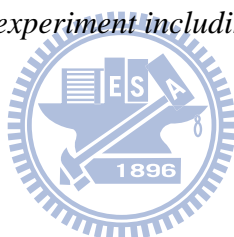
- To use eletrowetting effect to control the surface properties. In additional the cell adhesion protein can be patterned on superhydrophobic surface and the cell will attach to the desired position.
- To develop three dimensional nanoporous structure inside microfluidic system.
- To use different size of nanostructures to study single DNA behavior with fluoresce microscopy.



Chapter 2

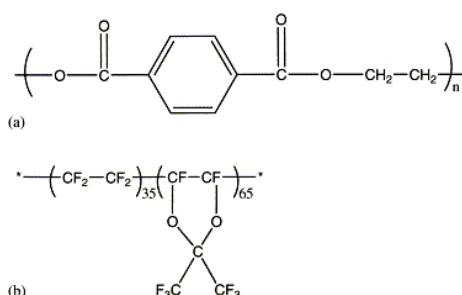
Materials and Experimental Techniques

A brief review of the materials used and the experimental details that we developed for superhydrophobic micro-device and nanofluidic system will be presented. The fabrication include spin-coated, oxygen plasma treatment, nanosphere lithography, nanoimprint, photolithography, microfluidic channel and electrode pattern. In the other hand, the cell was chosen in this experiment including NIH 3T3, CHO and HeLa cell.



2.1 Materials

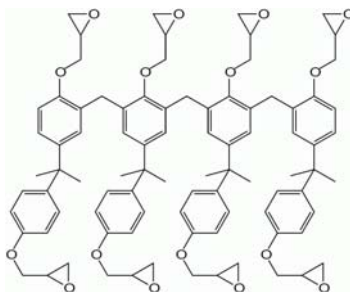
- (1) Poly[tetrafluoroethylene-co-2,2-bis(trifluoromethyl)-4,5-difluoro-1,3-dioxole] are spin-coated as 5-micron thick film on glass from Teflon AF, DuPont, US.



- (2) Indium Tin Oxide (ITO) glass substrate: ITO glass substrates were first patterned by lithograph as a design 200×200 μm square arrays, then cleaned with detergent, and ultrasonicated in acetone and isopropyl alcohol, subsequently dried on hot plate at

150 °C for 5 min, and finally treated with oxygen plasma for 5 min. The thickness of ITO is 200 nm.

- (3) Polystyrene and Silica nanospheres were chosen by different size from Bangs Laboratories, Inc., Fishers, IN
- (4) S1813 is positive photoresist system engineered to satisfy the microelectronics industry's requirement for advanced IC device fabrication.
- (5) SU-8 is a negative, epoxy-type, near-UV photoresist (365 nm) from MicroChem.



2.2 Cell Line

- (1) The NIH3T3 is a standard fibroblast cell line, which is a type of cell that synthesizes and maintains the extracellular matrix of many animal tissues.
- (2) The CHO cell is a cell line derived from Chinese hamster ovary cell.
- (3) The HeLa cell is derived from cervical cancer cell, which belongs to an immortal cell line.

2.3 Experimental Techniques

2.3.1 Preparation of Fluoropolymer Films

The poly[tetrafluoroethylene-co-2,2-bis(trifluoromethyl)-4,5-difluoro-1,3-dioxole] was first spin-coated as 5-micron thick film on glass from Teflon AF, DuPont, US. and heated with hotplate upon 250°C for 30 minutes to evaporate the solvent.

2.3.2 Photolithography and Oxygen Plasma Treatment for

Superhydrophobic Micro Device

A layer of photoresist (S1813, Shipley) was spun on top of the fluoropolymer coating and a photolithographic process was used to define the superhydrophobic area on the photoresist. The superhydrophobic microarray can be manufactured using an oxygen plasma treatment (Oxford Plasmalab 80 Plus, 80W) with a gas O_2 (2 sccm) at a total pressure of 25 mTorr. After plasma treatment the photoresist was removed by washing the surface with acetone. Only the areas exposed to the oxygen plasma exhibited the superhydrophobic behavior (Figure 2.1).

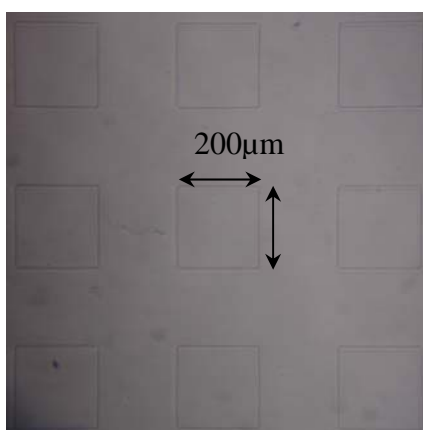


Figure 2.1 The superhydrophobic micro arrays was formed on substrate after oxygen plasma etching and remove photoresist. (Square size: $200\mu\text{m}\times 200\mu\text{m}$)

2.3.3 Nanosphere Lithography

Nanosphere lithography [30-33] is a well-established technique for patterning large-area periodic nanosphere arrays. By spin-coating the monodisperse polystyrene beads solution on substrate surfaces, self-organized close-packed nanostructures can be easily achieved. In this experiment, it has been shown that both single- and double-layer close-packed polystyrene arrays over a few square centimeter area can be obtained by

adjusting the speed of the spin-coater and the concentration of the surfactants in the polystyrene solution. A monodispersed polystyrene dispersion with 400 nm diameter beads (Bangs Laboratories, Inc., Fishers, IN) was used to produce self-assembled close packed two-dimensional colloidal crystals on a silicon wafer (Figure 2.2).

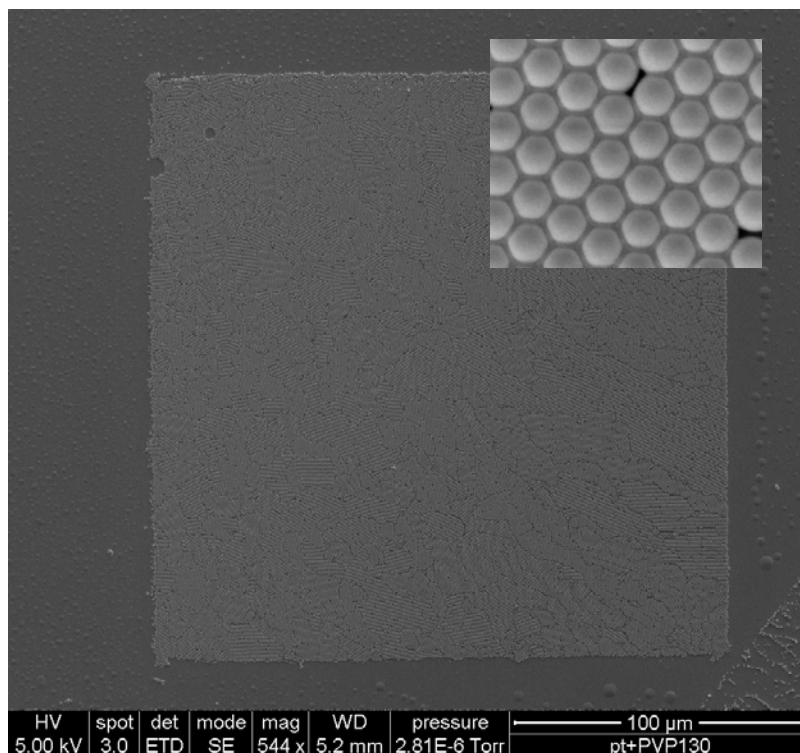


Figure 2.2 Single layer polystyrene beads close-packed in pattern area on silica substrate.

(Size: 400nm)

2.3.4 Fabrication of Nanostamp in Silicon Base

To prepare silicon nanomold for nanoimprint process, these two-dimensional colloidal crystals were then used as the template to produce stamps for nanoimprint. To vary the surface fraction of the nanoimprint stamp, the size of the polystyrene beads was trimmed by oxygen plasma etching (Oxford Plasmalab 80 Plus, 50 W, 20 sccm O₂), which

reduced the diameter of the polystyrene beads while keeping their separation distance unchanged. The diameter of the polystyrene beads could be changed from 400 nm to 200 nm. To fabricate nanoimprint stamp, a 50 nm thick chromium layer was deposited on top of the trimmed polystyrene beads. Then the polystyrene beads were dissolved in dichloromethane (Figure 2.3). A dry etching process was used to etch the silicon wafer in an RIE etcher (Oxford Plasmalab 80 Plus, 110 W, 45 sccm SF₆, 5 sccm O₂). After the dry etching process and removing chromium layer by CR-7 etchant, the silicon stamp (30 × 30 mm²) with periodic nanopores was obtained (Figure 2.4).

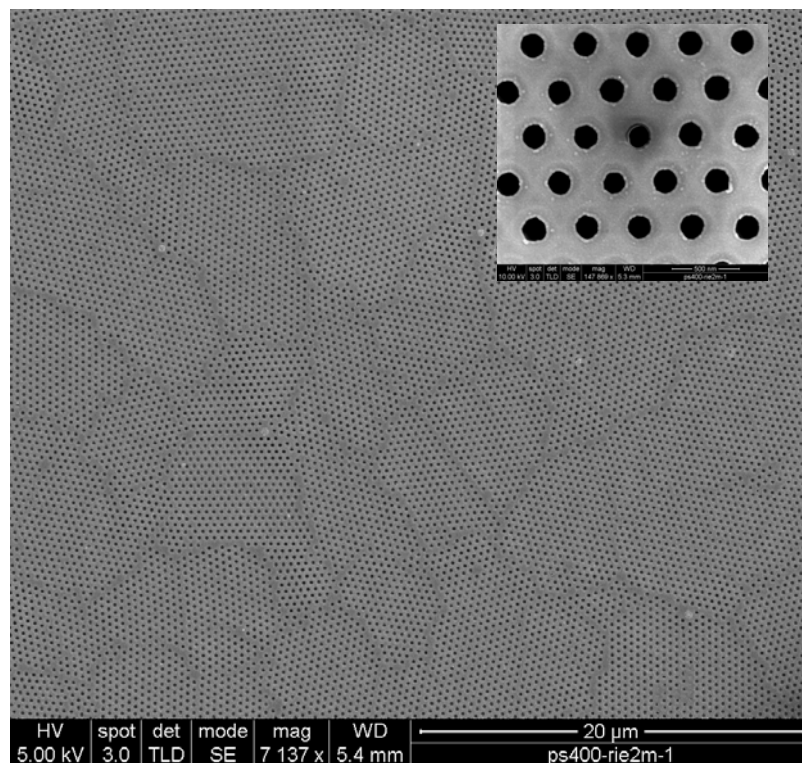


Figure 2.3 The periodic chromium network on silicon substrate after oxygen plasma reducing the size of nanosphere and metal depositing. (Hole size: 200nm)

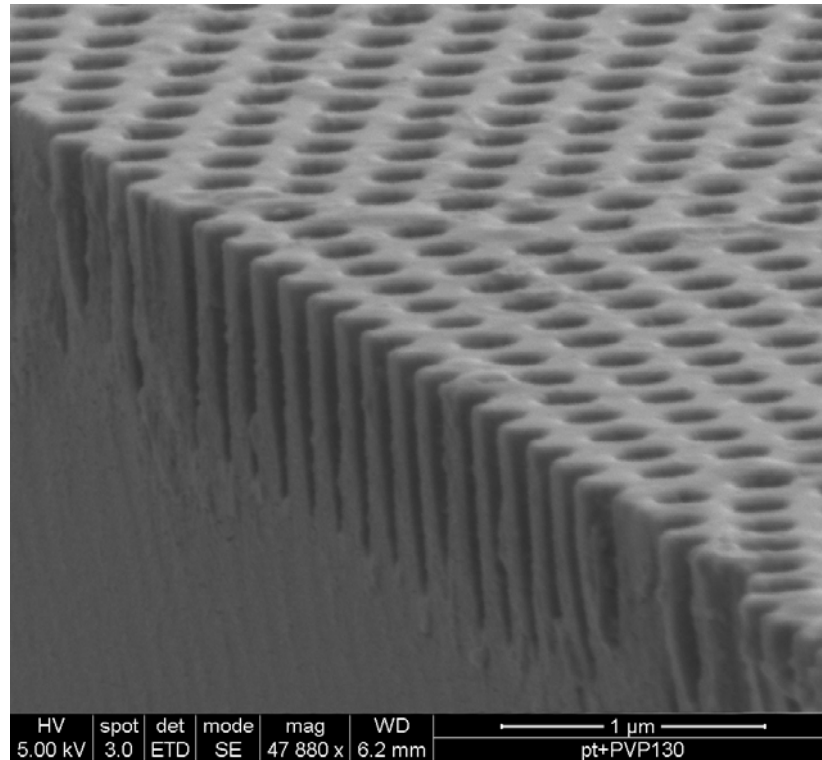
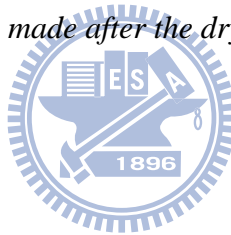


Figure 2.4 The silicon stamp was made after the dry etching process and removing chromium layer by CR-7 etchant.



2.3.5 Nanoimprint

To create a nanostructure on polymer as superhydrophobic microdevice by the nanoimprint process, a 1 μm thick layer of fluoropolymer was coated on the ITO glass. Then the nanoimprint stamp was pressed against the polymer coated ITO glass under 70 mbar pressure at 150.C for 30 min. After removing the stamp, nanostructures with desired dimension can be fabricated on the device surfaces (Figure 2.5).

2.3.6 Switchable Superhydrophobic Surfaces

To fabricate a switchable superhydrophobic surface, electrowetting was employed to modify the surface energy through charging the surface with electric field. To avoid

breakdown of the fluoropolymer at high voltage, a layer of silicon oxide (~300 nm) was deposited on top of the ITO electrode by PECVD before coating the surface with Teflon AF. To induce a transition from the superhydrophobic state to the completely wetted state, an AC voltage (300V, 150 Hz) was applied to the ITO glass. The water contact angle on the roughened fluoropolymer surface could be switched from $\sim 167^\circ$ to $< 10^\circ$ as shown in Figure 2.6

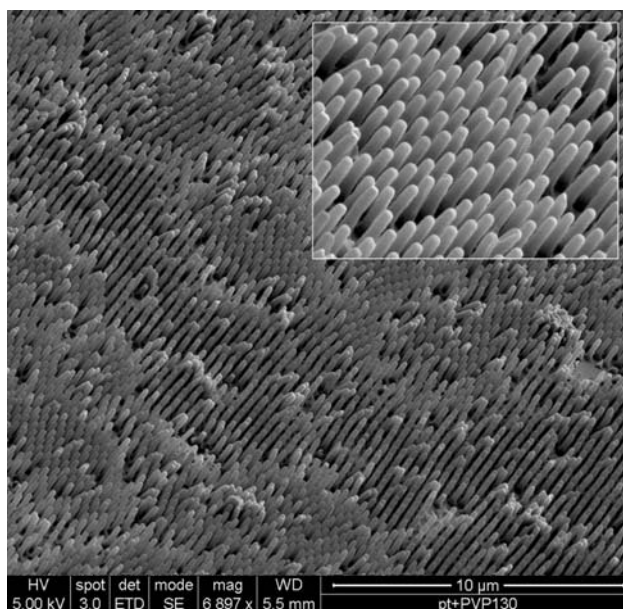


Figure 2.5 Polymeric nanostructure obtained by nanoimprint process.

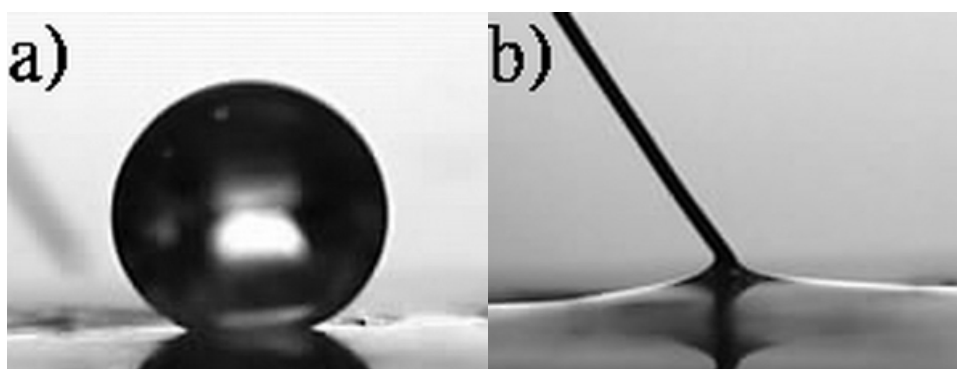


Figure 2.6 Optical images of water droplet on the roughened fluoropolymer surface before (a) and after (b) applying 300 VAC to the ITO glass.

2.3.7 Nanostructure in Microfluidic Channel

To fabricate size-controlled porous nanostructures inside the microfluidic channels, a cover slip (Technical Glass Product, Painesville Twp, OH) was used as the substrate. A layer of 15 μm thick cured SU-8 photoresist was used as the base layer. A second layer of SU-8 photoresist was then spun on the base layer and then the microchannels were created in the second layer using a standard photolithography process. The microchannels were then temporally sealed by conformal contact with a 5 mm thick polydimethylsiloxane (PDMS) slab. Well-ordered colloidal crystals could be grown in the microchannel using evaporation induced self assembly process. The void spaces in the colloidal crystal were then filled with SU-8 photoresist. A photomask was used to define the location of the nanoporous structures inside the microfluidic channel. After dissolving silica colloidal particles in buffer oxide etch (BOE) solution, well-ordered nanoporous structures inside the microfluidic system can be obtained (Figure 2.7). These nanoporous structures were consisted of cavities with a diameter of d_c , which represented the size of the original silica nanoparticles, and interconnecting pores with a diameter of d_p . These interconnecting pores and cavities could be used as the sieving materials for separating biomolecules. The colloidal particles used in this experiment were 300 nm and 570 nm silica nanoparticles (Bangs Laboratories, Fisher, IN, USA).

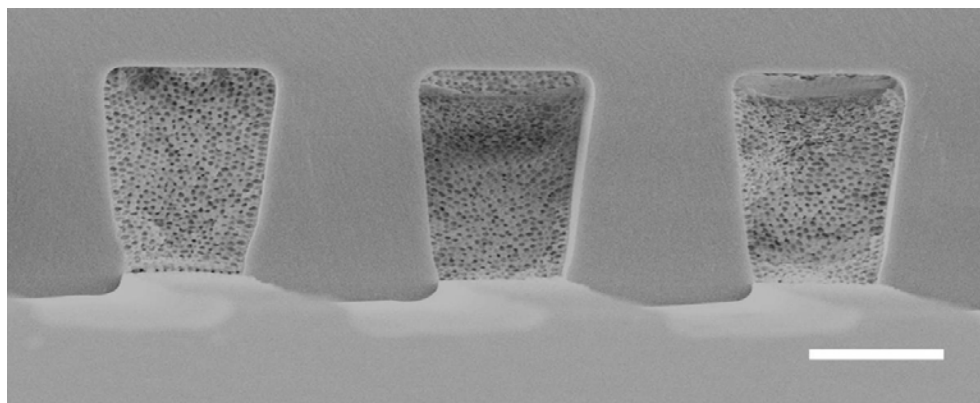


Figure 2.7 Cross-sectional SEM images of nanoporous structures inside the microchannels. Bar: 4 μm .

2.3.8 Cell Culture on Superhydrophobic Micro Arrays

The entire cell was incubated in the chamber with superhydrophobic micro arrays with total volume 1000ml at 37°C and 5% CO₂ in an incubator for 6 hours (Figure 2.8). The concentration of the cell was used 10⁵ cell/c.c. in this process. Then the suspends cell could be removed by PBS washing and taken the DIC image by confocal microscopy (IX 71, Olympus) for counting the number of the cell on different rough surface.

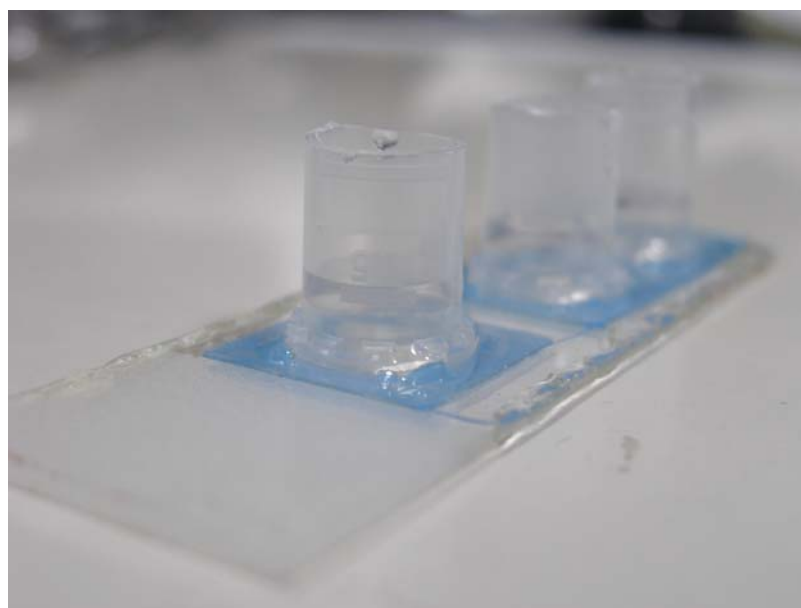
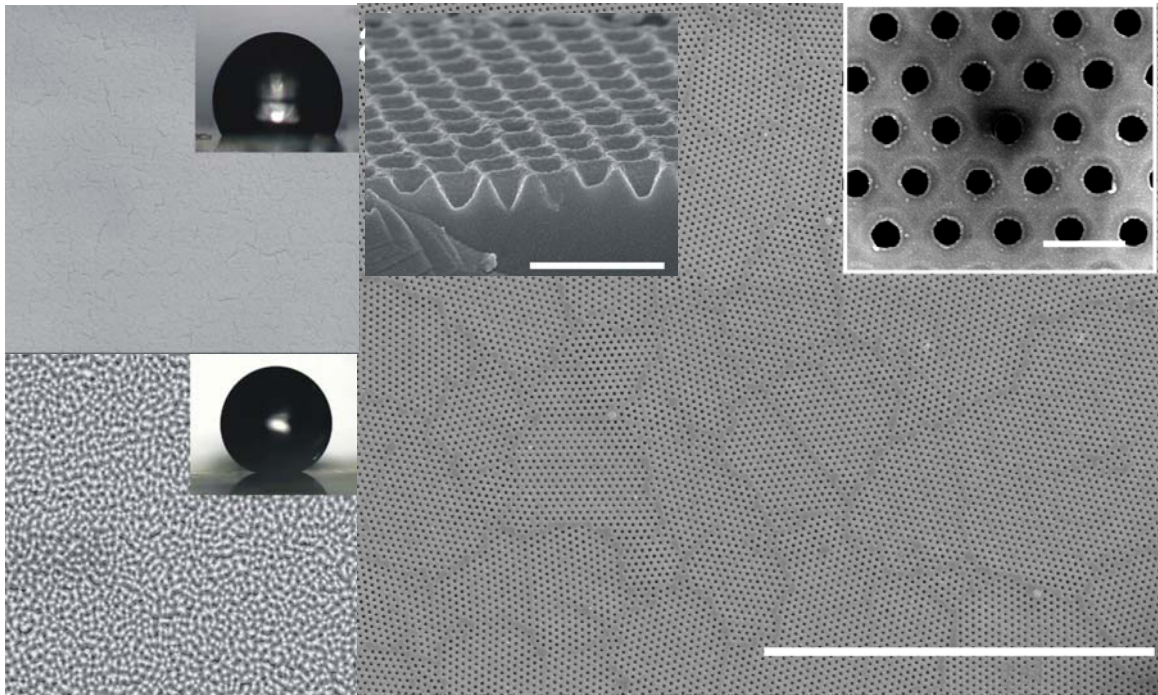


Figure 2.8 Cell seed on superhydrophobic micro arrays with volume 1000ml.

Chapter 3

Superhydrophobic Coatings for Microdevices



In this chapter, there are two simple techniques to impart superhydrophobic properties to the surfaces of microdevices. In the first approach, thin films of a fluoropolymer were spin-coated on the device surfaces followed by an oxygen plasma treatment. By varying the oxygen plasma treatment time, the water contact angles on device surface could be tuned from 120° to 169° . In the second approach, a nanoimprint process was used to create nanostructures on the devices. To fabricate nanoimprint stamps with various feature sizes, nanosphere lithography was employed to produce a monolayer of well-ordered close-packed nanoparticle array on the silicon surfaces. After oxygen plasma trimming, metal deposition and dry etching process, silicon stamps with different nanostructures were obtained. These stamps were used to imprint nanostructures on

hydrophobic coatings, such as Teflon, over the device surfaces. The water contact angle as high as 167° was obtained by the second approach.

3.1 Introduction

In the development of modern technology, it is often useful to learn from nature. Many new ideas and inventions have originated from the observation of the behavior of natural materials. One recent example is the so-called “superhydrophobic” materials, which exhibit a water contact angle larger than 150°. Such superhydrophobic materials have lately attracted considerable attention because of their self-cleaning properties. In the past, it was known that a very high water contact angle could be obtained by treating the Teflon surface with oxygen plasma [34, 35]. However, it was only until the discovery of the relationship between the microand nano-structures of the plant surfaces and their water-repellent behavior [36, 37], that researchers started to realize that such superhydrophobic materials might have some important applications. For example, it has been suggested that contamination, oxidation and current conduction can be inhibited on such superhydrophobic surfaces [38], and the flow resistance in the microfluidic channels can also be reduced using the super water-repellent materials [39]. In another example, it was demonstrated that the superhydrophobic surfaces could resist the adhesion of cells and proteins [40]. The self-cleaning and anti-adhesion properties of the superhydrophobic surface could be beneficial to various applications where a clean surface is always required. However, one of the most important issues to incorporate superhydrophobic surfaces into the existing applications is that the surface modification process should be compatible with the current manufacturing techniques, especially the micro-fabrication process.

In the past few years, a variety of fabrication procedures have been proposed to prepare superhydrophobic surfaces. In general, superhydrophobic surfaces can be fabricated by coating a rough surface with low surface energy molecules, such as fluoroalkylsilanes [41] or by roughening the surface of hydrophobic materials. Many superhydrophobic surfaces have been produced by these approaches including fluoroalkylsilane modified inverse opal surfaces [42], plasma polymerization [43], anodic oxidation of aluminum [44], gel-like roughened polypropylene [45], plasma fluorination of polybutadiene [46], oxygen plasma treated poly(tetrafluoroethylene) [34, 47], densely packed aligned carbon nanotubes [48], aligned polyacrylonitrile nanofibers [49], and solidification of alkylketene dimer [50]. If superhydrophobic surfaces are to be used in a microdevice, the modification process should be compatible with the micro-fabrication techniques. For example, if one would like to engineer the surface of a microfluidic device with superhydrophobic properties to reduce the flow resistance, the superhydrophobic material should be integrated into the microfluidic system [39, 51]. Since the surfaces of the microdevices are always flat and smooth, superhydrophobic surfaces can be produced only by roughening a hydrophobic coating. However, almost none of the above-mentioned techniques can be used directly in such type of applications. Therefore, an alternative approach for producing superhydrophobic coatings on the device surface is needed.

Here we describe two simple fabrication processes to modify the surface of the device to achieve a very high water contact angle. In the first approach, the device was first coated with a thin film of hydrophobic materials, fluoropolymer in this case, and then oxygen plasma was used to create superhydrophobic surfaces. However, only in some cases, the chemical properties of the hydrophobic materials could be altered by the oxygen plasma treatment [52]. Therefore, a second technique has been developed where the nanostructures can be created on the device surfaces by a nanoimprint process [53]. Both

of these approaches are compatible with the micro-fabrication process.

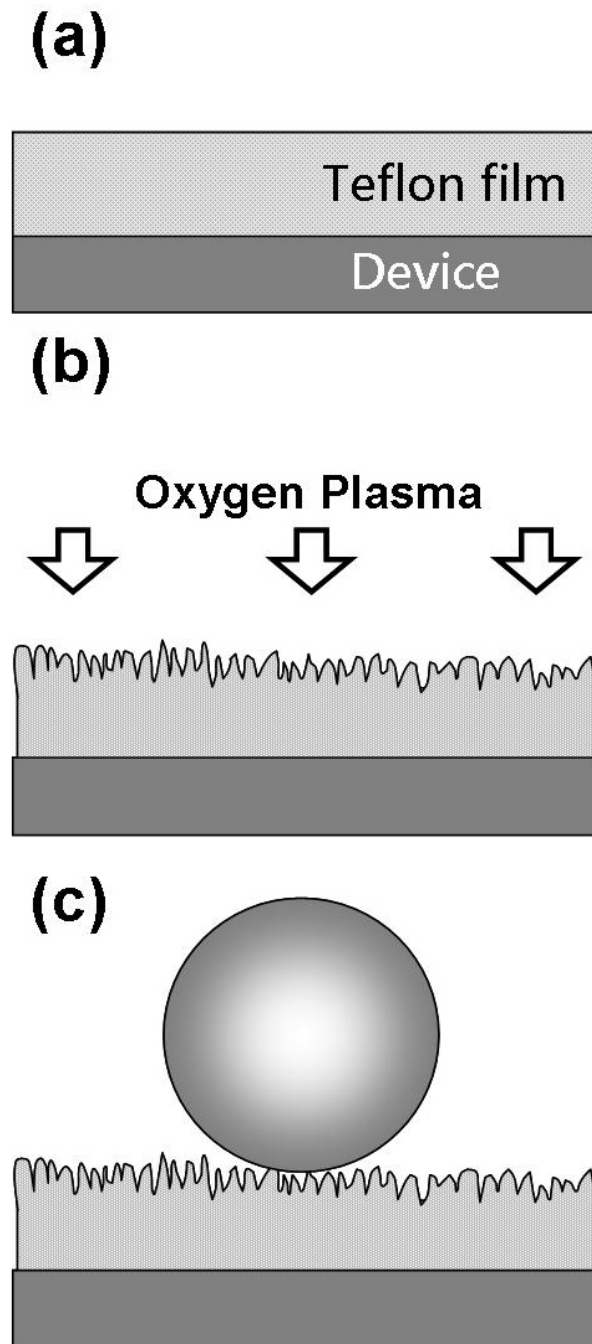


Figure 3.1 Schematic for producing a superhydrophobic coating on device surfaces using oxygen plasma treatment. (a) The surface of the device is coated with a layer of fluoropolymer (Teflon). (b) Oxygen plasma treatment is used to roughen the surface of fluoropolymer. (c) A superhydrophobic surface is obtained after the oxygen plasma treatment.

3.2 Experimental Section

3.2.1 Oxygen Plasma Treatment

One simple approach to create a superhydrophobic surface on a device is to coat the device with a layer of hydrophobic material followed by an oxygen plasma treatment, which roughens the surface of the coating material. The schematic for such process is depicted in Figure 3.1. Since ITO glasses are widely used as the substrates in many industrial applications, such as liquid crystal displays, touch panels, solar cells and microfluidic systems, ITO glasses have been used to mimic the device surface in these experiments [54–56]. In the first step of this process, a thin layer of fluoropolymer poly [tetrafluoroethylene-co-2,2-bis(trifluoromethyl)-4,5-difluoro-1,3-dioxole] (Teflon AF, DuPont) was spin coated on the ITO glass at 1000 rpm for 1 min. The thickness of the fluoropolymer was measured to be about 5 μm . The fluoropolymer covered ITO glass was then baked on a hot plate at 150.C for 30 min. After baking, the water contact angle was measured to be 120.. The water contact angle was measured by the sessile drop method where the image of a sessile drop on the sample surface was recorded from its edge through an optical microscope and the contact angle was evaluated from the image by a Dataphysics- SCA20 program. The superhydrophobic surface could be produced by using an oxygen plasma treatment (Oxford Plasmalab 80 Plus, 80W) with O₂ gas (20 sccm) at a total pressure of 25 mTorr.

3.2.2 Nanoimprint Process

An alternative approach to fabricate a superhydrophobic surface on a device is to utilize the nanoimprint technique to create nanostructures on the chip surfaces, which are coated with a thin film of hydrophobic materials. The fabrication scheme for a superhydrophobic surface using nanoimprint is illustrated in Figure 3.2 To conduct nanoimprint lithography, the first step is to fabricate the stamp for nanoimprint. Previously

[57–59], we demonstrated a simple technique to fabricate nanoimprint stamp by nanosphere lithography. In this process, a monodispersed polystyrene dispersion with 400 nm diameter beads (Bangs Laboratories, Inc., Fishers, IN) was used to produce self-assembled close packed two-dimensional colloidal crystals on a silicon wafer. These two-dimensional colloidal crystals were then used as the template to produce stamps for nanoimprint. To vary the surface fraction of the nanoimprint stamp, the size of the polystyrene beads was trimmed by oxygen plasma etching (Oxford Plasmalab 80 Plus, 50 W, 20 sccm O₂), which reduced the diameter of the polystyrene beads while keeping their separation distance unchanged. The diameter of the polystyrene beads could be changed from 400 nm to 200 nm. To fabricate nanoimprint stamp, a 50 nm thick chromium layer was deposited on top of the trimmed polystyrene beads. Then the polystyrene beads were dissolved in dichloromethane. A dry etching process was used to etch the silicon wafer in an RIE etcher (Oxford Plasmalab 80 Plus, 110 W, 45 sccm SF₆, 5 sccm O₂). After the dry etching process and removing chromium layer by CR-7 etchant, the silicon stamp (30 × 30 mm²) with periodic nanopores was obtained.

To create a superhydrophobic surface on the ITO glass by the nanoimprint process, a 1 μm thick layer of polymer (Teflon AF) was coated on the ITO glass. Then the nanoimprint stamp was pressed against the polymer coated ITO glass under 70 mbar pressure at 150°C for 30 min. After removing the stamp, nanostructures with desired dimension can be fabricated on the device surfaces.

3.3 Result and Discussion

3.3.1 Oxygen Plasma Treatment

It has been demonstrated that the oxygen plasma can be used to roughen the surface of Teflon to produce superhydrophobic surfaces [34]. The same concept has been modified in this experiment by using the fluoropolymer coating (Teflon AF), which can be easily

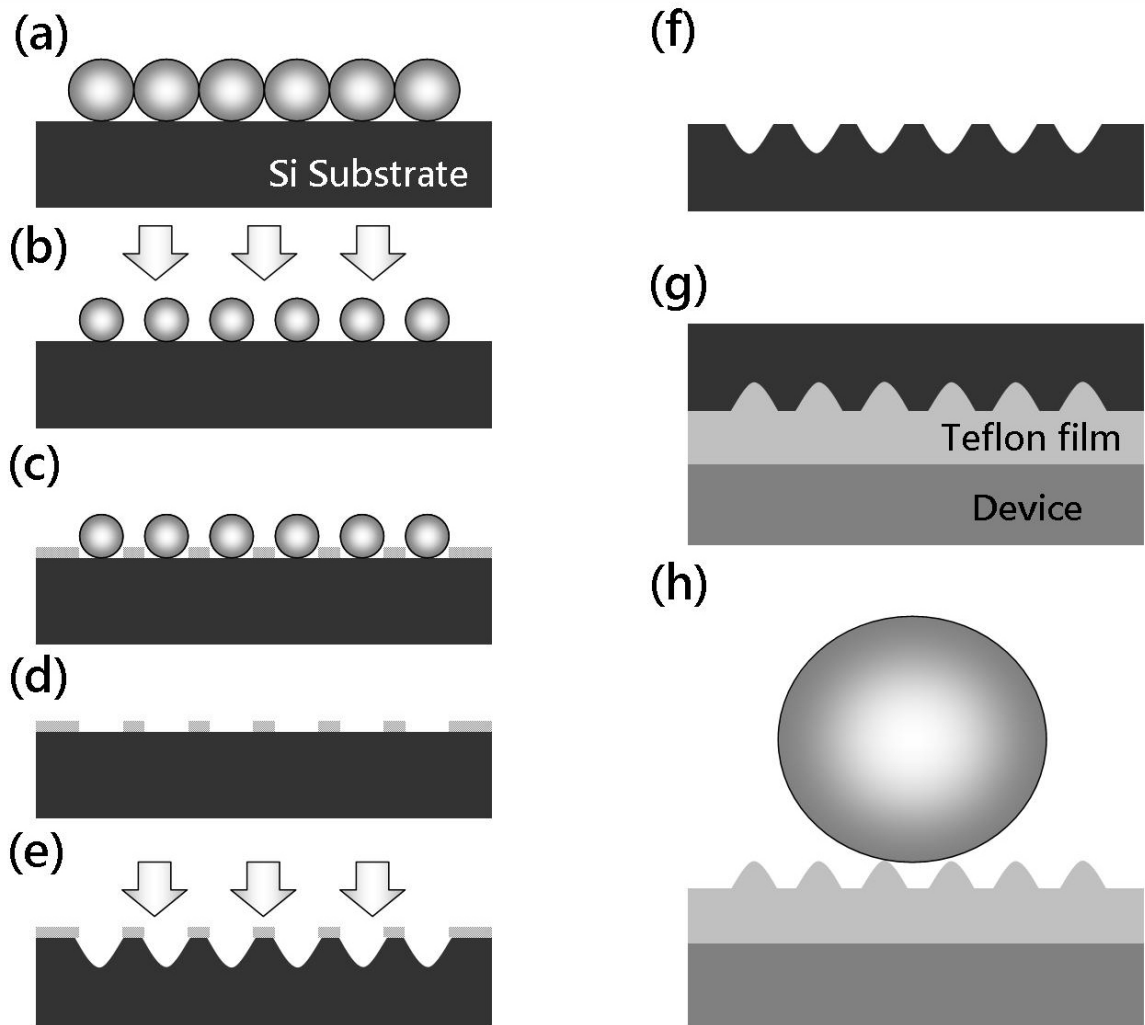


Figure 3.2 Schematic for creating a superhydrophobic coating on device surfaces using nanoimprint process. (a) The silicon substrate is coated with a single layer of well-ordered polystyrene beads. (b) Oxygen plasma is used to reduce the size of polystyrene beads. (c) A layer of chromium is coated on top of the polystyrene beads. (d) Polystyrene beads are then removed by CH_2Cl_2 solution. (e) The silicon wafer is etched by RIE. (f) The nanoimprint stamp is obtained by removing the chromium layer using CR-7 etchant. (g) The stamp is pressed against the device coated with fluoropolymer. (h) After removing the stamp from the device surface, nanostructure on the surface is obtained.

applied to device surfaces. Shown in Figure 3.3 are the SEM images of the fluoropolymer before and after 12 min of oxygen plasma treatment. As a result of oxygen plasma roughening, nanostructures with diameters in the range of 100 nm can be seen from the SEM images. Depending on the time of oxygen plasma treatment, the surface roughness increased from 0.5 nm to 35 nm, whereas

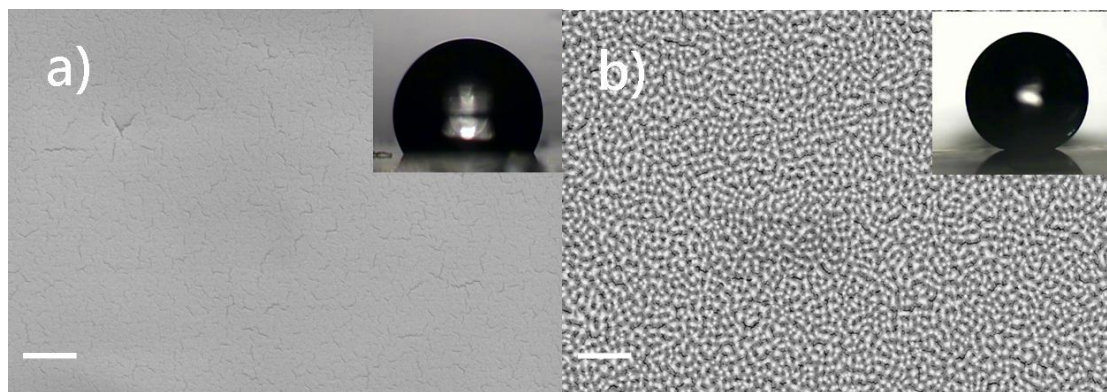
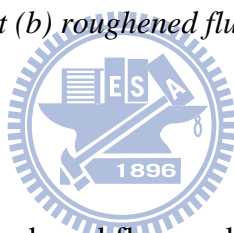


Figure 3.3 SEM images of (a) flat (b) roughened fluoropolymer surfaces. Inset: water droplets on both surfaces.



the water contact angle on the roughened fluoropolymer surface varied from 120° to 167° as depicted in Figure 3.4. In a word, the hydrophobicity of the surface can be tailored by controlling the oxygen plasma treatment time.

In some applications, it may be desirable to use thin film coatings other than fluoropolymer. However, the oxygen plasma treatment may change the surface chemistry of the coating materials. In the case of Teflon AF, the major effect of oxygen treatment is etching. No significant changes in peak shape and position were observed in the XPS spectra of the fluoropolymer (Figure 3.5) before and after oxygen plasma treatment. And the percentages of the XPS peak areas changed only slightly from 77% (F), 13% (C), 10% (O) for the flat fluoropolymer to 75.6% (F), 12.7% (C), 11.7% (O) for the roughened fluoropolymer (Figure 3.6).

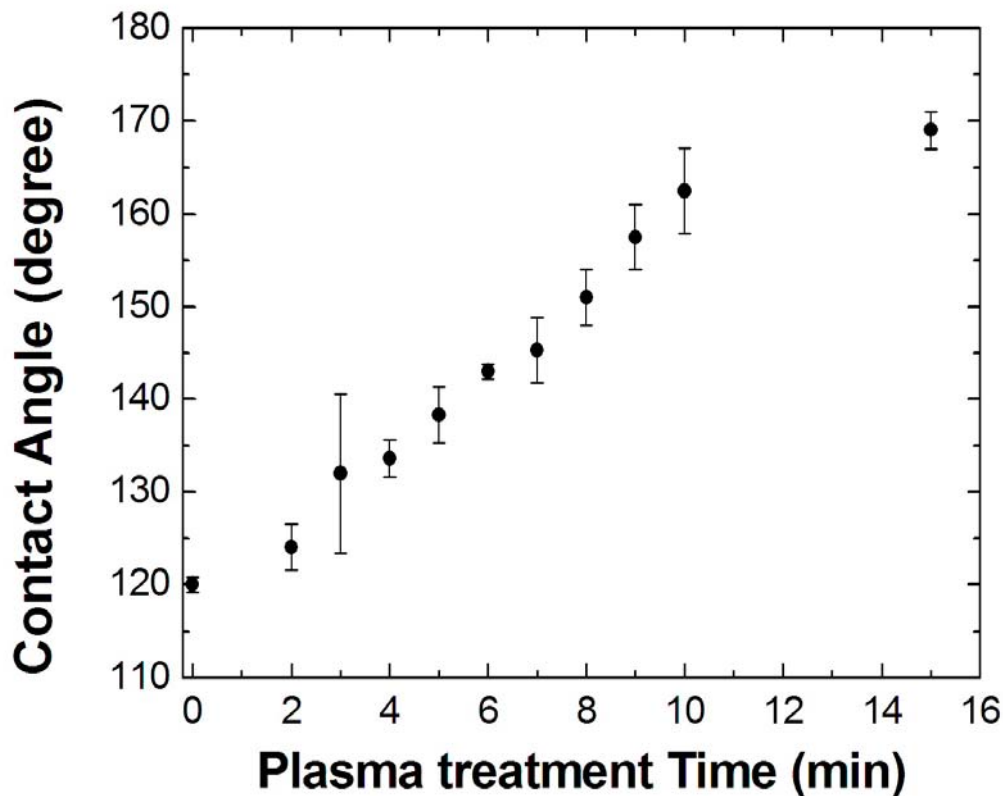


Figure 3.4 Water contact angle measured on the roughened fluoropolymer surface as a function of oxygen plasma treatment time.

No peak shift or additional peak was observed in the in the FTIR for the roughened fluoropolymer (Figure 3.7). However, if other types of coatings are used, such as SU8 photoresist, poly(dimethylsiloxane) (PDMS) or polyethylene, additional oxygen peaks in the XPS spectra were observed indicating that the surfaces had been chemically modified. In fact, the surfaces of the SU-8 photoresist and PDMS changed from hydrophobic to hydrophilic after the oxygen plasma treatment [52]. Therefore, the oxygen plasma roughening process may not be extended to other types of coatings.

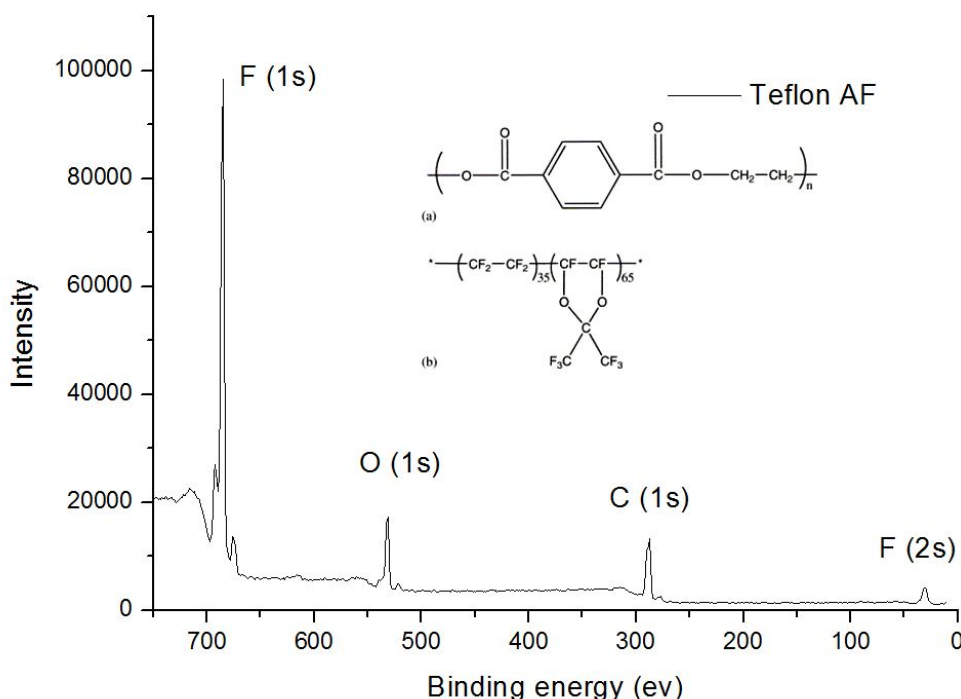


Figure 3.5 The XPS data of the fluoropolymer coating without oxygen plasma treatment.

3.3.2 Nanoimprint Process

In a previous experiment, we had utilized nanosphere lithography to create wellordered nanostructures with tunable hydrophobicity on the surface [59]. However, such process is not compatible with micro-fabrication process. We have modified this technique by transferring the pattern of nanostructure into the silicon stamp and the nanostructures can be replicated by nanoimprint process. In other experiments, we had demonstrated that it was possible to create nanoimprint stamp with different dimensions of nanostructures by a combination of nanosphere lithography and oxygen plasma etching [57, 58]. The silicon nanopillar arrays with different shapes and diameters have been obtained by this approach. Following the fabrication process described in the Experimental Section, arrays of nanopores with 200 nm diameter and 300 nm in depth were created as shown in Figure 3.8. To prepare a superhydrophobic coating on the device, the device was first coated with a layer of hydrophobic polymer (Teflon AF in this case). Then the stamp was pressed against the device for 30 min. After removing the stamp, a layer of nanostructure on the surface was obtained. Figure 3.9 shows SEM image of the imprinted

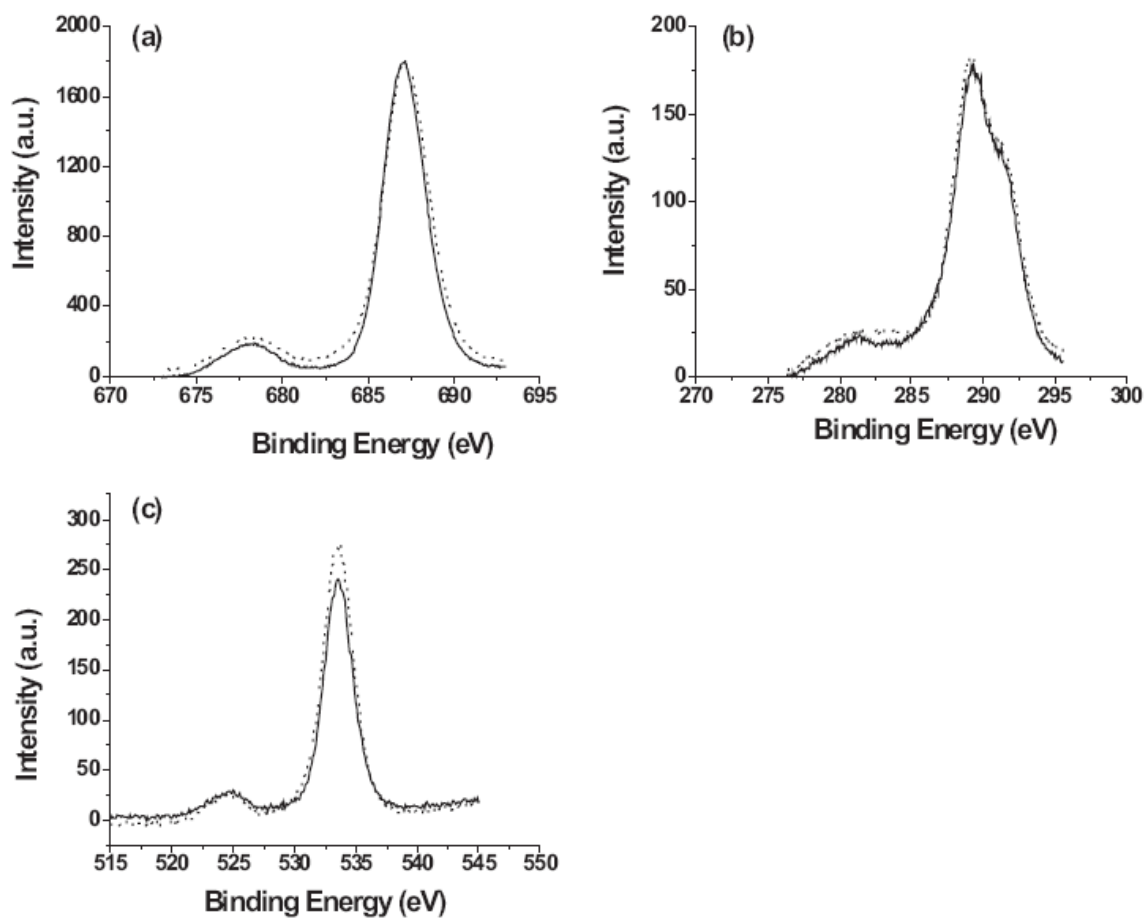


Figure 3.6 The XPS spectra of a) F (1s), b) C (1s), c) O (1s) peaks for both the flat Teflon AF (solid line) and the roughened Teflon AF after 10 min of oxygen plasma treatment (dotted line).

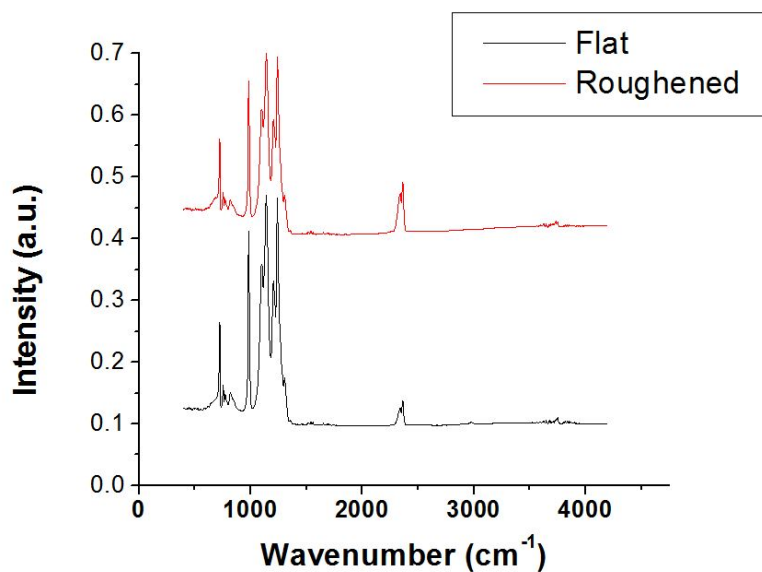


Figure 3.7 FTIR spectra of the flat (black) and roughened (red) Teflon AF.

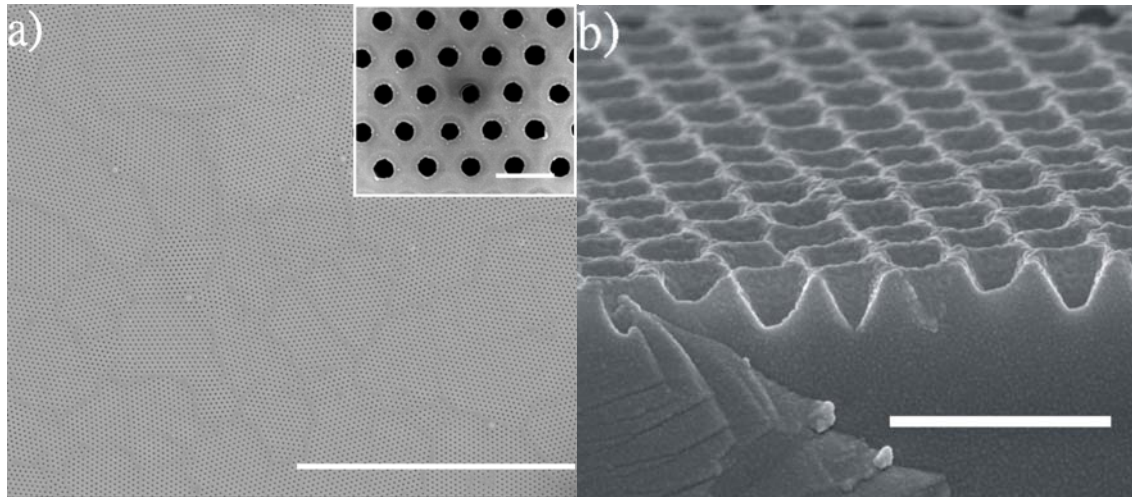


Figure 3.8 SEM images of the nanoimprint stamp created by nanosphere lithography. (a) Dissolve nanosphere after deposit layer of metal(Cr) 50nm, br: 2 μm ; inset bar: 500 nm; (b) Silicon nanomold, bar: 1 μm , the angle of SEM view: 60°.

nanostructures on the ITO glass surface. A water contact angle up to 168. was obtained by this approach. Both approaches described here can be used to create superhydrophobic coatings on the device. The advantage of the oxygen plasma is the ease in the fabrication process. However, the oxygen plasma treatment often introduces chemical modification on the surface. For example, the PDMS surface could be changed to hydrophilic after oxygen plasma etching due to the formation of OH. groups on the surface. On the other hand, there is no chemical modification on the surface in the nanoimprint process. Therefore, the nanoimprint process can be extended to all types of hydrophobic coatings.

3.4 Conclusion

In summary, we have developed two techniques to impart superhydrophobic property to the surfaces of devices. In the first approach, oxygen plasma treatment was used to roughen the Teflon coating whose surface water contact angle could be tuned from

120° to 168° by varying the oxygen plasma treatment time. However, the application of the oxygen plasma process is limited to fluoropolymers. In the second approach, nanoimprint process was used to create nanostructures on the device surfaces where the water contact angle as high as 167° was obtained. In principle, the nanoimprint process can be applied to all types of hydrophobic coatings.

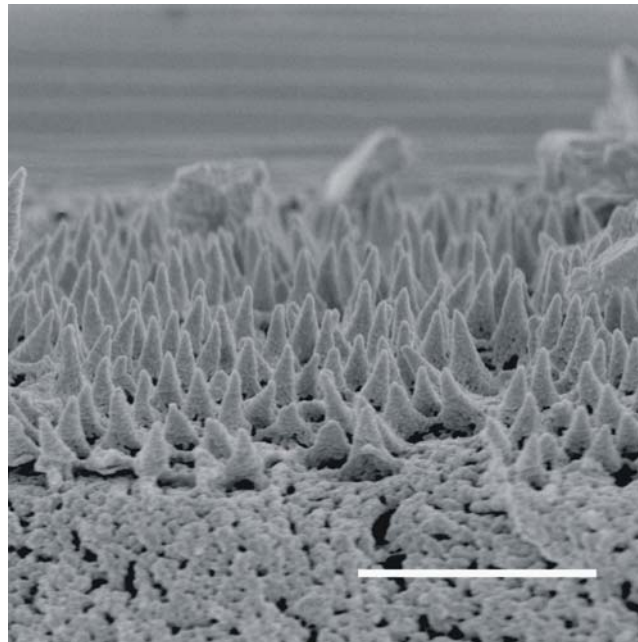
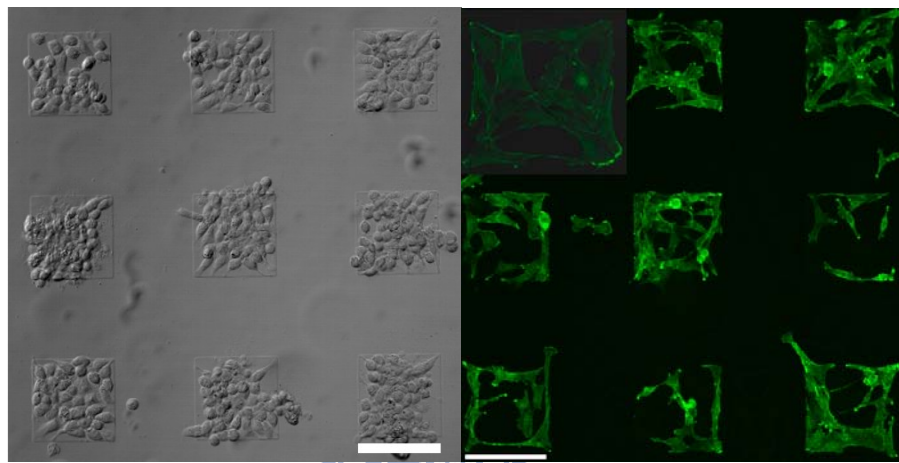


Figure 3.9 SEM image of the imprinted nanostructure on the ITO glass surface. Bar: 1.5 μm , the angle of SEM view: 60°.

Chapter 4

Observation of Enhanced Cell Adhesion and Transfection Efficiency on the Superhydrophobic Surfaces



The patterned nanostructure fluoropolymer surfaces were used for the study of the cell adhesion. By a combination of photolithography and oxygen plasma treatment, patterned fluoropolymer surfaces with various roughnesses have been obtain. The water contact angles measured on the surface were range from 120° to 163° , and surface roughness was measured from 2 nm to 65 nm. When these pattern surfaces were used as the substrates for the cell cultures of HeLa, NIH3T3, and CHO cells, it was found that those cell lines did not adhere to the flat fluoropolymer surfaces. However, the number of NIH3T3 and CHO cells adhered on the surfaces increase with the surface roughness. Such nanostructure materials could be used the scaffold for selected cell growth. In conclusion, we report a surprising observation of enhanced cell adhesion and transfection efficiency on the patterned superhydrophobic surfaces, which could be used as cell microarrays.

4.1 Introduction

Ever since the discovery of the importance of the surface roughness to the water repellent behavior of plant leaves, [60] material scientists have developed various strategies [62] to produce the so-called “superhydrophobic surfaces”, whose water contact angles are larger than 150° . It is generally believed that the water repellent properties of the superhydrophobic materials could reduce the water contact area on the surfaces, therefore, minimizing the adsorption of particles or molecules. In the past few years, several potential applications of the superhydrophobic surfaces have been identified including coatings for self-cleaning, fog condensation, contamination reduction, oxidation reduction, oil water separation, and rapid water spreading. [62] However, there are very limited research activities in exploring the possibility of using the superhydrophobic materials for biological applications. The reduced contact area between the solution and surface may minimize the adsorption of biomolecules, therefore, improving the protein resistance on the superhydrophobic surface. It has been shown that the short-term protein resistance on the superhydrophobic surfaces was very similar to the poly (ethylene glycol) (PEG) surfaces, a well-known protein resistance coating, allowing the selective deposition of proteins on the patterned superhydrophobic surfaces. [63] The bioanalytical readout in the protein microarrays fabricated on the superhydrophobic surfaces have been greatly improved owing to the reduced protein adsorption on the superhydrophobic surfaces.[64] It was also shown that the superhydrophobic surfaces could suppress the protein adsorption and promote the flow-induced protein detachment in the microfluidic system.[65] The adhesion of the blood cells was found to be minimized on the superhydrophobic surfaces.[66] Here we report a surprising observation of enhanced cell adhesion and transfection efficiency on the patterned superhydrophobic surfaces, which could be used as cell microarrays.

One of the great challenges in material science is to engineer the surfaces of substrates or devices to regulate the spatial and the temporal behavior of living cells while maintaining their functions.[67] Most of the normal cells need to adhere on the surfaces to proliferate. In vivo, cells are bound to the extracellular matrix (ECM) within tissues. [68] In the cell culture, cells are immobilized to the substrate surfaces through ECM proteins. Therefore, it is very important to investigate the cell-substrate interactions, which is essential to the understanding of biocompatibility, cell culture, cell spreading and tissue engineering. It is recognized that the adhesion of cells on materials depends on the surface characteristics such as wettability, surface charge, surface chemistry, chirality and roughness. [69] Among them, surface wettability is known to be a key factor to the non-specific protein adsorption. It is known that proteins could adsorb rapidly on the hydrophobic surfaces through non-polar interactions while hydrophilic surfaces are less susceptible to the non-specific protein adsorption.[68] Some hydrophilic surfaces, such as PEG modified surfaces, which could bind strongly to the water molecules, have been engineered to resist the protein adsorption. On the other hand, protein adsorption on the hydrophobic surfaces often leads to conformational changes, unfolding or denature of proteins, therefore, permanently contaminating the surfaces. The situation is somewhat different on the superhydrophobic surface. Because the contact between solution and surface is greatly reduced by the surface nanostructures, the protein adsorption was observed to be minimized on such surface for short time.[63] However, as the proteins adsorb on the surface nanostructures, the surface wettability would be changed and the protein adsorption would be accelerated. Since the superhydrophobic surfaces are composed of nanostructures, their surface areas are much larger than the flat surfaces. Therefore, we expect the superhydrophobic surfaces could accumulate more proteins than the flat surfaces of the same materials, if the contact time with the solution is increased.

4.2 Experimental Section

4.2.1 Fabrication of superhydrophobic arrays

To prepare a superhydrophobic surface, the approach was used the same with description of chapter 2, which thin layer of fluoropolymer poly[tetrafluoroethylene-co-2,2-bis(trifluoromethyl)-4,5-difluoro-1,3-dioxole] (Teflon, AF, DuPont) was spin-coated on a cover slip at 3000 rpm for 1 min (Figure 4.1A). The thickness of the fluoropolymer was measured to be about 5 μm . The fluoropolymer coated cover slip was then baked on a hot plate at 110⁰ for 30 min. After these processes, the water contact angle measured on the fluoropolymer was about 120⁰. A fluoropolymer surface were then roughened by oxygen plasma treatment (Oxford Plasmalab 80 Plus, 80W) with a gas O₂ (2 sccm) at a total pressure of 25 mTorr. The water contact angles on the roughened fluoropolymer surfaces were measured to be 123⁰, 135⁰, 142⁰, 148⁰, 158⁰, 163⁰ for 2, 4, 6, 8, 10 and 12 minutes of oxygen treatment whereas the surface roughness for these surfaces were 10, 25, 35, 42, 52 nm and 65 nm, respectively. For the cell culture, the chip was designed to have two different roughness states on the same surface (Inside pattern: different rough surface; Outside pattern: flat surface). First, a layer of photoresist (S1813, Shipley) was spun on top of the fluoropolymer and a photolithographic process was used to define the superhydrophobic area (200 \times 200 μm) on the photoresist (Figure 4.1B). The superhydrophobic microarray was manufactured using oxygen plasma treatment (Oxford Plasmalab 80 Plus, 80 W) with O₂ gas (2 sccm) at a total pressure of 25 mTorr. After plasma treatment the photoresist was removed by washing the surface with acetone. Only the areas exposed to the oxygen plasma exhibited the superhydrophobic behavior (Figure 4.1C and D). For cell incubation, the chip was formed as a chamber which was stuck a plastic tube on the top and the area was about 1 cm (Figure 4.1E).

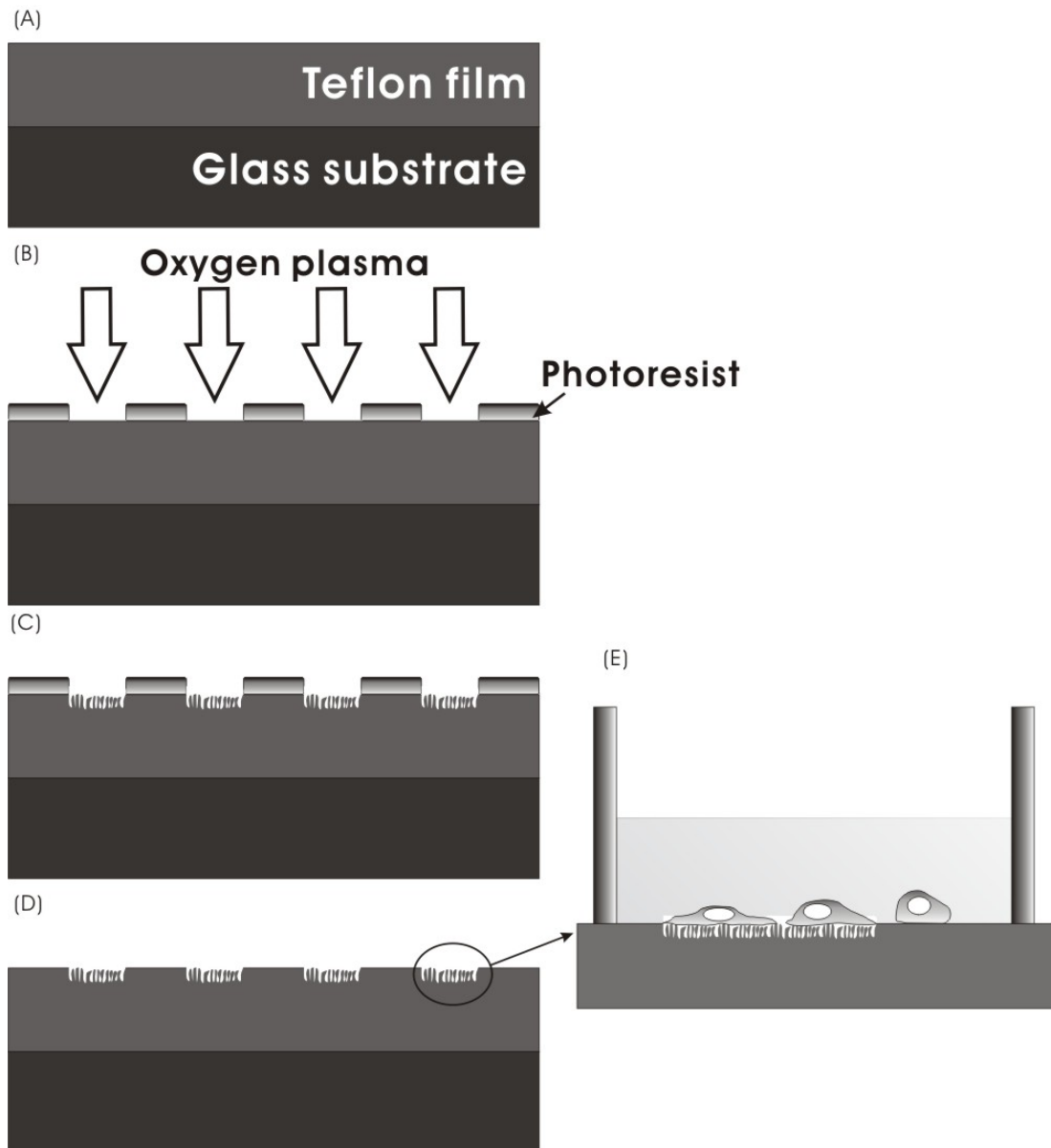
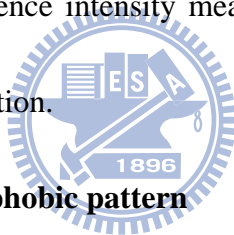


Figure 4.1 Patterning process for switchable superhydrophobic surfaces: A) the fluoropolymer was coated on glass substrate. B) A layer of patterned photoresist was used as the mask for the oxygen plasma treatment. C) After oxygen plasma treatment, the unprotected area was roughened. D) The superhydrophobic microarray was obtained by removing the photoresist. E) The cell was cultured on superhydrophobic microarray.

4.2.2 Protein absorption with different different surface

To measure the amount of the fibronectin adsorbed on the superhydrophobic surfaces, roughened fluoropolymers with a water contact angle of 163° was used in this experiment. Clean glasses, PEG glasses (Microsurfaces, Inc), and flat fluoropolymers were used as the control. These substrates were dipped into solution containing $50\mu\text{g/ml}$ fibronectin conjugated with Oregon Green (Invitrogen) for a given amount of time and washed by PBS buffer solution before the fluorescence measurement. The fluorescence of intensity was measured by a fluorescence microscopy (IX 71, Olympus). All fluorescence intensities were normalized to the fluorescence intensity measured on a flat glass after 6 hours of incubation in the fibronectin solution.



4.2.3 Cell Culture on superhydrophobic pattern

For the cell adhesion measurement, the patterned superhydrophobic surfaces were prepared on the cover slips. The detail procedure for preparing the patterned superhydrophobic surfaces can be found in a previous publication. [63] The dimension for each pattern was $200\ \mu\text{m} \times 200\ \mu\text{m}$. Three cell lines, NIH 3T3, CHO and HeLa, were seeded on the patterned superhydrophobic surfaces and placed on a confocal microscope (Fluoview 1000, Olympus) equipped with an incubator (MIU-IBC-IF, Olympus) at 37°C and $5\% \text{CO}_2$ for 6 hours. The density of the cells was about 10^5 cell/ml. To count the number of cell attached to the patterned area, the suspension cells were removed by PBS

solution and the DIC image was taken at each condition.

4.2.4 Transfection of Cell

For the transfection experiment, PolyFect (Qiagen) was used as a transfection reagent and the Kaede fluorescence protein expression vector (PKaede-MC1, MBL International), which can express a fluorescence protein Kaede, was used. To conduct transfection, the CHO cells were cultured on the patterned superhydrophobic surfaces at 37°C for 6 hours. After washing the suspension cells with PBS solution, the PolyFect mixed with plasmid DNA was introduced at room temperature for 10 minutes. The fluorescence images were monitored during the expression process on a confocal microscope (Fluoview 1000, Olympus).



4.3 Result and Discussion

4.3.1 Water Contact Angle and Surface Roughness Measurement

In oxygen plasma process, the roughness of the fluoropolymer was higher by increasing etching time. The surface topography and roughness were measured by commercial AFM (VEECO Innova SPM), stored with a standard silicon tip (Budget sensor) on the cantilever, scanned with tapping mode. The resonance frequency of the cantilever was 300 kHz. The topography of the flat and rough Teflon were measured in area 5×5 μm. Figure 4.2a was shown the top view of fluoropolymer coating without any plasma etching and Figure 4.2b was roughed by oxygen plasma for 12 minute. Root mean square (RMS) was measured on areas of 50 μm×50 μm by AFM and the water contact angle was measured by homemade instrument and calculated by Dataphysics-SCA20 program. The way of the measurement was that the image of a sessile drop on the fluoropolymer surface

was taken image by digital camera from its edge so-called ‘sessile drop method’. The Dataphysics-SCA20 program was auto-fix the contract of the drop image and measure the water contact angle. The water contact angles on the roughened fluoropolymer surfaces were measured to be 123°, 135°, 142°, 148°, 158°,163° for 2, 4, 6, 8,10 and 12 minutes of oxygen treatment whereas the surface roughness for these surfaces were 10, 25, 35, 42, 52 nm and 65 nm, respectively (Figure 4.3 and 4.4).

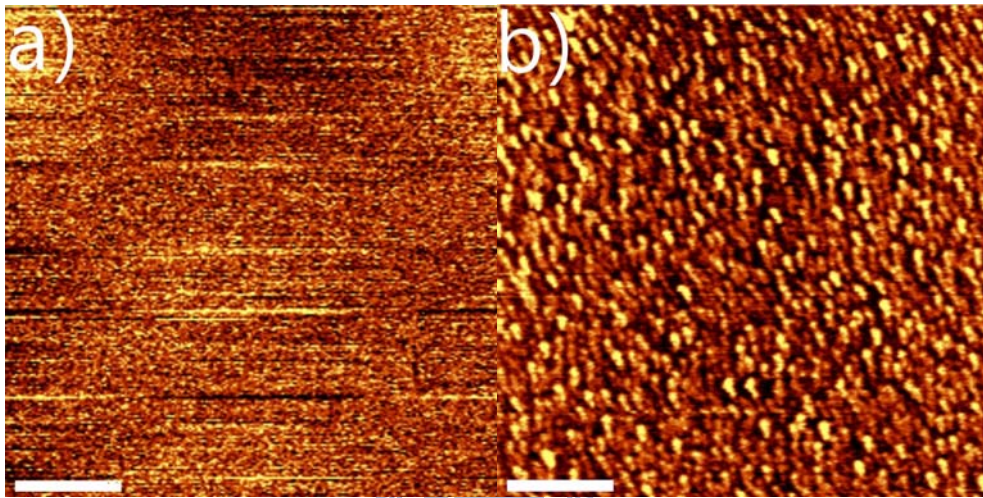


Figure 4.2 The AFM images of (a) flat and (b) roughened Teflon AF. Bar: 1 μ m. (Measured by VEECO Innova SPM)

4.3.2 Counting Cell Number on Pattern Surface

To realize the behavior of the cell attachment on various roughness surface, the cell will first culture on micro-pattern chip for 6 hours then take the DIC image by confocal microscopy. It has been counted that the number of the cell between inside and outside pattern area where combine 9 square pattern and total area keep in 1 mm². Fig is shown that the optical image of the HeLa cell growth on roughness micro-pattern arrays by etching time 12 minute. The result is shown that the number of the cell inside pattern is more than outside area. In a word, HeLa cell prefers to stay in the roughness surface more than flat surface. For serious analysis, the HeLa cell has been cultured in different

roughness chip by different etching

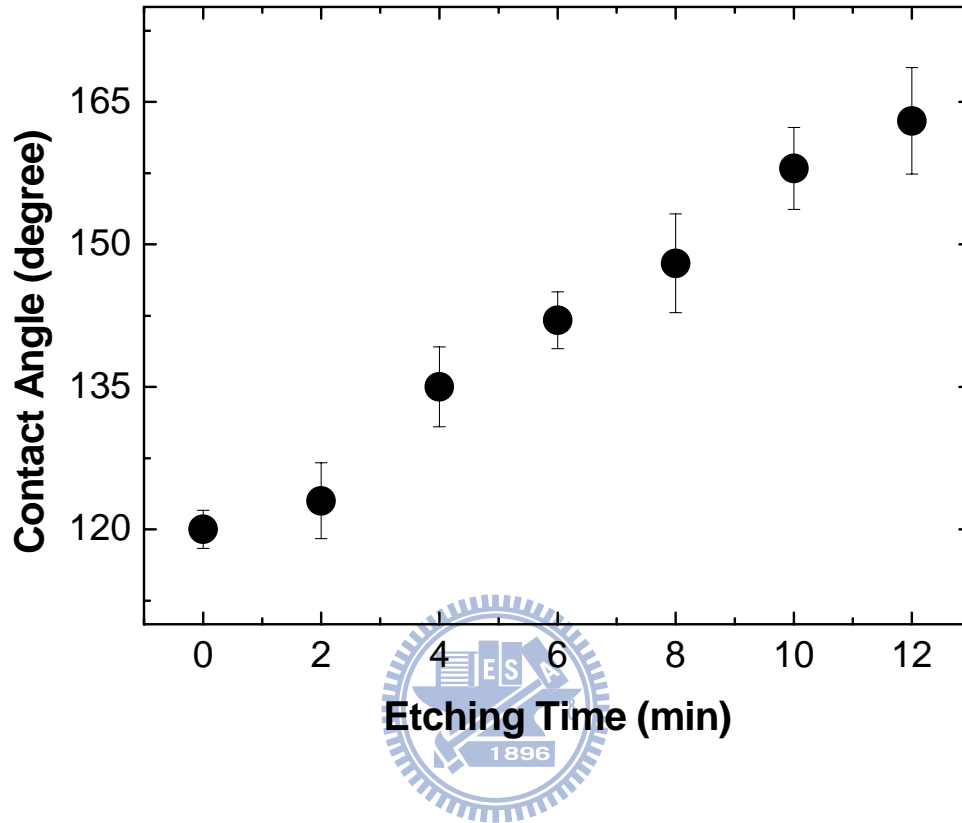


Figure 4.3 The contact angles on the roughened Teflon AF surfaces as a function of etching time.

time and the result is shown in fig. With the increasing time of the etching, the number of the HeLa cell inside pattern increased from 170 to 630 and outside area increased from 50 to 210. In NIH 3T3 and CHO cell case, there are conspicuously increased in the number on inside pattern and without increased in outside pattern. Considering the PC12 cell, there is abnormal distribution in the number of cell on different roughness area. Therefore, we concluded that HeLa cell has preferred to grow on the roughness surface with increasing time of the oxygen plasma treatment, but also increased in flat surface. Comparing NIH 3T3 and CHO cell, they both have particularly selected to attach on more roughness

surface. In general, the size of the cell in suspension is similar but the size of fibroblast (NIH 3T3) are larger and the number is less than epithelium (CHO) cell in etching time 12 minute chip. It is meaning that the fibroblast has well attachment on roughness surface.

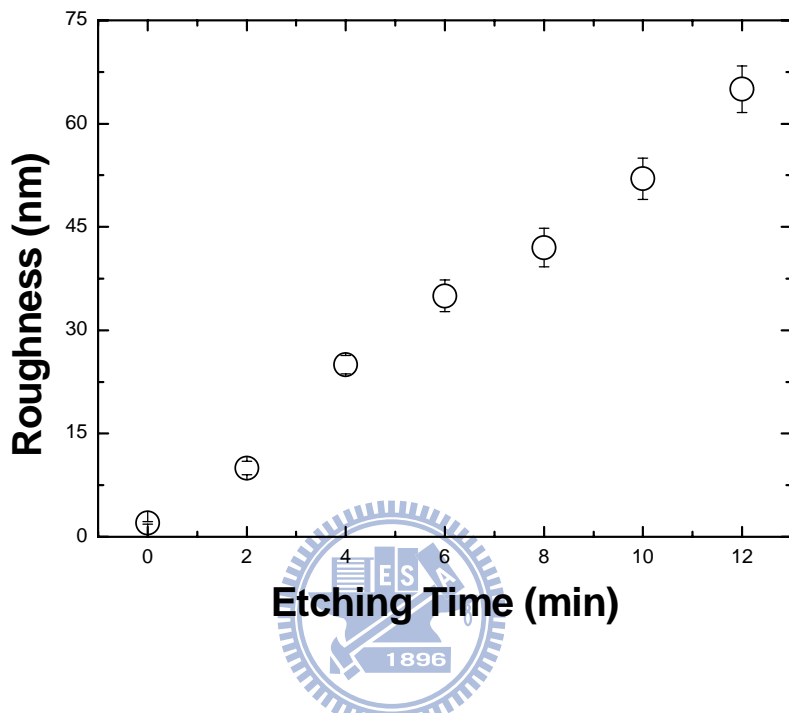


Figure 4.4 The surface roughness on the roughened Teflon AF surfaces as a function of etching time. (Measured by VEECO Innova SPM)

4.3.3 Protein Absorption Analysis

To test how proteins adsorb on the superhydrophobic surfaces, I have investigated the adsorption of a fluorescence dye labeled fibronectin, an ECM protein, on the superhydrophobic surfaces, which were fabricated by roughening thin films of fluoropolymers (Teflon AF, DuPont) using oxygen plasma. It has been demonstrated that the oxygen plasma treated fluoropolymers could exhibit superhydrophobic behaviors without altering the surface chemistry of the fluoropolymers. [63] The detail characterization of the oxygen plasma treated fluoropolymers can be found in a previous publication.[63] The water contact angle and the surface roughness of the roughened

fluoropolymers used in this experiment were measured to be 163 ± 5.6^0 and 65 ± 3.4 nm, respectively. The amounts of fibronectins adsorbed on different surfaces were measured through the fluorescence intensity, which is plotted in Figure 4.5 as a function of solution contact time. In the first thirty minutes, the protein resistance of the superhydrophobic surface was very similar to the PEG surfaces whereas substantial amounts of fibronectins were found to adsorb on the flat fluoropolymers within the same period of time. However, when the fibronectin solution stayed on the superhydrophobic surfaces for more than one hour, the accumulation of fibronectin molecules on the superhydrophobic surfaces became evident and eventually surpassed those adsorbed on the flat fluoropolymers. It should be noted that very little amount of fibronectins was observed on the PEG modified surfaces at all time. This result is not surprising since the superhydrophobic surfaces were made of hydrophobic materials with surface nanostructures. In a superhydrophobic surface, the protein solution stays on the top of the surface nanostructures with air bubbles trapped underneath. The protein adsorption is minimized in short term due to the reduced solution contact area on the surfaces. However, as more and more proteins adsorbed on the top of nanostructures, the surface wettability would be altered and the protein solution could slowly fill in the nanostructures (a Wenzel state). [70] Since the Wenzel model predicts that the surface nanostructures enhance the changes in wettability, [63] the protein adsorption on the superhydrophobic surface would accelerate the wetting process and results in increase in protein adsorption. Similar time-dependent adsorption behavior on the roughened fluoropolymers was also observed for other proteins.

The result shown in Figure 4.5 suggested that the superhydrophobic surface could be used as the protein resistance coating as long as the protein solution is removed in short time as those demonstrated in the protein array applications. [63] When the contact time with the protein solution is increased, the superhydrophobic surface can accumulate more fibronectin molecules than the flat surface made of the same materials, which may be used

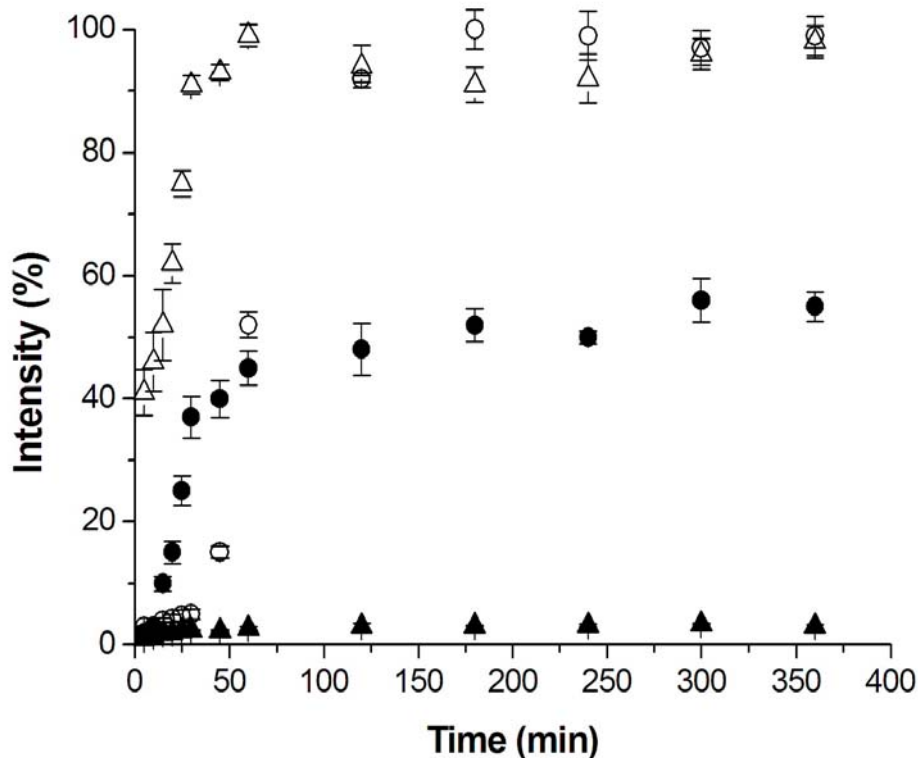


Figure 4.5 The fluorescence intensity of the dye conjugated fibronectins on various surfaces as a function of solution contact time. Open triangles: glass surfaces. Close triangles: PEG presenting surfaces. Open circles: roughened fluoropolymers with a contact angle of 163° . Close circles: flat fluoropolymers

to regulate the adhesion of cells on the surfaces. In the past two decades, a lot of surface modification schemes have been proposed to promote the adhesion of cells on the surfaces. Most of them rely on self-assembly monolayers or polymers that provide ligands for cell adhesion.[71] One of the most commonly used approaches to regulate the spatial arrangement of cells on the surface is to employ the micro-contact printing [72] where ECM molecules such as fibronectins, vitronectin and collagens are first patterned on the surfaces. Then the adhesion of cells could be guided through the binding to these ECM molecules. Since the superhydrophobic surfaces can accumulate more ECM molecules than the flat surfaces, we can fabricate the patterned superhydrophobic surfaces where the

concentration of ECM molecules can be modulated spatially, which can be used to guide the growth of cells. To fabricate the patterned superhydrophobic surfaces, a standard photolithography was used to create patterns on the photoresist over the fluoropolymers. After subsequent development and oxygen treatment, the patterned superhydrophobic surfaces have been obtained. These patterned superhydrophobic surfaces were used as the substrates in the cell cultures. Three cell lines, NIH 3T3, CHO and HeLa, were cultured on the patterned superhydrophobic surfaces for 6 hours. The results are depicted in Figure 4.6 where all three tested cell lines were found to adhere preferentially on the roughened area. For the adherent cells such as NIH 3T3 and CHO cells, the cells adhered mostly on the roughened area. However, the effect of the selective growth on the patterned superhydrophobic surfaces was not so prominent for HeLa cells, which can grow in the suspension. To understand the origin of the preferential growth of cells on the patterned superhydrophobic surfaces, time-lapse DIC images of the cells on the patterned superhydrophobic surfaces were recorded as shown in Figure 4.7. The cells were observed to be randomly distributed on the surfaces when the cells were first seeded. However, more and more cells were found to migrate toward the roughened area during the incubation. After 3 hours of incubation, most cells were found inside the roughened area. When the patterned surfaces were washed with PBS solution, the weakly adhered cells were removed as shown in Figure 4e. Since the cells prefer to stay on the more adhesive surfaces, the preferential growth of the cells on the roughened area can be attributed to the accumulation of more ECM molecules from the serum containing growth medium in the roughened area.

To further explore the relationship between the number of the adhered cells and the surface roughness, we have investigated the cell adhesion on the roughened fluoropolymers with surface roughness ranging from 2 nm to 65 nm, and the corresponding water contact angle from 120° to 163° . Shown in Figure 4.8 are the averaged number of cells adhered on

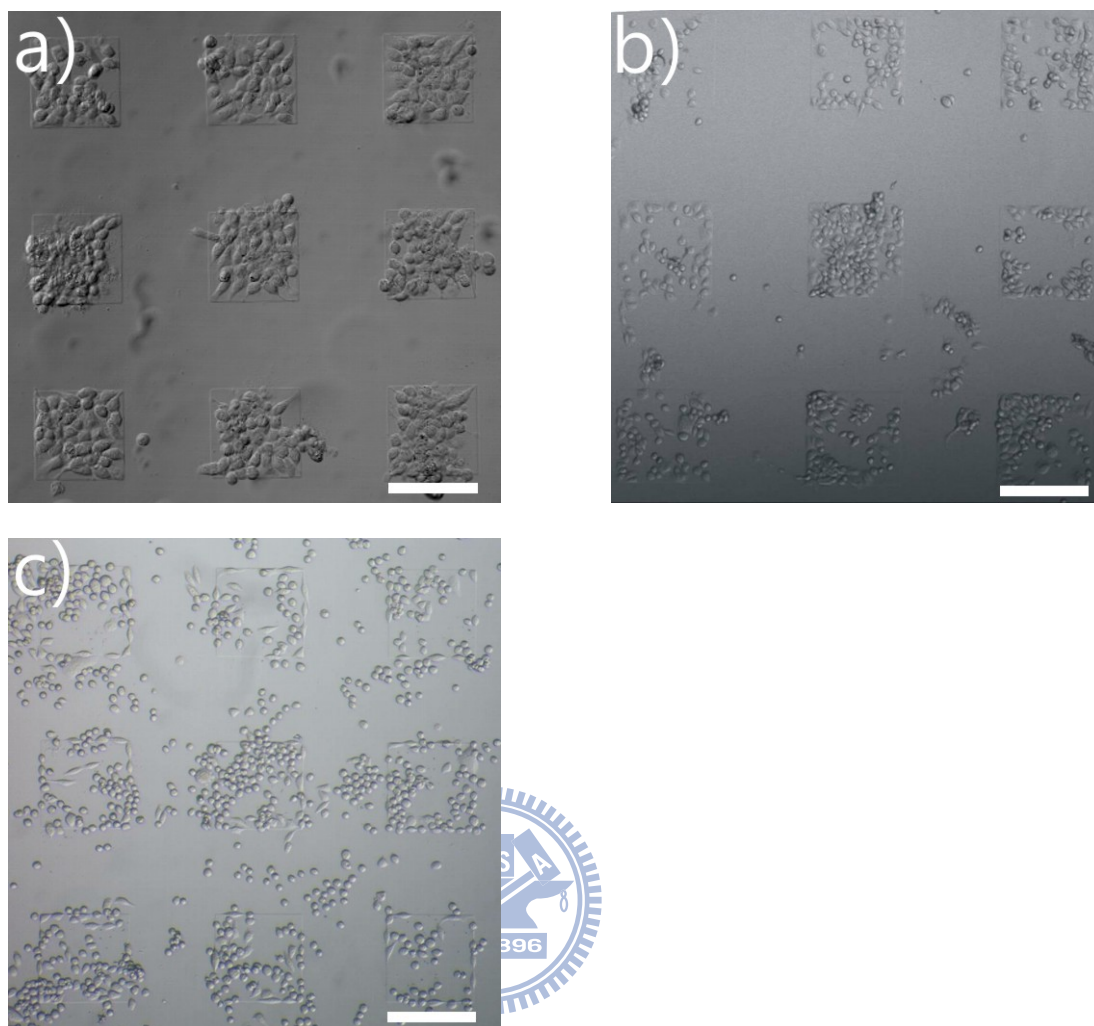


Figure 4.6 The DIC images of (a) NIH 3T3 (b) CHO and (c) HeLa cells on the patterned superhydrophobic surfaces after 6 hours of incubation. Bar: 200 μm.

various roughened fluoropolymers for three cell lines. It can be seen that very little amount of cells could adhere on the flat fluoropolymer. However, the number of cells attached to the roughened fluoropolymer increased as the surface roughness increased. When the surface was in the superhydrophobic state (larger than 150°), the number of cells attached to the roughened surfaces surpassed the surface coated with collagens. No measurable cytotoxicity was observed for the cells grown on the superhydrophobic surfaces over seven days. In another word, the biocompatibility of the fluoropolymers has been improved by converting them into the superhydrophobic surfaces. Our result was different

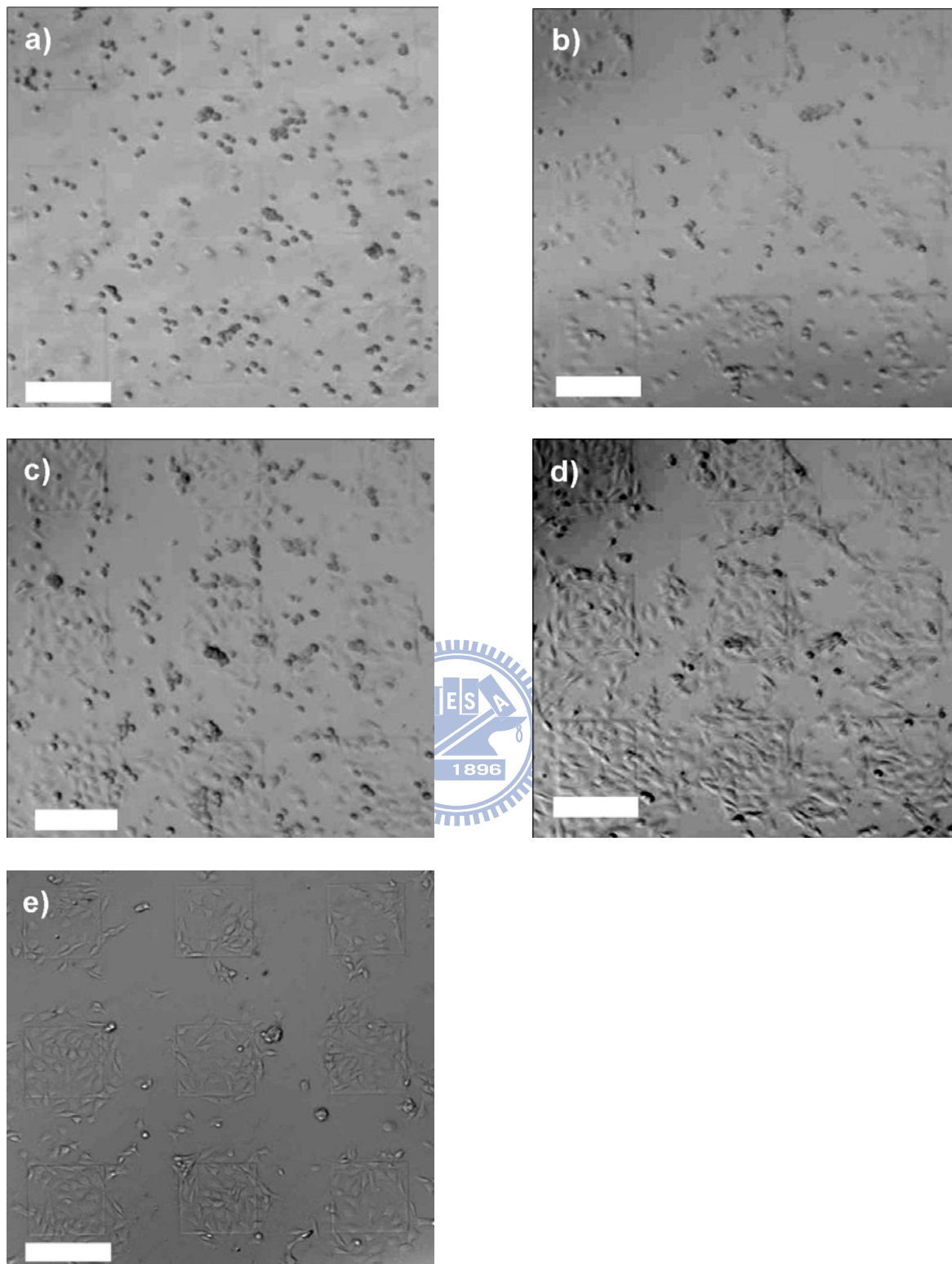


Figure 4.7 The time-lapse DIC images of NIH 3T3 cells on the patterned superhydrophobic surfaces after a) 0 minute, b) 50 minutes c) 100 minutes d) 3 hours of incubation. e) After washing the sample with PBS solution. Bar: 200 μm .

from the rough poly (L-lactic acid) (PLLA) surfaces where no cells were observed to adhere on the superhydrophobic PLLA surfaces.[73] Only when the rough PLLA surfaces were treated with Ar plasma, significant amount of cell adhesion was observed. The difference between these two experiments may be attributed to different cell lines used in the experiment. It is known that the adhesion behavior of different cells can be quite different.

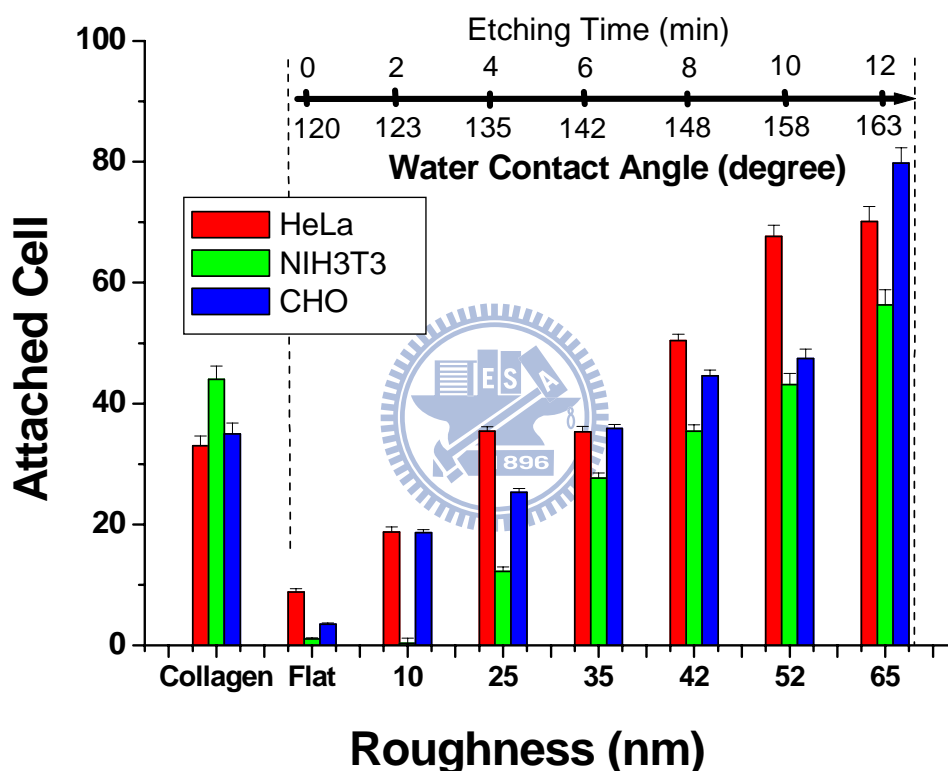


Figure 4.8 The averaged cell number attached on the roughened fluoropolymer surfaces as a function of water contact angle. The patterned area is 200 μm x 200 μm . The collagen coated glass and flat fluoropolymer were used as controls.

Since the spatial distribution of cells on the patterned superhydrophobic surfaces can be regulated, the patterned superhydrophobic surfaces may be used to produce cell

microarray. Cell microarrays have been used to investigate the expression of genes and the

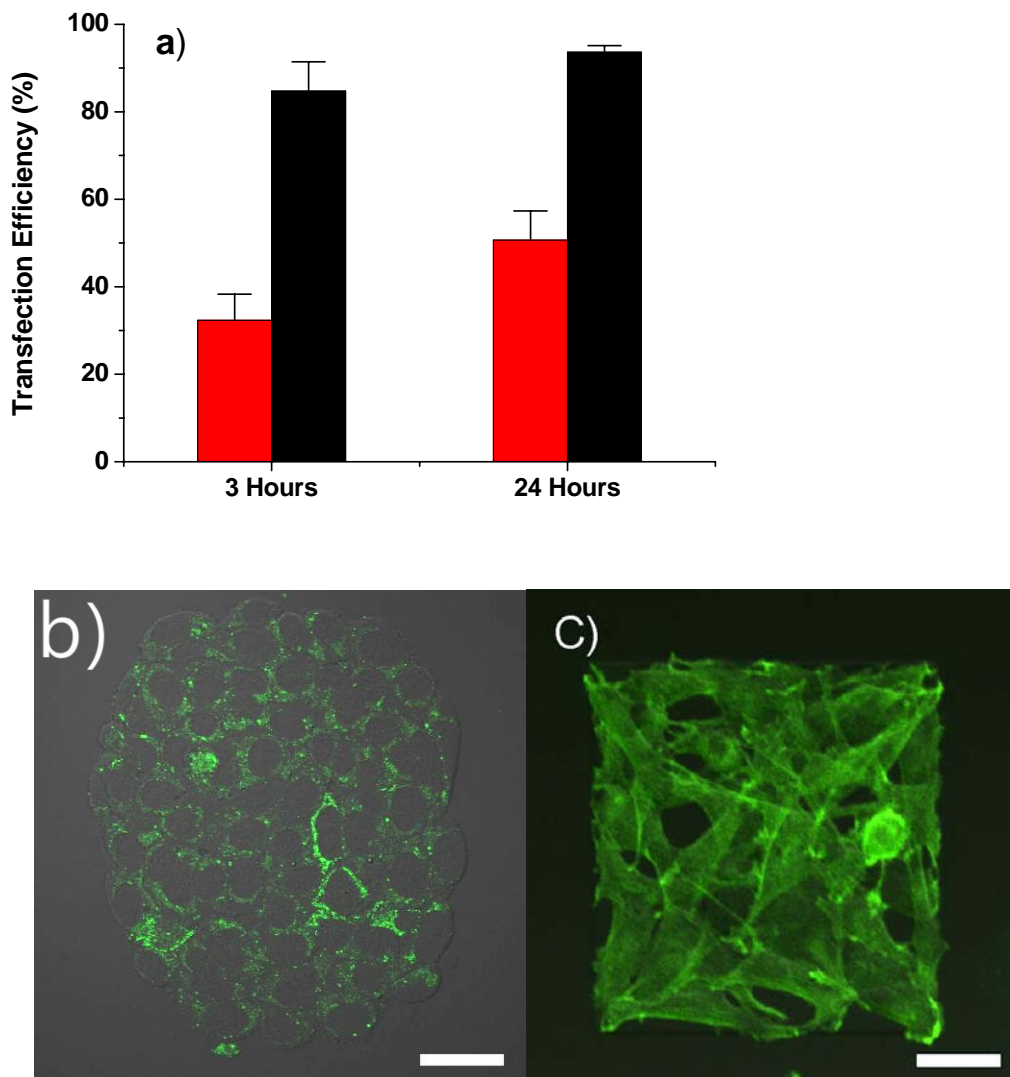


Figure 4.9 a) Transfection efficiency measured for the CHO cells on the poly D-lysine (red) and superhydrophobic surface (black). b) The CHO cells on the patterned superhydrophobic surfaces transfected with fluorescence proteins, Kaede. Bar 50 μm . (c) The NIH 3T3 cells on the patterned superhydrophobic surfaces transfected with fluorescence proteins, GFP-actin. Bar 50 μm

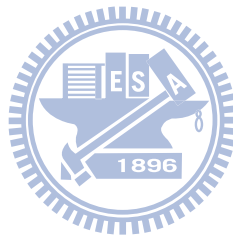
function of proteins in living cells where the native environments could facilitate correct biomolecular reactions. [74] However, the cell microarray technology is still far from mature. There are several challenges needed to be overcome including the improvement of

cell adhesion and transfection efficiency, and colony separation.[75] On the patterned superhydrophobic surfaces, we have shown that the adhesion have been improved and the cell colonies were already separated by their spatial patterns. The only question remained for using the patterned superhydrophobic surfaces as the cell microarrays is the transfection efficiency for the cells grown on such surfaces. To test the transfection efficiency of the cells on the patterned superhydrophobic surfaces, CHO cells were transfected by a commercial fluorescence protein construct PKaede-MC1, which can be used to express a fluoresce protein, Kaede, in the cells. The CHO cells on the poly D-lysine coated culture dish were used as the control. Figure 4.9a summarizes the transfection efficiency measured on both surfaces after 3 hours and 24 hours of transfection. It can be clearly seen that the transfection efficiency on the patterned superhydrophobic surfaces were much higher than those measured on the normal culture dishes in short time. After 24 hour of transfection, all CHO cells on the patterned superhydrophobic surfaces exhibited fluorescence indicating 100% transfection efficiency on such surface (Figure 4.9b).The enhanced observed transfection efficiency may be attributed to the surface nanostructures. It has been suggested that the surface nanostructures may help to retain the cells therefore, the gene delivery. [76] Similar result was also observed for the NIH 3T3 cells as shown in Figure 4.9c.

4.4 Conclusions

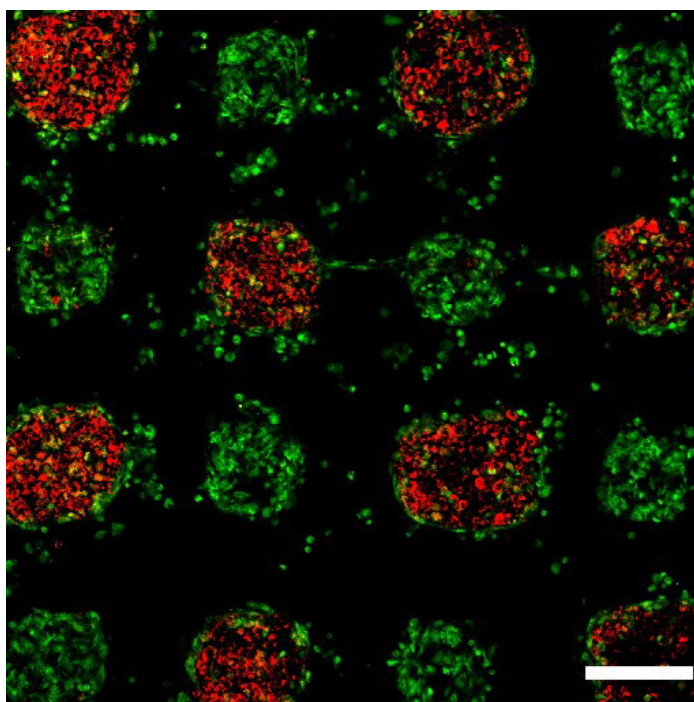
In conclusions, the superhydrophobic surfaces were found to exhibit short-term resistance to the protein adsorption. However, the superhydrophobic surfaces could accumulate more fibronectins than the flat surface of the same materials. When the patterned superhydrophobic surfaces were used in the cell culture, it was observed that the cells attached preferentially on the roughened area allowing the formation of cell microarrays. The biocompatibility of the fluoropolymer was improved by converting the fluoropolymers into the superhydrophobic materials. It was also found that the transfection

efficiency of the CHO cells and NIH 3T3 cells was greatly improved on the superhydrophobic surfaces. Therefore, we conclude that the patterned superhydrophobic surfaces could be used as cell microarrays with the advantages of improved cell adhesion, nature separation of colonies and enhanced transfection efficiency.



Chapter 5

Addressable Cell Microarrays by Switchable Superhydrophobic Surfaces



In this chapter, we describe an approach to fabricate addressable cell microarrays, which are based on the patterned switchable superhydrophobic surfaces. The switchable superhydrophobic surfaces were prepared by roughening the surface of fluoropolymers on the electrodes. Upon the application of 150 V, the water contact angle on the roughened fluoropolymer surface could be changed from 163° to less than 10° allowing the deposition of fibronectin, which could guide the growth of the cell. Our result indicated that it was possible to grow two different of cells on the desired area on the cell microarrays.

5.1 Introduction

In the era of genomics and proteomic, there are increasing demands in the development of novel patterning techniques to create arrays of functional biomolecules or cells on the miniaturized devices, which could be used in various large-scale biomedical applications such as biosensing, proteomic, immunoassays or drug screening [77, 78]. Several processes have been demonstrated capable of patterning biomolecules with very high degree of spatial control including dip-pen lithography, nanopipet, inkjet printing, photolithography, nanoimprinting and etc [79-86]. While the serial writing techniques provide the individual addressability, the parallel printing processes offer easy and fast protein patterning. However, very few of the above mentioned techniques are capable of patterning cells. The cell microarrays, which provide the native environments for various biochemical reactions, are often used to investigate the expression of genes and the function of proteins [87]. In the past few years, a lot of schemes have been proposed to fabricate the cells microarrays [88]. One of the most popular approaches is to print biomolecules on a chip where the desired types of cells are cultured. However, in such type of cell microarray, the cells are not confined. The separation of different colony sometime becomes problematic. Another approach is to employ micro-contact printing where the extracellular matrix (ECM) molecules such as fibronectins, vitronectin and collagens are first patterned on the surfaces [89]. Then the growth of cells on the surfaces was guided through the binding to these ECM molecules. However, in these two cases, only one type of cells can be used on a chip. Here we report the use of the switchable superhydrophobic surfaces to create cell microarrays where two or more types of cells can be cultured on different area of the same chip.

Superhydrophobic surfaces, whose water contact angles are larger than 150° , have been one of the most popular research topics for material scientists recently. The studies of

the superhydrophobic surfaces allow the investigation of the influence of the surface nanostructures to the water-repellent behavior similar to those observed in many living organs [90]. The understanding of the origin of the water-repellent behavior may help us in developing new industrial applications such as self-cleaning, anti-adhesion and oxidation resistant coatings [91]. To prepare superhydrophobic surfaces, there are two general approaches: roughening the surfaces of hydrophobic materials or coating the surface with a layer of hydrophobic nanostructured materials [92]. In these processes, the surface hydrophobicity can be controlled via proper surface engineering. However, the surface wettability can not be changed using these approaches once the materials are fabricated. A switchable surface is always desirable because of its great potential in many applications including fluidic manipulation, actuation, and the study of cell adhesion [93]. In a previous publication [94], we have demonstrated a novel class of nanostructured material, switchable superhydrophobic surfaces, for the fabrication of functional multi-component protein arrays where the electrowetting effect was employed to convert a superhydrophobic state into a complete wetted state, allowing fast but addressable protein deposition on the otherwise protein-resistant superhydrophobic surfaces. In such switchable superhydrophobic surfaces, the contact between protein solution and surface is minimized. Therefore, the protein deposition is only taking place on the arrays, which are activated by applying voltage. Because the protein solution only stays on the top of device for a few seconds, it is very unlikely that proteins would accidentally deposit on area already patterned with other proteins. To pattern different types of cells on such device, we propose to prepare addressable cell microarray by patterning the extracellular matrix (ECM) molecules, such as fibronectins, sequentially to the pre-determined areas, and then the microarray is cultured with the desired cell type. By repeating this process, two different types of cells can be cultured on to the same chip with spatial control.

5.2 Experimental section

The detail fabrication process for the addressable superhydrophobic microarray can be found in a previous publication [94]. In short, to fabricate the addressable cell microarrays, the patterned switchable superhydrophobic surfaces were prepared on the ITO glass. A layer of 5 μm thick fluoropolymer poly [tetrafluoroethylene-co-2,2-bis(trifluoromethyl)-4,5-difluoro -1,3-dioxole] (Teflon AF, DuPont) was first coated on the ITO glass with pre-patterned electrodes, which were covered with a layer of silicon oxide (~300 nm thick) for insulation purpose. Then a layer of photoresist (S1813, Shipley) was spun on top of the fluoropolymers and a photolithographic process was used to define the superhydrophobic area on the photoresist. The superhydrophobic microarray can be manufactured using an oxygen plasma treatment (Oxford Plasmalab 80 Plus, 80W) with a gas O_2 (2 sccm) at a total pressure of 25 mTorr. After plasma treatment, the photoresist was removed by washing the surface with acetone. Only the areas exposed to the oxygen plasma exhibited the superhydrophobic behavior, whose surface contact angle was measured to be 163° and the surface roughness was 65 nm. The switchable superhydrophobic chip is shown in figure 1.

Shown in scheme 1 is the patterning process for ECM molecules and cells. To guide the growth of the cells, ECM molecules such as fibronectins were patterned on the superhydrophobic microarray (Figure 5.1a). A drop (~15 μl) of fibronectin solution was pipetted onto the top of the microarray, which covered the whole superhydrophobic microarray. A platinum wire (0.1 mm in diameter) was inserted into the droplet, which served as the counter electrode. A 150 V voltage was applied to the selected ITO electrodes for a few seconds to switch the surface wettability of individual superhydrophobic microarrays (Figure 5.1b). After washing the chip with PBS solution, the fibronectin patterned microarrays on the desired area could be obtained (Figure 5.1c).

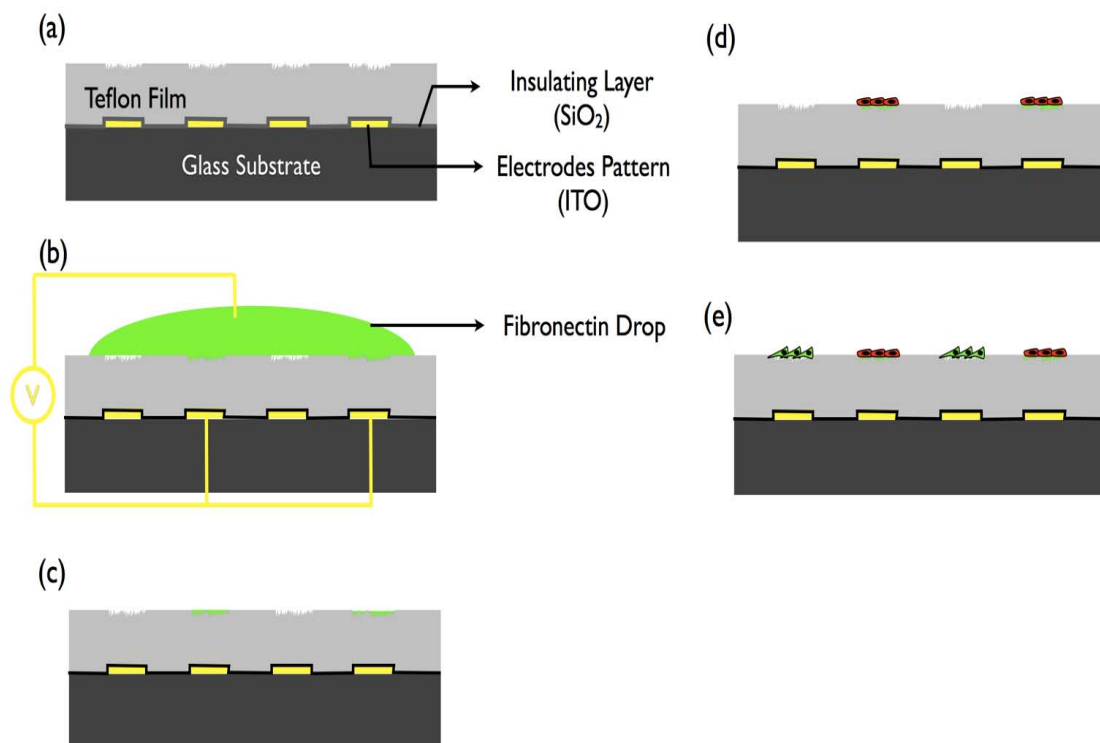


Figure 5.1 (a) The switchable superhydrophobic surface is fabricated by roughening a layer of fluoropolymer on the pre-patterned ITO electrodes. (b) A drop of fibronectin solution is added to the surface and a 150V is applied to the desired electrodes. (c) Fibronectin molecules are deposited to the array with underneath electrode activated. (d) The microarray is then used for cell culture. The cells will only attach to the area coated with fibronectin. (e) The procedure is repeated to culture the second type of cells.

The chip was then used to culture the first type of cells for a short time. Cells would attach to the area patterned with fibronectin (Figure 5.1d). The process was repeated once to culture the second type of cells on other patterned area (Figure 5.1e)

To create cell microarrays, a 4 x 4 switchable superhydrophobic microarray was used. The dimension for each array was 200 μm x 200 μm . Two cell lines, NIH 3T3 and HeLa, were seeded on the patterned superhydrophobic surfaces and placed on a confocal microscope (Fluoview 1000, Olympus) equipped with an incubator (MIU-IBC-IF,

Olympus) at 37°C and 5% CO₂ for 6 hours. The density of the cells was about 10⁵ cell/ml. Before measurement, the suspension cells were removed by PBS solution and the DIC or fluorescence image was taken.

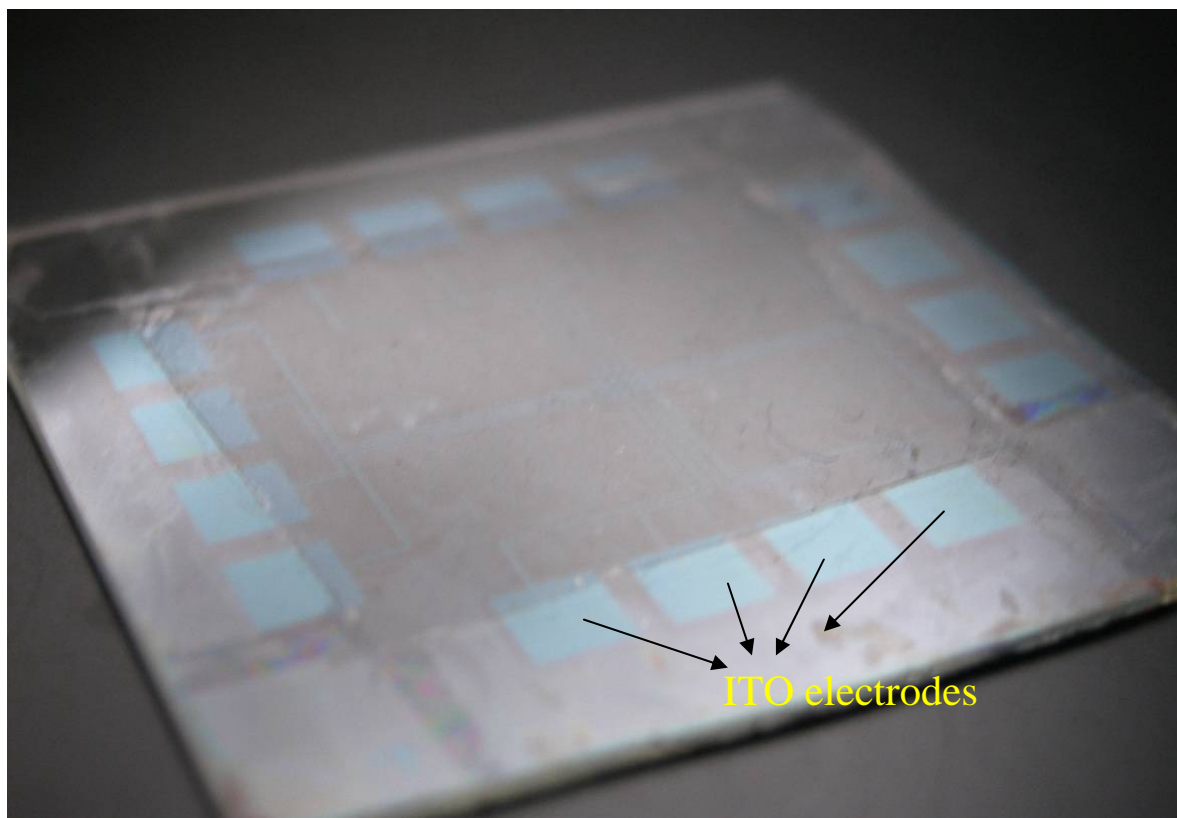


Figure 5.2 Optical image of an addressable chip containing 4 x 4 switchable superhydrophobic microarrays.

5.3 Results and Discussions

Shown in Figure 5.2 is an addressable chip containing 4 x 4 switchable superhydrophobic microarrays. In a previous experiment [94], we have demonstrated that the water contact angle on the switchable superhydrophobic surface can be switched from 163⁰ to less than 10⁰ by applying 150 V to the underneath electrodes and five different proteins can be selectively deposited into the individual elements of the microarrays. To produce cell microarrays with different types of cells, ECM molecules were deposited into the desired area and followed by culturing the first type of cells. After the cells were

attached to the desired area, the ECM molecules could be deposited into another area and followed by culturing the second type of cells.

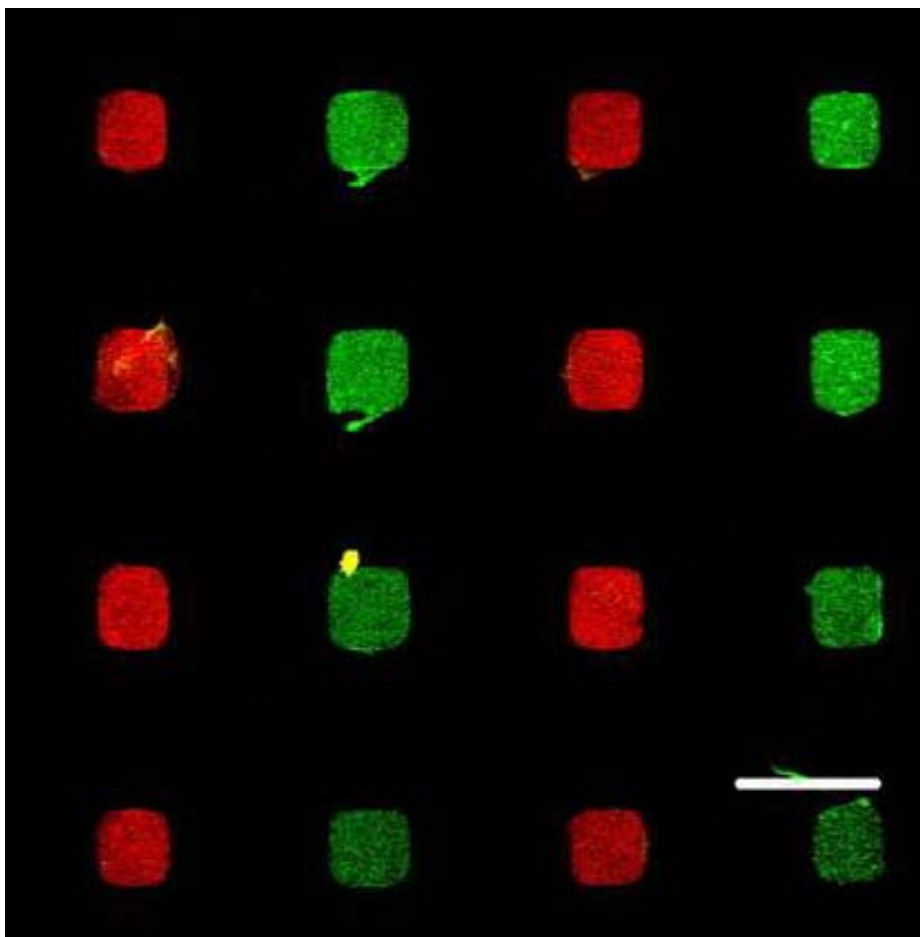


Figure 5.3 Fluorescence image of the patterned FITC conjugated anti-chicken IgG (green) and cy3 conjugated anti-rabbit IgG (red). Bar: 400 μ m.

Before using the switchable superhydrophobic microarray for cell patterning, the chip was tested by depositing two different protein solutions. To deposit proteins on the switchable superhydrophobic microarray, a drop (15 μ l) of phosphate buffered saline (PBS) solution containing green-fluorescent FITC conjugated anti-chicken IgG (5 μ g/ml, Sigma-Aldrich) was first placed on the superhydrophobic microarray for 1 second with 150 V applied voltage, and then washed by PBS solution. A second drop of protein

solution containing cy3 conjugated anti-rabbit IgG (10 $\mu\text{g/ml}$, red, Sigma-Aldrich), was then added on the chip and the procedure was repeated. The result is depicted in Figure 5.3 It can be clearly seen that the area deposited with anti-chicken IgG (green) and anti-rabbit IgG (red) was well separated and there was very little cross contamination (<2%).

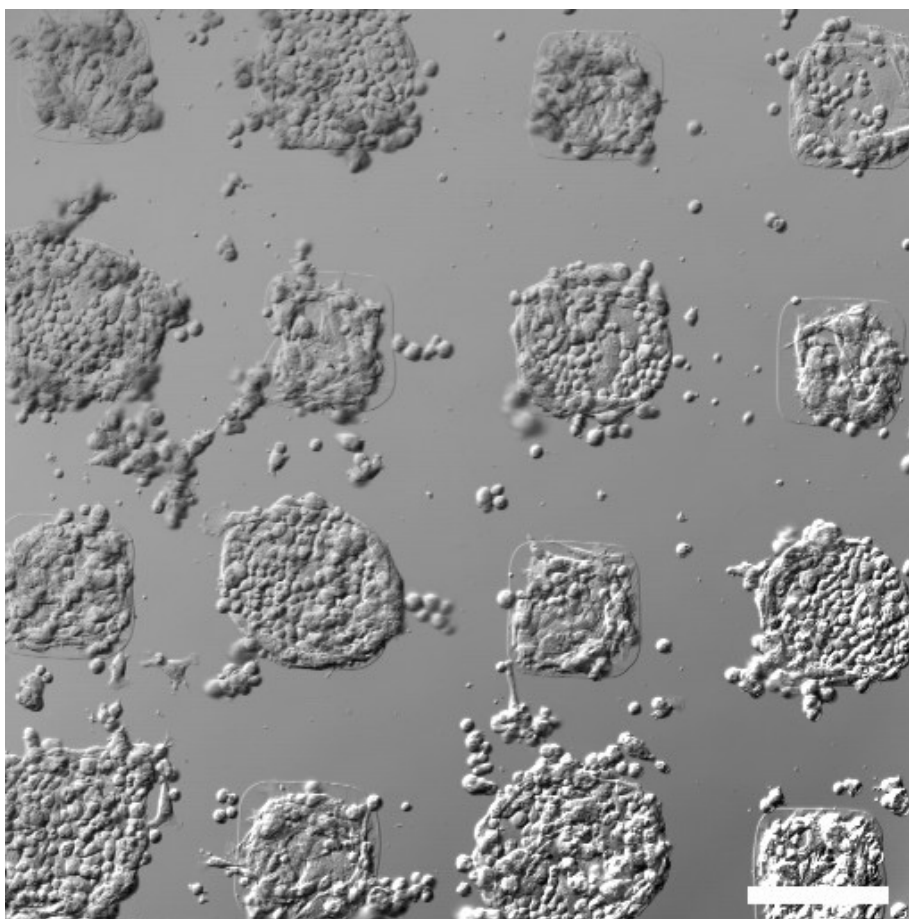


Figure 5.4 HeLa cells patterned on the switchable superhydrophobic microarrays. Bar: 200 μm

Knowing that the protein could be selectively deposited on the switchable superhydrophobic microarray, the protein solution containing fibronectins (50 $\mu\text{g/ml}$) was then deposited into a 4 x 4 microarrays. The fibronectins as shown in Figure 5.4. Since the HeLa cells can grow even in the suspension, some HeLa cells were found to grow on the flat area (no fibronectin deposition). During the cell culture, the HeLa cells were found to

migrate from the flat area to the patterned area. For those HeLa cells attached on the flat area, they tended to aggregate. The situation is a little bit different for the adherent cell line. When the fibroblast cells were seeded on the alternative patterned microarrays, it was found the fibroblast cells were attached exclusively on the arrays patterned with fibronectins as shown in Figure 5.5. No fibroblast cell was found in the roughened region without the fibronectin deposition. chip was then placed in the cell culture dish and seeded with HeLa cells at a concentration of 10^5 cell/ml. After 6 hours of incubation at 5% of CO_2 and 37°C , HeLa cells were found to attach to all the arrays patterned with

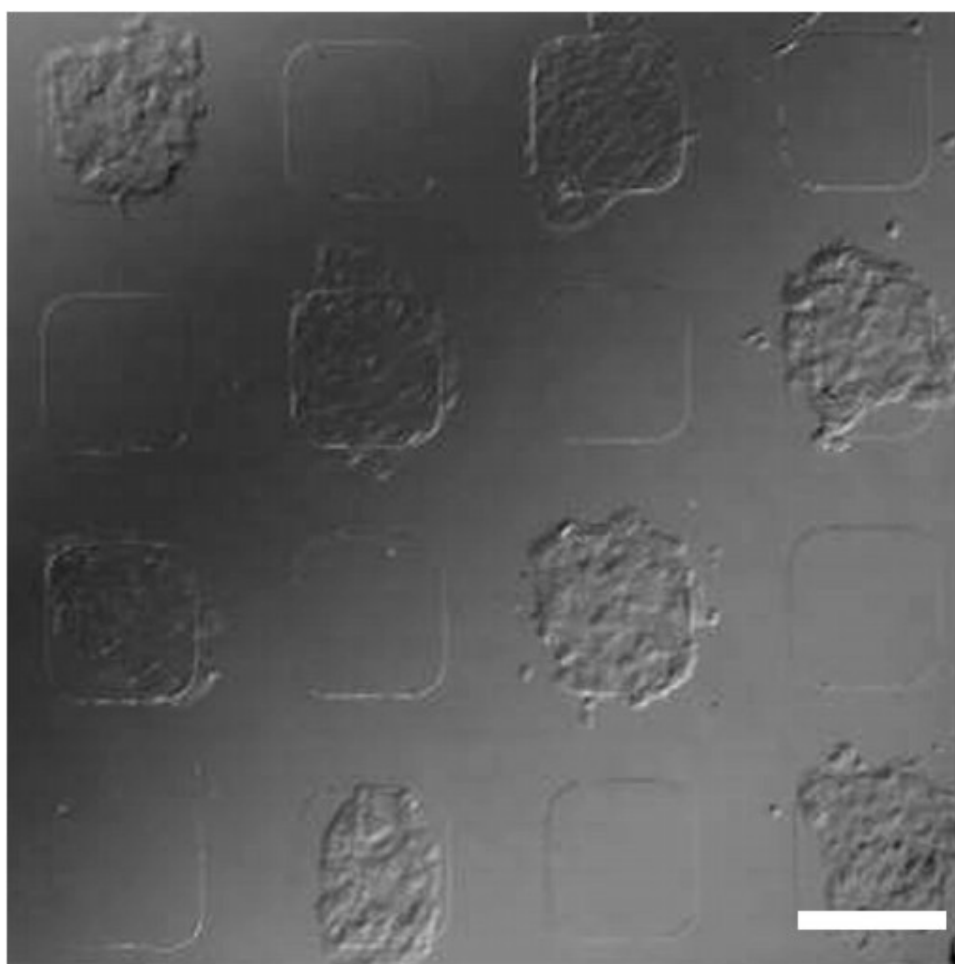


Figure 5.5 *Fibroblast cells patterned on the switchable superhydrophobic microarrays.*

Bar: 200 μm

To culture different cells on the same chip, the fibronectin solution was deposited on the alternative arrays similar to those shown in Figure 5.5 and then seeded with fibroblast

cells. After 30 minutes of incubation, the fibronectins were deposited to the rest of the microarrays and the HeLa cells were added to the culture dish. To distinguish two different cells, the fibroblast cells were stained by a red cell tracker dye and the HeLa cells were stained by a green cell tracker dye. Shown in Figure 5.6 is the fluorescence image of the cells on the switchable superhydrophobic array. It can be clearly seen that two different cells can be grown in the desired region in an addressable fashion. Therefore, we conclude that our approach can be used to co-culture two different cells on the same chip with spatial control. In principle, this approach can be extended to pattern more than two types of cells.

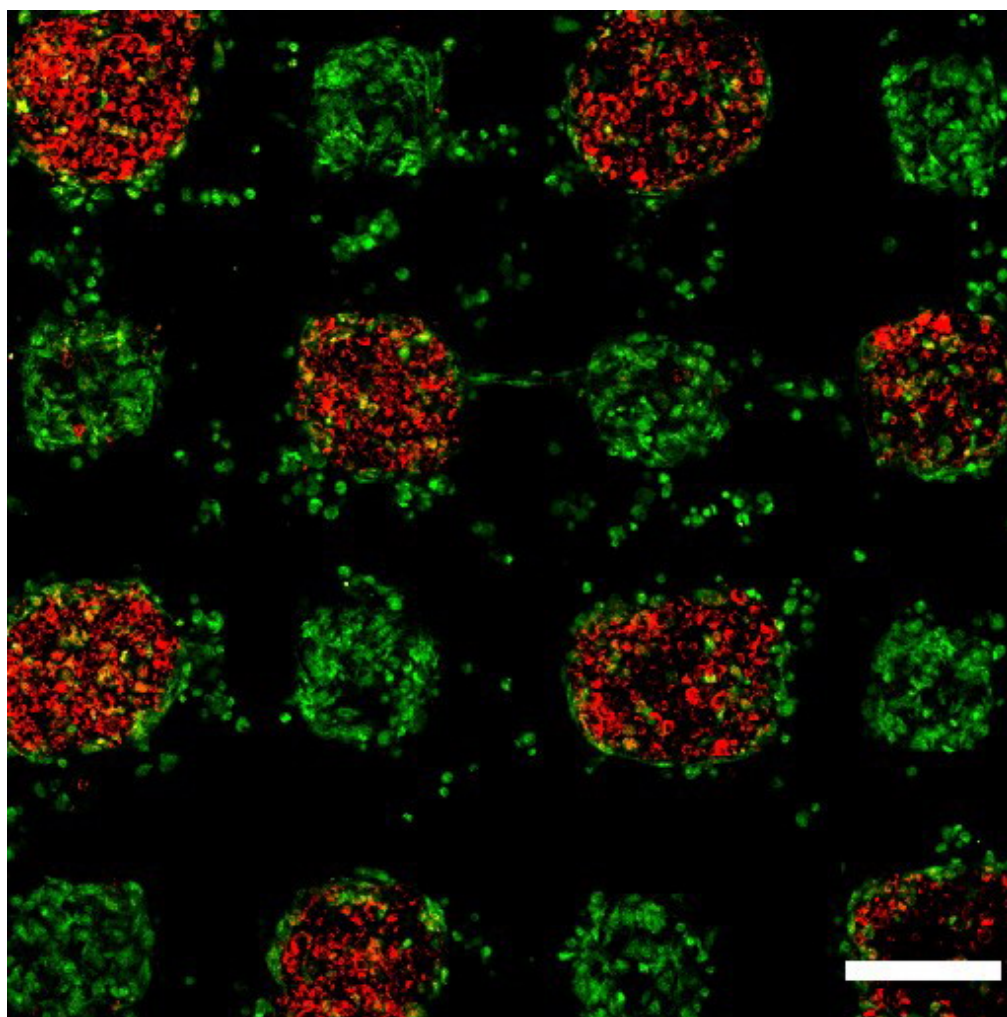


Figure 5.6 Fibroblast cells (red) were first patterned on switchable superhydrophobic microarray then followed by the HeLa cells (green). Bar: 200 μm .

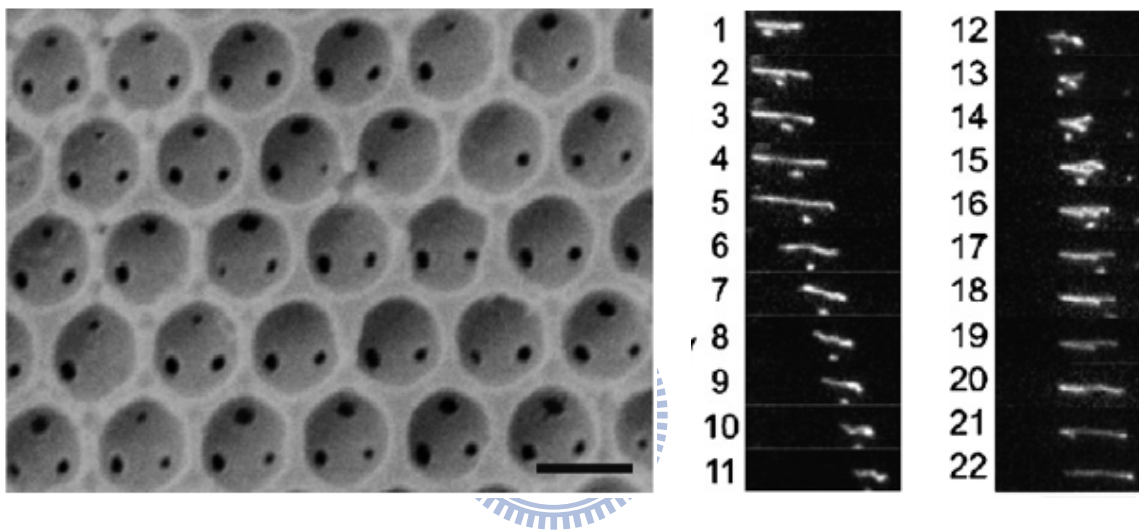
5.4 Conclusions

In conclusion, we have demonstrated a novel cell patterning technique using the switchable superhydrophobic surfaces. It has been shown that each element on the switchable superhydrophobic microarray could be addressed individually and different types of functional biomolecules could be selectively deposited on the microarray. It has also been demonstrated that two different types of cells could be cultured on the same chip at any desired area.



Chapter 6

Behavior of single DNA molecules in the well-ordered nanopores



In this chapter I describe a simple approach to fabricate robust three-dimensional periodic porous nanostructures inside the microchannels. In this approach, the colloidal crystals were first grown inside the microchannel using an evaporation-assisted self-assembly process. Then the void spaces among the colloidal crystals were filled with epoxy-based negative tone photoresist. After subsequent development and nanoparticle removal, the well-ordered nanoporous structures inside the microchannel could be fabricated. Depending on the size of the colloidal nanoparticles, periodic porous nanostructures inside the microchannels with cavity size of 330 and 570nm have been obtained. The dimensions of interconnecting pores for these cavities were around 40 and 64nm, respectively. The behavior of single λ -phage DNA molecules in these nanoporous structures was studied using fluorescence microscopy. It was found that the length of DNA

molecules oscillated in the nanoporous structures. The measured length for λ -phage DNA was larger in the 330nm cavity than those measured in the 570nm cavity.

6.1 Introduction

Gel electrophoresis has been proven to be a very useful tool for separating biomolecules. However, the extension of gel electrophoresis for the separation of larger biomolecules was found to be problematic. To separate large biomolecules, there have been increasing research activities in developing nano fluidic systems where the dimensions of biomolecules are larger than the dimension of nanofluidic system. To optimize the separation efficiency of the nanofluidic system, it is necessary to understand the influence of geometric parameters in the nanofluidic system, such as channel dimension and geometry, to the biomolecules. Therefore, it is very important to investigate the behavior of single DNA molecules in various nanofluidic systems [95–98]. To construct nanofluidic systems, MEMs (micro-electromechanical systems)-based fabrication techniques are often used. One- and two-dimensional nanofluidic channels have been fabricated on the silicon-based substrates for the separation of DNA and protein molecules, for example, two-dimensional micron scale obstacles were integrated into microfluidic channels allowing the separation of DNA molecules [99–101]. Larger DNA or protein molecules could be also separated by nanofluidic devices consisted of entropic traps [102–105]. However, these fabrication techniques often required the use of sophisticated lithographic techniques and the access to the clean room, which may deter many researchers in the field. Self-assembly of colloidal particles, on the other hands, is an alternative approach to construct well-ordered nanostructures without the access to the conventional lithographic tools where the close packed colloidal particles can be used as templates to fabricate various types of nanostructures. It has been shown by Colvin and coworkers [106] that three-dimensional periodic nanostructures could be produced by the self-assembly process

of colloidal particles using capillary force where the size of these periodic nanostructures can be tuned using colloidal nanoparticles with different diameters. This approach was later modified by Ozin and coworker using micropatterns where the evaporation induced self-assembly process drove the colloidal particles into the pre-designed patterns forming colloidal crystals with controlled orientation [107]. Such approach allowed the construction of heterostructure in the microchannels [108] as well as the integration with the detection system [109]. Since the diameters of the colloidal nanoparticles are in the range of nanometer, the void spaces between nanoparticles form nanofluidic channels, which have been used as the sieving matrix in the microfluidic system for the separation of DNA molecules [110]. Because the close-packed colloidal crystals offered well-ordered size-controlled nanofluidic system, they have been utilized to investigate the behavior of single DNA molecules in the confined spaces [111–113] as well as the separation of small dye molecules [114] and biomolecules [115]. Previously, we have developed an addressable microfluidic system to control the growth of colloidal crystals at any position inside one- or two-dimensional microfluidic system using electrocapillary effect [116,117]. Here, I present a similar approach to construct monolithically integrated periodic porous nanostructures in the microfluidic system using SU-8 photoresist (MicroChem, Newton, MA, USA) [118]. It is known that the cured SU-8 photoresist is highly resistant to acids and bases and they exhibit excellent mechanical properties and thermal stability. It has also been shown that the electrokinetic properties of SU-8 were similar to the commercial glass microdevices [119]. In addition, the photo patternable property of the photoresist would allow fabricating nanostructures at any desired location inside the microfluidic system. Therefore, it is advantageous to use SU-8 to construct nanofluidic system. In our approach, the SU-8 photoresist was used to fill up the void space inside the colloidal crystals. Upon the removal of the colloidal nanoparticles, the SU-8 photoresist formed an inverse structure of the colloidal crystals where cavities with diameter of the original

colloidal nanoparticles as well as interconnecting nanopores could be obtained. These interconnecting nanopores were then served as sieving materials for the separation of biomolecules. The behavior of single DNA molecules was investigated in the nanofluidic system formed by the interconnecting nanopores as a function of applied electric field and cavity size.

6.2 Materials and Methods

6.2.1. Chip Fabrication

The size-tunable nanoporous chips were fabricated by a combination of photolithography and self-assembly of colloidal crystal, as described previously [114]. The schematic for the chip fabrication is illustrated in Figure 6.1. The close packed colloidal crystal was first grown inside the SU-8 microchannels using an evaporation induced self-assembly process (Figure 6.1a). The void spaces in the colloidal crystal were then filled with SU-8 photoresist. A photomask was used to define the location of the nanoporous structures inside the microfluidic channel (Figure 6.1b). After dissolving silica colloidal particles in buffer oxide etch (BOE) solution, well-ordered nanoporous structures inside the microfluidic system can be obtained (Figure 6.1c). These nanoporous structures were consisted of cavities with a diameter of d_c , which represented the size of the original silica nanoparticles, and interconnecting pores with a diameter of d_p (Figure 6.1d). These interconnecting pores and cavities could be used as the sieving materials for separating biomolecules. The colloidal particles used in this experiment were 300 and 570nm silica nanoparticles (Bangs Labs., Fisher, IN, USA).

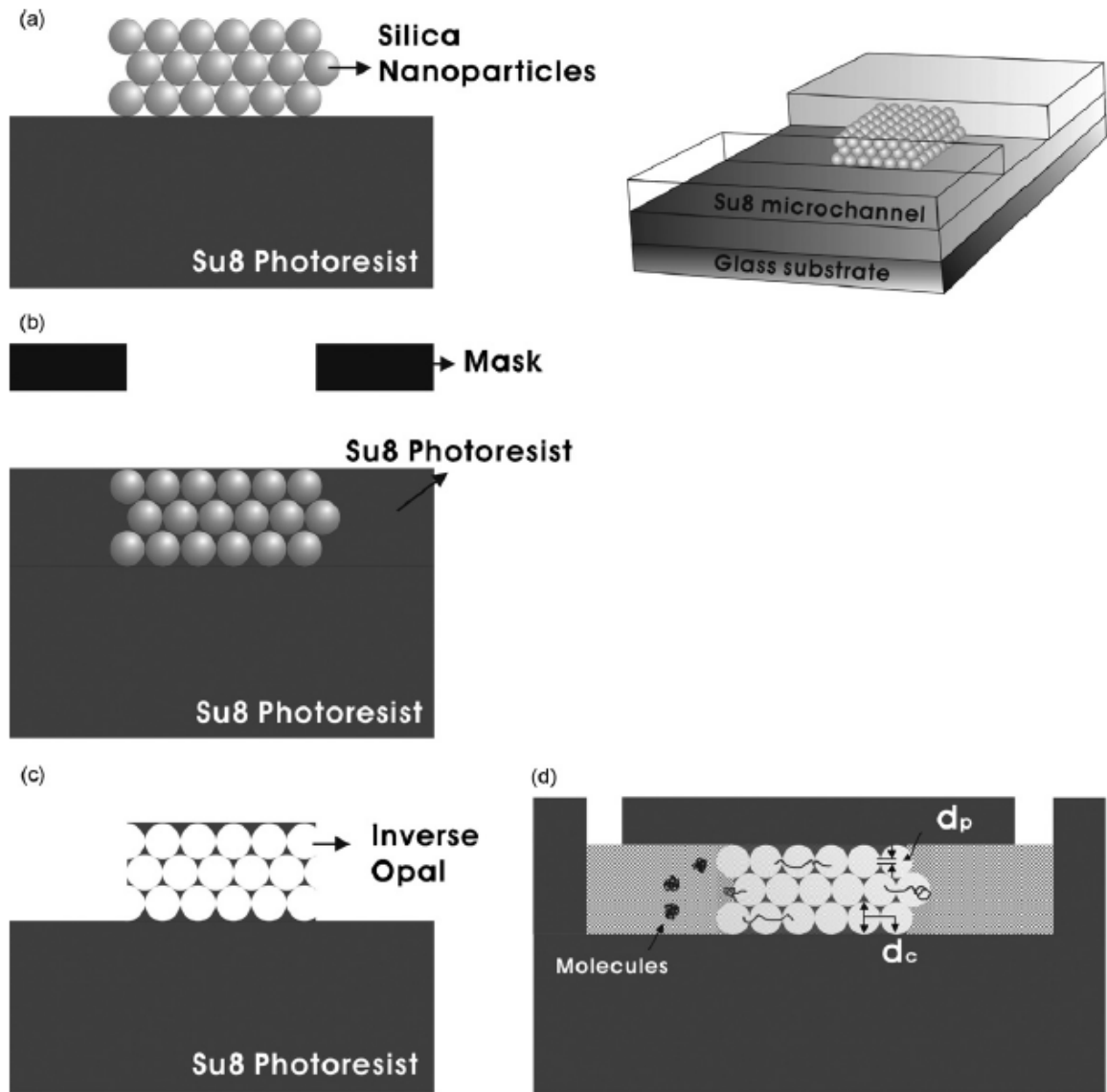


Figure 6.1 Schematic for the fabrication of well-order nanoporous structure in the microchannel using SU-8 photoresist. (a) Silica colloidal crystals are first grown inside the SU-8 microchannel. (b) The void spaces of the colloidal crystals are filled with SU-8 photoresist and cured in the desired area using UV radiation. (c) Inverse opal structures can be obtained after removing the silica nanoparticles with BOE solution and sealing with another layer of SU-8 photoresist. (d) The nanoporous structures are consisted of cavity d_c and interconnecting pore d_p .

6.2.2. DNA Separation

To investigate the behavior of single DNA in the well-ordered nanoporous structure, λ -phage (MW: 48.5 kilo base pairs (kbp), Sigma) and M13mp18 (MW: 7.25 kbp, Sigma) DNA molecules were used. In this experiment, the DNA molecules were mixed with YOYO-1 dye (nucleic acid dye, trade name, Invitrogen, Carlsbad, CA, USA) at a ratio of 5:1 (base pair/dye) in $5\times$ Tris borate EDTA buffer (TBE, pH 8.3, Sigma–Aldrich). An electrokinetic injection was used to introduce the DNA molecules to the sieving area. The fluorescence images of DNA molecules were taken on an Olympus IX71 inverted microscope equipped with a Cascade 512B CCD (charge coupled device) camera (Roper Scientific, Duluth, GA, USA).

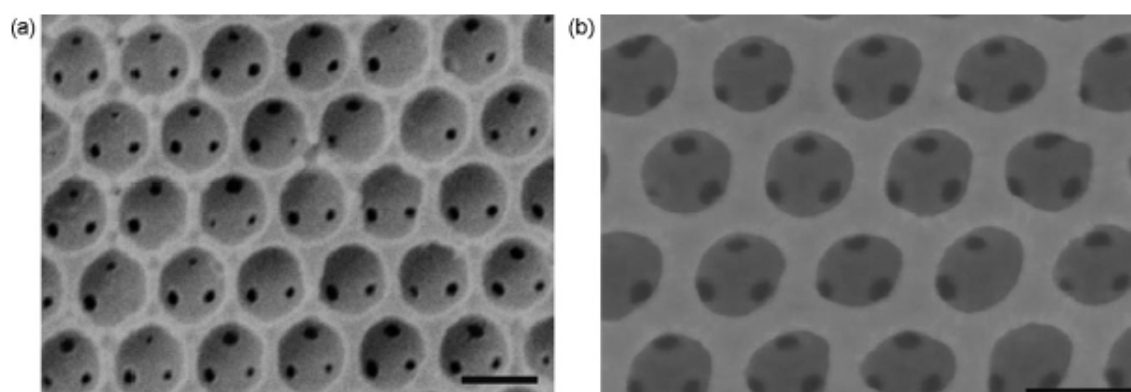


Figure 6.2 SEM images of nanoporous structures. Silica nanoparticle size (a) 300 nm, bar: 300 nm; (b) 570 nm, bar: 500 nm.

6.3 Results and Discussions

6.3.1 Monolithic Integration of SU-8 Microchannels

In this experiment, the three-dimensional ordered nanoporous structures were fabricated using SU-8 photoresist. There were two different dimensions in the well-ordered nanostructures: cavities (d_c), which were an inverse replica of the original silica nanoparticles, and interconnecting pores (d_p) where the close packed silica nanoparticles contacted each other. While the cavity size should be the same as the

diameter of the silica nanoparticles, the diameter of the interconnecting pore was found to be about 10% of the diameter of the silica. The size tuning in this approach was achieved by varying the size of the silica nanoparticles. Shown in Figure 6.2 are the cross-sectional scanning electron microscopy (SEM) images of two different nanoporous structures. The nanoporous structure formed by 300nm silica nanoparticles is shown in Figure 6.2a, while the nanostructure fabricated by 570nm nanoparticle is depicted in Figure 6.2b. From these SEM images, it can be clearly seen that the cavities were arranged in hcp (hexagonally close packed) close packed structures, which was the result of the self-assembly process. The cavity and interconnecting pore sizes were measured to be 297 and 40nm when the 300nm silica nanoparticles were used, whereas the colloidal crystals formed by 570nm nanoparticles produced cavities with 575nm diameter and 64nm interconnecting pores. The dimension of the different nanostructures used in this experiment was summarized in Table 6.1.

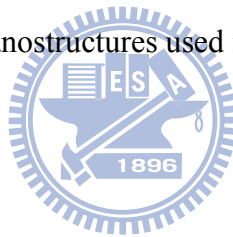


Table 6.1

The relationship between the silica beads, cavity size and pore size Silica particles size

Silica particles size (nm)	Cavity size d_c (nm)	Pore size d_p (nm)
300	297 ± 8	40 ± 10
570	575 ± 10	64 ± 20

6.3.2 Behavior of Individual DNA Molecules

To see the influence of the nanostructure to the behavior of biomolecules in the nanofluidic system, we have investigated the behavior of single λ -phage DNA molecules in the nanoporous fluidic system at various applied d.c. electric fields. To observe the λ -phage DNA molecules in the nanoporous structure, the nanoporous structure was filled with 5 \times Tris borate EDTA buffer and the DNA molecules were labeled with fluorescence

dye (YOYO-1) and the images of single DNA molecules were recorded by a fluorescence microscope (Olympus IX71) equipped with high speed camera (Cascade 512B EM CCD). Shown in Figure 6.3 are the sequential images of λ -DNA molecules migrating inside the nanoporous structure toward the anode at an applied field of 5 V/cm. The time interval between each frame was 0.1 s. Two different sizes of nanoporous structures were used in this experiment, the cavity size were 300nm (Figure 6.3a) and 570nm (Figure 6.3b), respectively.

Since the radius of gyration for λ -phage DNA molecules was larger than diameters of cavities and interconnecting pores in both cases, it was found that the λ -phage DNA molecules were stretched when they passed through these nanoporous structures. And the longest observed length was measured to be around 20 μm , which was about the contour length of λ -DNA molecules. Therefore, the λ -phage DNA molecules could be fully stretched in these nanoporous structures. Comparing with the averaged length of λ -phage DNA molecules measured in two different cavities, it was found that the length of DNA molecules measured in smaller cavity (300 nm) was larger than those measured in larger cavities (570 nm). In another word, the DNA molecules could recoil back to the coiled state more easily when they were in the larger cavities. The average length of the DNA molecules in two different cavities as a function of time was depicted in Figure 6.4a. The time origin was randomly selected at the frame where the length of the DNA molecules was measured to be the smallest. The length distribution of DNA molecules in two different cavities is shown in Figure 6.4b. It was found that the length of the DNA molecules oscillated with the same frequency in these nanoporous structures. However, the exact origin of this phenomenon was not known at this time.

6.3.3 Mobility Measurement

To utilize the nanoporous sieving materials to separate the biomolecules, it is very

important to measure the mobility of the biomolecules in these media. Shown in Figure 6.5a is the measured electrophoretic mobility of λ -phage DNA molecules in two different sizes of cavities whereas the mobility of smaller M13mp18 DNA molecules in the same media was depicted in Figure 6.5b. The electrophoretic mobility measured in the cavities formed by nanoparticles with a diameter of 300 nm was similar to those measured previously [118]. However, the mobility of both DNA molecules in the cavities formed by 570 nm colloidal particles was slightly higher at higher applied field. Since the sizes of the interconnecting pores in both cases were much smaller than the radius of gyration of both DNA molecules, we expect the entropic trapping effect to dominate in such type of sieving materials.

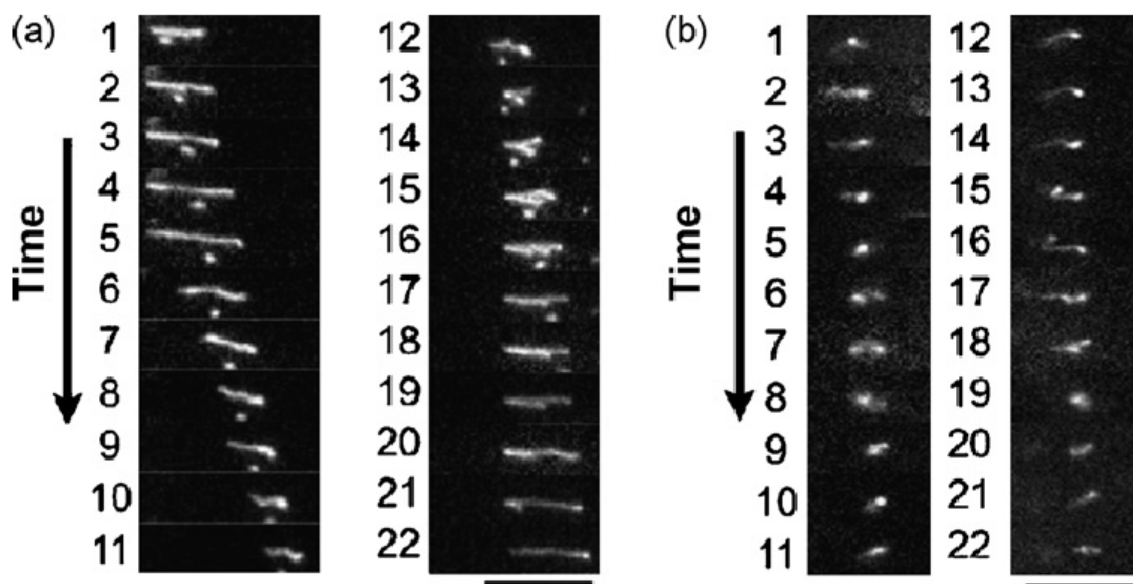


Figure 6.3 Sequential images of λ -DNA migrating inside the nanoporous structure toward the anode at an applied field of 5 V/cm. Elapsed time between frames is 0.1 s. Cavity size: (a) 300 nm, bar: 20 μ m and (b) 570 nm; bar: 20 μ m.

6.4 Conclusions

In summary, we have constructed well-ordered nanoporous structures inside the microfluidic channels using self-assembly process of colloidal nanoparticles. It was found that the cavity size of these nanoporous structures was the same as the diameter of the original colloidal nanoparticles whereas the size of the interconnecting pores was found to be about 10% of the cavity size. The influence of the nanostructures to the DNA molecules

was measured on a single molecular level where the time dependent stretch-recoil

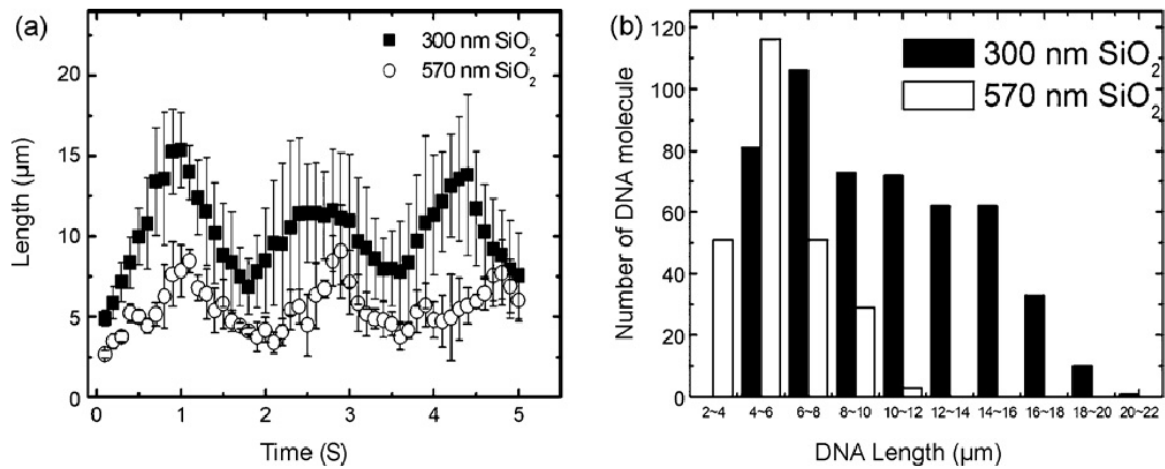


Figure 6.4 (a) Averaged DNA length in two different nanoporous structures. Applied field: 5 V/cm. 300nm (black square), 570 nm (open circles). (b) DNA length distribution in the nanoporous materials with two different cavity sizes (average of 500 DNA molecules).

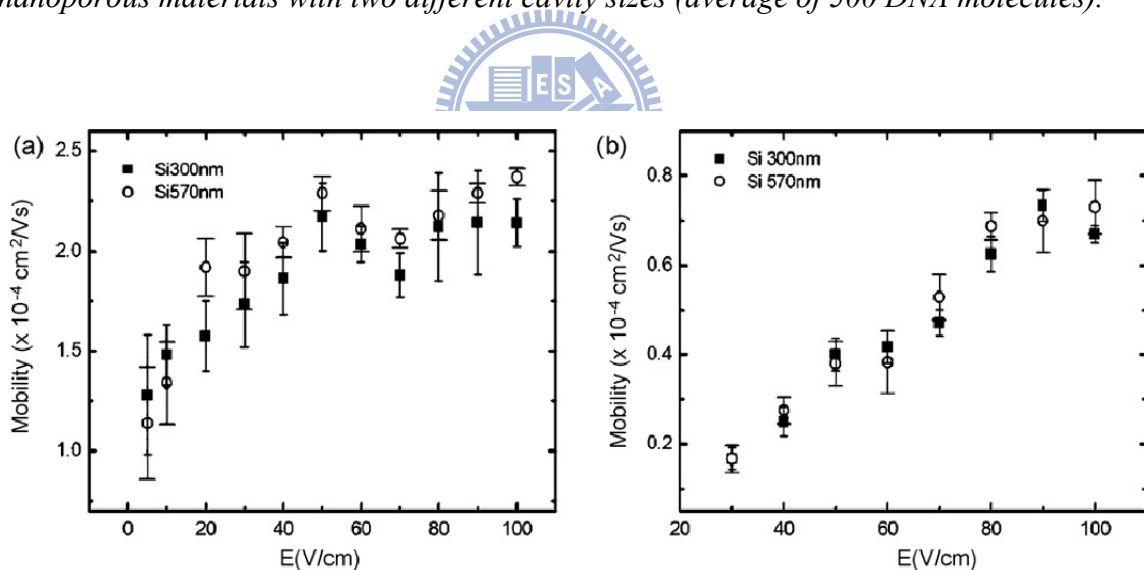
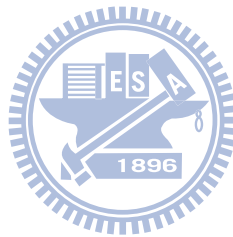


Figure 6.5 The electrophoretic mobility of (a) λ -DNA and (b) M13mp18 vector as a function of the applied electric field with two different cavity size of nanoporous structures: 300 nm (black square), 570 nm (open circles) (average of 50 DNA molecules).

behavior of the λ -phage DNA was recorded. The average length for λ -phage DNA molecules was found to be larger in the 300 nm cavity than those measured in the 570 nm cavity. The mobility of both λ -phage and M13mp18 DNA molecules was measured as a

function of applied field. It was found that the electrophoretic mobility for the smaller M13mp18 DNA molecules was smaller than the much larger λ -phage DNA molecules, which indicated that the well-ordered nanoporous structures could be used to construct integrated nanofluidic system for the separation of large biomolecules.



Chapter 7

Conclusions and Prospects

In this dissertation, I report the fabrication and characterization of superhydrophobic surface as a microdevice, which was used to study cell-substrate interaction. First, I developed two ways to prepare polymeric superhydrophobic microdevice. The first one is to combine spin-coated and oxygen plasma treatment on the fluoropolymer, which become more hydrophobic by increasing etching time. After 12 minutes etching process, the fluoropolymer become superhydrophobic surface with water angle more than 160° . Second, the nanoimprint process was used to create nanostructures on the devices, which included many thermal soluble polymers. The stamps were formed by silicon substrates, which were fabricated by nanosphere lithography and inductively coupled plasma reactive ion etching process. These stamps were used to imprint nanostructures on hydrophobic coatings, such as Teflon, over the device surfaces. The water contact angle as high as 167° has been obtained by the second approach. This approach was highly reproducible to make nanostructure on polymer. Then, these superhydrophobic pattern surfaces were used as substrate for the cell cultures of HeLa, NIH3T3, and CHO cells. It was found that these cell lines did not adhere to the flat fluoropolymer surfaces. However, the number of NIH3T3 and CHO cells adhered on the surfaces increase with the surface roughness. Such nanostructure materials could be used as the scaffold for selected cell growth. The transfection efficiency was also enhanced when cells were attached on superhydrophobic surface. Finally, the switchable surface fabricated by superhydrophobic coating and electrowetting effect was used to pattern two different types of cells on the same chip. Furthermore, I report the single DNA behavior detection by using three dimensional

nanoporous inside microfluidic channel system. The primary results obtained in this dissertation and prospects are summarized as follows:

- (1) I have developed two techniques to impart superhydrophobic property to the surfaces of devices. In the first approach, oxygen plasma treatment was used to roughen the Teflon coating whose surface water contact angle could be tuned from 120° to 168° by varying the oxygen plasma treatment time. However, the application of the oxygen plasma process is limited to fluoropolymers. In the second approach, nanoimprint process was used to create nanostructures on the device surfaces where the water contact angle as high as 167° was obtained. In principle, the nanoimprint process can be applied to all types of hydrophobic coatings.
- (2) The superhydrophobic surfaces were found to exhibit short-term resistance to the protein adsorption. However, the superhydrophobic surfaces could accumulate more fibronectins than the flat surface of the same materials. When the patterned superhydrophobic surfaces were used in the cell culture, it was observed that the cells attached preferentially on the roughened area allowing the formation of cell microarrays. The biocompatibility of the fluoropolymer was improved by converting the fluoropolymers into the superhydrophobic materials. It was also found that the transfection efficiency of the CHO cells and NIH 3T3 cells was greatly improved on the superhydrophobic surfaces. Therefore, we conclude that the patterned superhydrophobic surfaces could be used as cell microarrays with the advantages of improved cell adhesion, nature separation of colonies and enhanced transfection efficiency.
- (3) I have demonstrated a novel cell patterning technique using the switchable superhydrophobic surfaces. It has been shown that each element on the switchable superhydrophobic microarray could be addressed individually and different types of

functional biomolecules could be selectively deposited on the microarray. It has also been demonstrated that two different types of cells could be cultured on the same chip at any desired area.

- (4) I have constructed well-ordered nanoporous structures inside the microfluidic channels using self-assembly process of colloidal nanoparticles. It was found that the cavity size of these nanoporous structures was the same as the diameter of the original colloidal nanoparticles whereas the size of the interconnecting pores was found to be about 10% of the cavity size. The influence of the nanostructures to the DNA molecules was measured on a single molecular level where the time dependent stretch-recoil behavior of the λ -phage DNA was recorded. The average length for λ -phage DNA molecules was found to be larger in the 300 nm cavity than those measured in the 570 nm cavity. The mobility of both λ -phage and M13mp18 DNA molecules was measured as a function of applied field. It was found that the electrophoretic mobility for the smaller M13mp18 DNA molecules was smaller than the much larger λ -phage DNA molecules, which indicated that the well-ordered nanoporous structures could be used to construct integrated nanofluidic system for the separation of large biomolecules.

References

- [1] C. A. Thomas, P. A. Springer, G. E. Loeb, Y. Berwald-Netter, L. M. Okun. *Exp. Cell Res.* **74**, 61 (1972).
- [2] G. W. Gross, B. K. Rhoades, H. M. E. Azzazy, M. C. Wu, *Biosens Bioelec.* **10**, 553 (1995).
- [3] M. Mrksich, G. M. Whitesides, *Trends Biotech.* **13**, 228 (1995)
- [4] M. V. Merritt, M. Mrksich, G. M. Whitesides, *Principles of tissue engineering.* Austin:R.G. Landes Co. 211 (1997).
- [5] R. S. Kane, S. Takayama, E. Ostuni, D. E. Ingber, G. M. Whitesides, *Biomaterials* **20**, 2363 (1999).
- [6] G. M. Whitesides, E. Ostuni, S. Takayama, X. Jiang, D. E. Ingber, *Annu. Rev. Biomed. Eng.* **3**, 335 (2001).
- [7] J. Reichert, S. Brückner, H. Bartelt, K. D. Jandt, *Adv. Eng. Mater.* **9**, 1104 (2007).
- [8] C. Neinhuis, W. Barthlott, *Ann. Bot.* **79**, 677 (1997).
- [9] W. Barthlott, C. Neinhuis, *Planta* **1**, 202 (1997)
- [10] A. Nakajima, A. Fujishima, K. Hashimoto, T. Watanabe, *Adv. Mater.* **11**, 1365 (1999).
- [11] T. Sun, H. Tan, D. Han, Q. Fu, L. Jiang, *Small* **1**, 959 (2005).
- [12] J. Y. Shiu, C. W. Kuo, P. Chen, C. Y. Mou, *Chem. Mater.* **16**, 561 (2004).
- [13] N. A. Patankar, *Langmuir* **19**, 1249 (2003).
- [14] L. Feng, S. Li, Y. Li, H. Li, L. Zhang, J. Zhai, Y. Song, B. Liu, L. Jiang, D. Zhu, *Adv. Mater.* **14**, 1857 (2002).
- [15] Z.-Z. Gu, H. Uetsuka, K. Takahashi, R. Nakajima, H. Onishi, A. Fujishima, O. Sato, *Angew. Chem., Int. Ed.* **42**, 894 (2003).

- [16] D. O. H. Teare, C. G. Spanos, P. Ridley, E. J. Kinmond, V. Roucoules, J. P. S. Badyal, *Chem. Mater.* **14**, 4566 (2002).
- [17] K. Tsujii, T. Yamamoto, T. Onda, S. Shibuchi, *Angew. Chem., Int. Ed.* **36**, 1001 (1997).
- [18] H. Y. Erbil, A. L. Demirel, Y. Avci, O. Mert, *Science* **299**, 1377 (2003).
- [19] I. Woodward, W. C. E. Schofield, V. Roucoules, J. P. Badyal, *Langmuir* **19**, 3432 (2003).
- [20] M. Morra, E. Occhiello, F. Garbassi, *Langmuir* **5**, 872 (1989).
- [21] M. Morra, E. Occhiello, F. J. Garbassi, *Colloid Interface Sci.* **132**, 504 (1989).
- [22] H. Li, X. Wang, Y. Song, Y. Liu, Q. Li, L. Jiang, D. Zhu, *Angew. Chem., Int. Ed.* **40**, 1743 (2002).
- [23] L. Feng, S. Li, H. Li, J. Zhai, Y. Song, L. Jiang, D. Zhu, *Angew. Chem., Int. Ed.* **41**, 1221 (2002).
- [24] S. Shibuichi, T. Onda, N. Satoh, K. Tsujii, *J. Phys. Chem.* **100**, 19512 (1996).
- [25] J. Bico, C. Marzolin, D. Quere, *Europhys. Lett.* **47**, 220 (1999).
- [26] Z. Yoshimitsu, A. Nanajima, T. Watanabe, K. Hashimoto, *Langmuir* **18**, 5818 (2002).
- [27] W. Chen, A. Y. Fadeev, M. C. Hsieh, D. Oner, J. Youngblood, T. J. McCarthy, *Langmuir* **15**, 3395 (1999).
- [28] D. Oner, T. J. McCarthy, *Langmuir* **16**, 777 (2000).
- [29] A. Nakajima, A. Fujishima, K. Hashimoto, T. Watanabe, *Adv. Mater.* **11**, 1365 (1999)
- [30] U. C. Fischer, H. P. Zingsheim, *J. Vac. Sci. Technol.* **19**, 881 (1981).
- [31] J. C. Hulteen, R. P. Van Duyne, *J. Vac. Sci. Technol. A* **13**, 1553 (1995).
- [32] C. L. Haynes, R. P. Van Duyne, *J. Phys. Chem. B* **105**, 5599 (2001).
- [33] C. W. Kuo, J. Y. Shiu, Y. H. Cho, P. Chen, *Adv. Mater.* **15**, 1065 (2003).

- [34] M. Morra, E. Occhiello, F. Garbassi, *Langmuir* **5**, 872 (1989).
- [35] J. P. Youngblood, T. J. McCarthy, *Macromolecules* **32**, 6800 (1999).
- [36] C. Neinhuis, W. Barthlott, *Annals of Botany* **79**, 667 (1997).
- [36] W. Barthlott, C. Neinhuis, *Planta* **202**, 1 (1997).
- [37] A. Nakajima, A. Fujishima, K. Hashimoto, T. Watanabe, *Adv. Mater.* **11**, 1365 (1999).
- [38] N. A. Patankar, *Langmuir* **19**, 1249 (2003).
- [39] T. L. Sun, H. Tan, D. Han, Q. Fu, L. Jiang, *Small* **1**, 959 (2005).
- [40] L. Feng, S. H. Li, Y. S. Li, H. J. Li, L. J. Zhang, J. Zhai, Y. L. Song, B. Liu, L. Jiang, D. B. Zhu, *Adv. Mater.* **14**, 1857 (2002).
- [41] Z. Z. Gu, H. Uetsuka, K. Takahashi, R. Nakajima, H. Onishi, A. Fujishima, O. Sato, *Angew. Chem Intl. Ed.* **42**, 894 (2003).
- [42] D. O. H. Teare, C. G. Spanos, P. Ridley, E. J. Kinmond, V. Roucoules, J. P. S. Badyal, S. A. Brewer, S. Coulson, C. Willis, *Chem. Mater.* **14**, 4566 (2002).
- [43] K. Tsujii, T. Yamamoto, T. Onda, S. Shibuichi, *Angew. Chem. Intl. Ed.* **36**, 1011 (1997).
- [44] H. Y. Erbil, A. L. Demirel, Y. Avci, Y. Avc, O. Mert, *Science* **299**, 1377 (2003).
- [45] I. Woodward, W. C. E. Schofield, V. Roucoules, J. P. S. Badyal, *Langmuir* **19**, 3432 (2003).
- [46] M. Morra, E. Occhiello, F. Garbassi, *J. Colloid Interface Sci.* **132**, 504 (1989).
- [47] H. J. Li, X. B. Wang, Y. L. Song, Y. Q. Liu, Q. S. Li, L. Jiang, D. B. Zhu, *Angew. Chem. Intl. Ed.* **40**, 1743 (2001).
- [48] L. Feng, S. H. Li, H. J. Li, J. Zhai, Y. L. Song, L. Jiang, D. B. Zhu, *Angew. Chem. Intl. Ed.* **41**, 1221 (2002).
- [49] S. Shibuichi, T. Onda, N. Satoh, K. Tsujii, *J. Phys. Chem.* **100**, 19512 (1996).
- [50] J. Bico, C. Marzolin, D. Quere, *Europhys. Letters* **47**, 743 (1999).

- [51] F. Walther, P. Davydovskaya, S. Zurcher, M. Kaiser, H. Herberg, A. M. Gigler, R. W. Stark, *J. Micromech. Microeng.* **17**, 524 (2007).
- [52] J. Chauvin, T. Kawai, M. Irie, *Jap. J. Appl. Phys. Part 1* **40**, 2518 (2001).
- [53] J. Y. Shiu, P. L. Chen, *Adv. Mater.* **17**, 1866 (2005).
- [54] J. Y. Shiu, C. W. Kuo, P. L. Chen, *J. Amer. Chem. Soc.* **126**, 8096 (2004).
- [55] J. Y. Shiu, P. L. Chen, *Adv. Functional Mater.* **17**, 2680 (2007).
- [56] C. W. Kuo, J. Y. Shiu, P. L. Chen, G. A. Somorjai, *J. Phys. Chem. B* **107**, 9950 (2003).
- [57] C. W. Kuo, J. Y. Shiu, P. L. Chen, *Chem. Mater.* **15**, 2917 (2003).
- [58] C. W. Kuo, J. Y. Shiu, Y. H. Cho, P. L. Chen, *Adv. Mater.* **15**, 1065 (2003).
- [59] J. Y. Shiu, C. W. Kuo, P. L. Chen, C. Y. Mou, *Chem. Mater.* **16**, 561 (2004).
- [60] W. Barthlott, C. Neinhuis, *Planta* **202**, 1 (1997).
- [61] a) Z.-Z. Gu, H. Uetsuka, K. Takahashi, R. Nakajima, H. Onishi, A. Fujishima, O. Sato, *Angew. Chem. Int. Ed.* **42**, 894 (2003). b) H.Y. Erbil, A.L. Demirel, Y. Avci, O. Mert, *Science* **299**, 1377 (2003). c) H. Li, X. Wang, Y. Song, Y. Liu, Q. Li, L. Jiang, D. Zhu, *Angew. Chem. Int. Ed.* **40**, 1743 (2002). d) L. Feng, S. Li, H. Li, J. Zhai, Y. Song, L. Jiang, D. Zhu, *Angew. Chem. Int. Ed.* **41**, 1221 (2002). e) J.Y. Shiu, C.W. Kuo, P. Chen, C.Y. Mou, *Chem. Mater.* **16**, 561 (2004).
- [62] a) A. Nakajima, A. Fujishima, K. Hashimoto, T. Watanabe, *Adv. Mater.* **11**, 1365 (1999). b) X. J. Feng, L. Jiang, *Adv. Mater.* **18**, 3060 (2006) c) Z. G. Guo, F. Zhou, J. C. Hao, W. M. Liu, *J. Am. Chem. Soc.* **127**, 15670 (2005). d) J.Y. Shiu, W.T. Whang, P. Chen. *J. Adh. Sci. Technol.* **22**, 1883 (2008).
- [63] J. Y. Shiu, P. Chen, *Adv. Funct. Mater.* **17**, 2680 (2007).
- [64] R. Anton, M. V. Gyorgy, L. Thomas, *Biotechnology Annual Review* **13**, 1387 (2007).

- [65] Y. Koc, A. J. de Mello, G. McHale, M. I. Newton, P. Roach, N. J. Shirtcliffe, *Lab Chip*, **8**, 582 (2008).
- [66] T. Sun, H. Tan, D. Han, Q. Fu, L. Jiang, *Small* **1**, 959 (2005).
- [67] a) R. Langer, D. A. Tirrell, *Nature*, **428**, 487 (2004). b) M. Mrksich, *MRS Bulletin* **30**, 180 (2005).
- [68] N. J. Sniadecki, R. A. Desai, S. A. Ruiz, C. S. Chen, *Annals of Biomedical Engineering*, **34**, 59 (2006).
- [69] a) B. G. Keselowsky, D. M. Collard, A. J. Garcia, *J. Biomed. Mater. Res.* **66**, 247 (2003). b) A. I. Teixeira, G. A. Mckie, J. D. Foley, P. J. Bertics, *Biomaterials* **27**, 3945 (2006). c) H. Chen, L. Yuan, W. Song, Z. Wu, D. Li, *Prog. Polym. Sci.* **33**, 1059 (2008). d) H. Gan, K. Tang, T. Sun, M. Hirtx, Y. Li, L. Chi. S. Butz, H. Fuchs, *Angew. Chem. Int. Ed.* **48**, 5282 (2009).
- [70] N. A. Patankar, *Langmuir* **19**, 1249 (2003).
- [71] P. P. Girard, E. A. Cavalcanti-Adam, R. Kemkemer, J. P. Spatz, *Soft Matter* **3**, 307 (2007).
- [72] a) C. S. Chen, M. Mrksich, S. Huang, G. M. Whitesides, D. E. Ingber, *Science* **276**, 1425 (1997). b) C. S. Chen, X. Jiang, G. M. Whitesides, *MRS Bulletin* **30**, 194 (2005).
- [73] W. Song, D.D. Veiga, C.A. Custodio, J. Mano, *Adv. Mater.* **21**, 1830 (2009).
- [74] J. Ziauddin, D. M. Sabatini, *Nature*, **411**, 107 (2001).
- [75] A. L. Hook, H. Thissen, N. H. Voelcker, *TRENDS in Biotechnology* **24**, 471 (2006).
- [76] W. Kim, J. K. Ng, M. E. kunitake, B. R. Conklin, P. D. Yang, *J. Am. Chem. Soc.* **129**, 7228 (2007).

- [77] G. MacBeath, S. L. Schreiber, *Science* **289**, 1760 (2000)
- [78] D. S. Wilson, S. Nock, *Angew. Chem. Int. Ed.* **42**, 494 (2003)
- [79] L. M. Demers, D. S. Ginger, S. J. Park, Z. Li, S. W. Chung, C. A. Mirkin, *Science* **296**, 1836 (2002)
- [80] A. Bruckbauer, D. Zhou, L. Ying, Y. E. Korchev, C. Abell, D. Klenerman, *J. Am. Chem. Soc.* **125**, 9834 (2003)
- [81] T. Okamoto, T. Suzuki, N. Yamamoto, *Nat. Biotech.* **18**, 438 (2000)
- [82] S. A. Brook, N. Dontha, C. B. Davis, J. K. Stuart, G. O'Neill, W. G. Kuhr, *Anal. Chem.* **72**, 3253 (2002)
- [83] L. M. Lee, R. L. Heimark, R. Guzman, J. C. Baygents, Y. Zohar, *Lab Chip* **6**, 1080 (2006)
- [84] J. Doh, D. J. Irvine, *J. Am. Chem. Soc.* **126**, 9170 (2004)
- [85] G. M. Whitesides, E. Ostuni, S. Takayama, X. Jiang, D. E. Ingber, *Annu. Rev. Biomed. Eng.* **3**, 335 (2001)
- [86] J. P. Renault, A. Bernard, D. Juncker, B. Michel, H. R. Bosshard, E. Delamarche, *Angew. Chem. Int. Ed.* **41**, 2320 (2002)
- [87] J. Ziauddin, D. M. Sabatini, *Nature*, **411**, 107 (2001).
- [88] W. Franks, S. Tosatti, F. Heer, P. Seif, M. Textor, A. Hierlemann, *Biosens. Bioelectron.* **22**, 1426 (2007)
- [89] C. S. Chen, X. Jiang, G. M. Whitesides, *MRS Bulletin*, **30**, 194 (2005)
- [90] (a) C. Neinhuis, W. Barthlott, *Ann. Bot.* **79**, 667 (1997) (b) W. Barthlott, C. Planta Neinhuis, **202**, 1 (1997)
- [91] (a) A. Nakajima, A. Fujishima, K. Hashimoto, T. Watanabe, *Adv. Mater.* **11**, 1365 (1999) (b) N. A. Patankar, *Langmuir* **19**, 1249 (2003)
- [92] See for example (a) Z. -Z. Gu, H. Uetsuka, K. Takahashi, R. Nakajima, H. Onishi, A. Fujishima, O. Sato, *Angew. Chem. Int. Ed.* **42**, 894 (2003) (b) D. O. H. Teare, C. G. Spanos, P. Ridley, E. J. Kinmond, V. Roucoules, J. P. S. Badyal, *Chem. Mater.*

- 14**, 4566 (2002) (c) K. Tsujii, T. Onda, T. Yamamoto, S. Shibuichi, *Angew. Chem. Int. Ed.* **36**, 1011 (1997) (d) H. Y. Erbil, A.L. Demirel, Y. Avci, O. Mert, *Science* **299**, 1377 (2003) (e) M. Morra, E. Occhiello, F. Garbassi, *Langmuir* **5**, 872 (1989) (f) H. Li, X. Wang, Y. Song, Y. Liu, Q. Li, L. Jiang, D. Zhu, *Angew. Chem. Int. Ed.* **40**, 1743 (2002) (g) L. Feng, S. Li, H. Li, J. Zhai, Y. Song, L. Jiang, D. Zhu, *Angew. Chem. Int. Ed.* **41**, 1221 (2002)
- [93] (a) J. Lahann, S. Mitragotri, T. -N. Tran, H. Kaido, J. Sundaram, I. S. Choi, S. Hoffer, G. A. Somorjai, R. Langer, *Science* **299**, 371 (2003) (b) B. Gallardo, V. K. Guta, F. D. Eagerton, L. I. Jong, V. S. Craig, R. R. Shah, N. L. Abbott, *Science* **283**, 57 (1999) (c) R. A. Hayes, B. J. Feenstra, *Nature* **425**, 383 (2003) (d) K. Ichimura, S. -K. Oh, M. Nakagawa, *Science* **288**, 1624 (2000) (e) S. Minko, M. Muller, M. Motornov, M. Nitschke, K. Grundke, M. Stamm, *J. Am. Chem. Soc.* **125**, 3896 (2003) (f) C.S. Chen, M. Mrksich, S. Huang, G. M. Whitesides, D. E. Ingber, *Science* **276**, 1425 (1997)
- [94] J.Y. Shiu, P. Chen, *Adv. Func. Mater.* **17**, 2680 (2007)
- [95] Y.C. Chan, Y.K. Lee, Y. Zohar, *J. Micromech. Microeng.* **16**, 699 (2006).
- [96] J. Han, H.G. Craighead, *J. Vac. Sci. Technol. A* **17**, 2142 (1999).
- [97] J.T.Mannion, C.H. Reccius, J.D. Cross, H.G. Graighead, *Biophys. J.* **90**, 4538 (2006).
- [98] Y.W. Lin, M.F. Huang, H.T. Chang, *Electrophoresis* **26**, 320 (2005).
- [99] C.F. Chou, O. Bakajin, S.W.P. Turner, T.A.J. Duke, S.S. Chan, E.C. Cox, H.G. Craighead, R.H. Austin, *Proc. Natl. Acad. Sci. U.S.A.* **96**, 13762 (1999).
- [100] L.R. Huang, J.O. Tegenfeldt, J.J. Kraeft, J.C. Sturm, R.H. Austin, E.C. Cox, *Nat. Biotechnol.* **20**, 1048 (2002).
- [101] L.R. Huang, E.C. Cox, R.H. Austin, J.C. Sturm, *Science* **304**, 987 (2004).
- [102] J. Fu, P. Mao, J. Han, *Appl. Phys. Lett.* **87**, 263902 (2005).
- [103] J. Han, S.W. Turner, H.G. Craighead, *Phys. Rev. Lett.* **83**, 1688 (1999).
- [104] J. Fu, J. Yoo, J. Han, *Phys. Rev. Lett.* **97**, 18103 (2006).
- [105] J. Han, H.G. Craighead, *Science* **288** 1026 (2000).

- [106] P. Jiang, J.F. Bertone, K.S. Hwang, V.L. Colvin, *Chem. Mater.* **11** 2132 (1999).
- [107] S.M. Yang, G.A. Ozin, *Chem. Commun.* **24** 2507 (2000).
- [108] S.M. Yang, H. Miguez, G.A. Ozin, *Adv. Funct. Mater.* **12** 425 (2002).
- [109] G.A. Ozin, S.M. Yang, *Adv. Funct. Mater.* **11** 95 (2001).
- [110] M. Tabuchi, M. Ueda, N. Kaji, Y. Yamasaki, Y. Nagasaki, K. Yoshikawa, K. Kataoka, Y. Baba, *Nat. Biotechnol.* **22** 337 (2004).
- [111] D. Nykypanchuk, H.H. Strey, D.A. Hoagland, *Science* **297** 987 (2002).
- [112] H. Zhang, M.J. Wirth, *Anal. Chem.* **77** 1237 (2005).
- [113] Y. Zeng, D.J. Harrison, *Electrophoresis* **27** 3747 (2006).
- [114] S. Zheng, E. Ross, M.A. Legg, M.J. Wirth, *J. Am. Chem. Soc.* **128** 9016 (2006).
- [115] Y. Zeng, D.J. Harrison, *Anal. Chem.* **79** 2289 (2007).
- [116] J.Y. Shiu, C.W. Kuo, P. Chen, *J. Am. Chem. Soc.* **126** 8096 (2004).
- [117] J.Y. Shiu, P. Chen, *Adv. Mater.* **17** 1866 (2005).
- [118] C.W. Kuo, J.Y. Shiu, K.H. Wei, P. Chen, *J. Chromatogr. A* **1162** 175 (2007).
- [119] T. Sikanen, S. Tuomikoski, R.A. Ketola, R. Kostianen, S. Franssila, T. Kotiaho, *Lab Chip* **5** 888 (2005).

List of Publications

Journal Publications

1. **Jau-Ye Shiu**, Chiung Wen Juo, Wha-Tzong Whang and Peilin Chen*, "Addressable Cell Microarrays via Switchable Superhydrophobic Surfaces" (Invited Paper) J. Adhes. Sci. Technol. 2009, 22 (Accepted)
2. **Jau-Ye Shiu**, Wha-Tzong Whang and Peilin Chen*, "Superhydrophobic Coatings for Microdevices" (Invited Paper) J. Adhes. Sci. Technol. 2008, 22, 1883
3. **Jau-Ye Shiu**, Wha-Tzong Whang* and Peilin Chen*, "Behavior of single DNA molecules in the well-ordered nanopores" J. Chromatogr. A, 2008, 1206, 72
4. Chiung-Wen Kuo, **Jau-Ye Shiu**, Kung Hwa Wei, and Peilin Chen*, "Functionalized Silver Nanowires for Live Cell Study" Chem. Lett., 2008, 37, 610
5. Po-Hung Shih, **Jau-Ye Shiu**, Po-Chiao Lin, Chun-Cheng Lin, Teodor Veres, Peilin Chen*, "On Chip Sorting of Bacterial Cells Using Sugar-Encapsulated Magnetic Nanoparticles", J. Appl. Phys. 2008, 103, 07A316 (This worked was selected by Virtual Journal of Biological Physics Research 2008, 15, 6) .
6. **J.Y. Shiu**, P. Chen*, "Addressable Protein Patterning via Switchable Superhydrophobic Microarrays" Adv. Func. Mater. 2007, 17, 2680
7. C. W. Kuo, **J.Y. Shiu**, K, H. Wei and P. Chen*, "Monolithic Integration of Well-Ordered Nanoporous Structures in the Microfluidic Channels for Bioseparation" J. Chromatogr. A, 1162, 175, 2007.
8. **J.Y. Shiu**, P. Chen*, "Active Patterning Using an Addressable Microfluidic Network" Adv. Mater., 17, 1869, 2005.
9. **J.Y. Shiu**, C.W. Kuo, P. Chen*, "Actively Controlled Self-Assembly of Colloidal Crystals in Microfluidic Networks by Electrocapillary Forces" J. Am. Chem. Soc., 126, 8096, 2004.
10. **J.Y. Shiu**, C.W. Kuo, P. Chen*, C.Y. Mou, "Fabrication of Tunable Superhydrophobic Surfaces by Nanosphere Lithography" Chem. Mater., 16, 561. 2004.
11. C.W. Kuo, **J.Y. Shiu**, P. Chen*, G.A. Somorjai, "Fabrication of Size-Tunable Large-Area Periodic Silicon Nanopillar Arrays with Sub-10 nm Resolution" J. Phys. Chem. B, 107, 9950, 2003.

12. C.W. Kuo, **J.Y. Shiu**, Y.H. Cho, P. Chen*, “Fabrication of Large-Area Periodic Nanopillar Arrays for Nanoimprint Lithography Using Polymer Colloid Masks” Adv. Mater., **15**, 1065, 2003.
13. C.W. Kuo, **J.Y. Shiu**, P. Chen*, “Size and Shape Controlled Fabrication of Large-Area Periodic Nanopillar Arrays” Chem. Mater., **15**, 2917, 2003

Patent

1. 可定址微流裝置及其方法 TW I296607
2. 快速切換超親水、超疏水表面 TW I265945



Resume

Jau-Ye Shiu



Personal Details

Name Jau-Ye Shiu
Citizenship Taiwan (TW)
Address 128 Academia Road,
Section 2, Nankang,
Taipei 115, Taiwan
tel. +886227898000ext55
email jyshiu@gate.sinica.edu.tw



Current Positions

2006 - Ph. D candidate, Department of Materials Science and Engineering, National

Chiao-Tung University, Taiwan (NCTU)

2003- Research assistant, Research Center for Applied Sciences (RCAS), Academia Sinica,

Taipei, Taiwan

Education

M.Sc. Physics (2002-2004), Department of Physics, National Chung Cheng University,
Taiwan

B.Sc. Physics (1998-2002), Department of Physics, Chinese Culture University, Taiwan

Research Interests

- Micro- and Nano-fluidic System Fabrication (Switchable Surfaces).

- Nanostructured surfaces for biological applications.

Research skills

I am well versed with Scanning electron Microscope (SEM), Confocal Raman Microscope, Atomic force microscopy (AFM), Scanning Tunneling electron Microscopy (STEM), X-ray Photoelectron spectroscopy (XPS) and clean room machines.

Research Publications

1. Jau-Ye Shiu, Chiung Wen Juo, Wha-Tzong Whang and Peilin Chen*, "Addressable Cell Microarrays via Switchable Superhydrophobic Surfaces" (Invited Paper) *J. Adhes. Sci. Technol.* 2009, 22 (Accepted)
2. Jau-Ye Shiu, Wha-Tzong Whang and Peilin Chen*, "Superhydrophobic Coatings for Microdevices" (Invited Paper) *J. Adhes. Sci. Technol.* 2008, **22**, 1883
3. Jau-Ye Shiu, Wha-Tzong Whang* and Peilin Chen*, "Behavior of single DNA molecules in the well-ordered nanopores" *J. Chromatogr. A*, 2008, **1206**, 72
4. Chiung-Wen Kuo, Jau-Ye Shiu, Kung Hwa Wei, and Peilin Chen*, "Functionalized Silver Nanowires for Live Cell Study" *Chem. Lett.*, 2008, **37**, 610
5. Po-Hung Shih, Jau-Ye Shiu, Po-Chiao Lin, Chun-Cheng Lin, Teodor Veres, Peilin Chen*, "On Chip Sorting of Bacterial Cells Using Sugar-Encapsulated Magnetic Nanoparticles", *J. Appl. Phys.* 2008, **103**, 07A316 (This worked was selected by *Virtual Journal of Biological Physics Research* 2008, 15, 6) .
6. J.Y. Shiu, P. Chen*, "Addressable Protein Patterning via Switchable Superhydrophobic Microarrays" *Adv. Func. Mater.* 2007, **17**, 2680
7. C. W. Kuo, J.Y. Shiu, K. H. Wei and P. Chen*, "Monolithic Integration of Well-Ordered Nanoporous Structures in the Microfluidic Channels for Bioseparation" *J. Chromatogr. A*, **1162**, 175, 2007.

8. J.Y. Shiu, P. Chen*, “Active Patterning Using an Addressable Microfluidic Network” *Adv. Mater.*, **17**, 1869, 2005.
9. J.Y. Shiu, C.W. Kuo, P. Chen*, “Actively Controlled Self-Assembly of Colloidal Crystals in Microfluidic Networks by Electrocapillary Forces” *J. Am. Chem. Soc.*, **126**, 8096, 2004.
10. J.Y. Shiu, C.W. Kuo, P. Chen*, C.Y. Mou, “Fabrication of Tunable Superhydrophobic Surfaces by Nanosphere Lithography” *Chem. Mater.*, **16**, 561, 2004.
11. C.W. Kuo, J.Y. Shiu, P. Chen*, G.A. Somorjai, “Fabrication of Size-Tunable Large-Area Periodic Silicon Nanopillar Arrays with Sub-10 nm Resolution” *J. Phys. Chem. B*, **107**, 9950, 2003.
12. C.W. Kuo, J.Y. Shiu, Y.H. Cho, P. Chen*, “Fabrication of Large-Area Periodic Nanopillar Arrays for Nanoimprint Lithography Using Polymer Colloid Masks” *Adv. Mater.*, **15**, 1065, 2003. C.W. Kuo, J.Y. Shiu, P. Chen*, “Size and Shape Controlled Fabrication of Large-Area Periodic Nanopillar Arrays” *Chem. Mater.*, **15**, 2917, 2003

Research Awards

- 2004 Best post award, Actively Controlled Self-Assembly of Colloidal Crystals by Electrocapillary Effect, Materials Research Society (MRS) fall meeting, US
- 2004 Paper reported by scientific magazine, *Lab on a Chip*, August, volume 4, No. 4
- 2004 Paper reported by scientific magazine, *MRS BULLETIN*, April, volume 29, No. 4